



Hochschule der Medien
Fakultät für Druck und Medien
Computer Science and Media

Generative Data Augmentation

Multi-Agent Diverse Generative Adversarial Networks
for Generative Data Augmentation

Dissertation submitted for the degree of
Master of Science

Topic: Generative Data Aufmentation

Author: Nicolas Reinhart - nr063@hdm-stuttgart.de
MatNr. 44100

Version of Date: May 4, 2025

1. Advisor: Prof. Dr.-Ing. Johannes Maucher
2. Advisor: Prof. Dr.-Ing. Oliver Kretzschmar

Abstract

asdf

Contents

List of Figures	5
List of Tables	6
List of Abbreviations	7
1 Introduction and Motivation	8
2 Related Work	10
3 Theoretical Background	12
3.1 Image Classification Models	12
3.1.1 Neural Networks for Classification	12
3.1.2 Classification Models for augmented Training	15
3.2 Data Augmentation - DA	15
3.2.1 Traditional Data Augmentation - TDA	16
3.2.2 Generative Data Augmentation - GDA	17
3.3 Generative Adversarial Network - GAN	18
3.3.1 Mathematical Formulation	18
3.3.2 Training Process	19
3.3.3 Challenges in GAN Training	19
3.4 Deep Convolutional Generative Adversarial Network - DCGAN	20
3.4.1 Architectural Adjustments	20
3.5 Conditional Generative Adversarial Network - cGAN	21
3.5.1 Mathematical Formulation	21
3.5.2 Architectural Adjustments	22
3.6 Multi-Agent Diverse Generative Adversarial Network - MADGAN	22
3.6.1 Mathematical Formulation	23
3.6.2 Architectural Adjustments	25
3.7 Adapting MAD-GAN for Conditional Generation with Explicit Diversity - CMADGAN	25
3.7.1 Mathematical Formulation	26
3.7.2 Architectural Adjustments	27
3.8 Image Scores	28
3.8.1 Inception Score - IS	28
3.8.2 Fréchet Inception Distance - FID	29
3.8.3 InceptionV3 Model	30
4 Experiments Setup	32
4.1 Preliminary Remarks	32
4.1.1 Scope Limitation Regarding Standard CIFAR-10	32
4.1.2 Datasets	33
4.1.3 GAN: Architecture, Training and Data Augmentation	33
4.1.4 Stratified Classifiers as measure for augmentation Quality	34
4.1.5 Labeling unconditioned data	34
4.1.6 Utilization of InceptionV3 for FID and IS	34
4.2 Experimental Workflow	35
4.3 Comparison of Classifier Performance	36

4.4	Hardware and Software Environment	36
4.4.1	Hardware	36
4.4.2	Software	37
5	Experiments Results	38
5.1	Key Research Questions	38
5.2	Key Research Question Answers	39
5.2.1	Question 1	39
5.2.2	Question 2	42
5.2.3	Question 3	51
5.2.4	Question 4	53
5.2.5	Question 5	53
6	Remarks	54
7	Outlook	55
8	Conclusion	56
List of References		57
Appendix		1
8.1	Network Architectures	1
8.1.1	Classifiers	1
8.1.2	Generator Model Architectures	2
8.1.3	Discriminator Model Architectures	3
8.2	FID and Inception Scores from MADGAN Architectures	5
8.2.1	MADGAN MNIST	5
8.2.2	MADGAN Fashion MNIST	6
8.2.3	cMADGAN MNIST	7
8.2.4	cMADGAN Fashion MNIST	8
8.2.5	DC MNIST	9
8.2.6	DC Fashion MNIST	9
8.2.7	Conditional MNIST	9
8.2.8	Conditional Fashion MNIST	9
8.3	Stratified Classifier Performances and Graphs	10
8.3.1	Dataset: MNIST, Architecture: MADGAN	10
8.3.2	Dataset: MNIST, Architecture: cMADGAN	14
8.3.3	Dataset: FASHION, Architecture: MADGAN	18
8.3.4	Dataset: FASHION, Architecture: cMADGAN	22
8.3.5	Dataset: MNIST, Architecture: Deep Convolutional GAN	26
8.3.6	Dataset: MNIST, Architecture: COND GAN	27
8.3.7	Dataset: FASHION, Architecture: DC GAN	28
8.3.8	Dataset: FASHION, Architecture: COND GAN	29
8.3.9	Dataset: MNIST, Architecture: TDA	30
8.3.10	Dataset: FASHION, Architecture: TDA	31
8.4	Data Creation Histograms	32
8.4.1	DCGAN MNIST	32
Declaration of Oath		33

List of Figures

1	Exemplary use of traditional augmentation techniques from the categories <i>geometric</i> (first row), <i>photometric</i> (second row), and <i>noise-corruption</i> (third row). The image shown is an image from the CIFAR10 dataset, assigned to the class "airplane".	17
2	Visualization of the vanilla GAN architecture. The figure shows the noise vector, flowing into the discriminator, as well as the real sample from P_d	18
3	Visualization of the MADGAN architecture. The figure shows the $k+1$ outputs of the discriminator and the k generators, with tied weights in the middle of the network.	23
4	Figure taken from the original paper [GKN ⁺ 18]. The visualization shows how different generators G_1 and G_2 are pushed to different modes M_1 and M_2	24
10	Depiction of the CNN achritecture used to classify unlabeled images from the MNIST GDA experiments and judge the effectiveness of said GDA. (Image created with [Gav20])	1
11	Depiction of the CNN achritecture used to classify unlabeled images from the FashionMNIST GDA experiments and judge the effectiveness of said GDA. (Image created with [Gav20])	1
12	Depiction of the CNN achritecture used to classify unlabeled images from the CIFAR10 GDA experiments and judge the effectiveness of said GDA. (Image created with)	1
13	Depiction of the generator used in the deep convolutional GAN dependent experiments. Used to train a generator and create fake image data based on the MNIST dataset.	2
14	Depiction of the generator used in the deep convolutional GAN dependent experiments. Used to train a generator and create fake image data based on the Fashion-MNIST dataset.	2
15	Depiction of the generator used in the Conditional GAN dependent experiments. Used to train a generator and create fake image data based on the MNIST and Fashion-MNIST datasets.	2
16	Depiction of the generators used in the MADGAN dependent experiments. Used to train a generator and create fake image data based on the MNIST and Fashion-MNIST datasets.	3
17	Depiction of the generators used in the cMADGAN dependent experiments. Used to train a generator and create fake image data based on the MNIST and Fashion-MNIST datasets.	3
18	Depiction of the discriminator used in the deep convolutional GAN dependent experiments. Used to train a generator based on the MNIST dataset.	3
19	Depiction of the discriminator used in the deep convolutional GAN dependent experiments. Used to train a generator based on the Fashion-MNIST dataset.	4
20	Depiction of the discriminator used in the Conditional GAN dependent experiments. Used to train a generator based on the MNIST and Fashion-MNIST datasets.	4

21	Depiction of the discriminator used in the MADGAN dependent experiments. Used to train a generator based on the MNIST and Fashion-MNIST datasets.	4
22	Depiction of the discriminator used in the cMADGAN dependent experiments. Used to train a generator based on the MNIST and Fashion-MNIST datasets.	4
23	A histogram chart depicting the class distribution of the generated data with the DCGAN generator trained on the MNIST dataset. The labels result from an auxiliary classifier as mentioned in 4.1.5.	32

List of Tables

1	Summary of commonly used benchmark datasets for image classification.	33
2	FID and IS results for GAN models on MNIST, comparing single-generator (DCGAN, cGAN) and multi-generator (MADGAN, cMADGAN; K=3-10) approaches.	40
3	FID and IS results for GAN models on Fashion-MNIST, comparing single-generator (DCGAN, cGAN) and multi-generator (MADGAN, cMADGAN; K=3-10) approaches.	41
4	Final F1 Scores after 50 epochs. Augmentation technique: MADGAN	43
5	Final F1 Scores after 50 epochs. Augmentation technique: TDA	43
6	Final F1 Scores after 50 epochs. Augmentation technique: MADGAN	45
7	Final F1 Scores after 50 epochs. Augmentation technique: TDA	45
8	Final F1 Scores after 50 epochs. Augmentation tech.: MADGAN (K=7)	47
9	Final F1 Scores after 50 epochs. Augmentation technique: TDA	47
10	Final F1 Scores after 50 epochs. Augmentation tech.: MADGAN (K=X)	49
11	Final F1 Scores after 50 epochs. Augmentation technique: TDA	49
12	Final F1 Scores after 50 epochs. Augmentation technique: MADGAN	52
13	Final F1 Scores after 50 epochs. Augmentation technique: TDA	52
14	Effect of varying the number of generators ($N = 3, 5, 7, 10$) in the MADGAN model on FID and Inception Score (IS \pm Std Dev) for the MNIST dataset. Results for each generator index are presented alongside baseline metrics.	5
15	Effect of varying the number of generators ($N = 3, 5, 7, 10$) in the MADGAN model on FID and Inception Score (IS \pm Std Dev) for the Fashion MNIST dataset. Results for each generator index are presented alongside baseline metrics.	6
16	Effect of varying the number of generators ($N = 3, 5, 7, 10$) in the cMADGAN model on FID and Inception Score (IS \pm Std Dev) for the MNIST dataset. Results for each generator index are presented alongside baseline metrics.	7
17	Effect of varying the number of generators ($N = 3, 5, 7, 10$) in the cMADGAN model on FID and Inception Score (IS \pm Std Dev) for the Fashion MNIST dataset. Results for each generator index are presented alongside baseline metrics.	8
18	FID and Inception Score (Mean \pm Std Dev) for a single DCGAN generator ($N = 1$) trained on the MNIST dataset. Baseline scores are included for reference.	9

19	FID and Inception Score (Mean \pm Std Dev) for a single DCGAN generator ($N = 1$) trained on the Fashion MNIST dataset. Baseline scores are included for reference.	9
20	FID and Inception Score (Mean \pm Std Dev) for a single Conditional GAN generator ($N = 1$) trained on the MNIST dataset. Baseline scores are included for reference.	9
21	FID and Inception Score (Mean \pm Std Dev) for a single Conditional GAN generator ($N = 1$) trained on the Fashion MNIST dataset. Baseline scores are included for reference.	9

1 Introduction and Motivation

Generative Adversarial Networks (GANs) [GPAM⁺14] and their variants revolutionized the field of computer vision in the year of 2014, enabling advancements in multiple areas of generating data. From *Text to Image Synthesis* [RAY⁺16], *Image Translation* [IZZE18], *Super Resolution* [LTH⁺17], *Image Inpainting* [PKD⁺16], *Style Transfer* [WWR⁺23] to *Data Augmentation* [SK19], GANs have been used in a variety of applications.

The idea of using GANs for *Generative Data Augmentation* (GDA) has already been applied successfully, e.g.: in computer vision [JLR25], [BNI⁺23] or for creating music [JLY20]. Especially the former survey *A Comprehensive Survey of Image Generation Models Based on Deep Learning* has, along *Variational Auto Encoders* (VAEs), a dedicated focus on GANs. Despite these achievements, in practice, GANs suffer from several challenges, complicating the training and inference process:

- Mode Collapse
- Lack of inter-class Diversity
- Failure to Converge
- Vanishing Gradients & Unstable Gradients
- Imbalance between Generator- and Discriminator Model

This thesis investigates the potential of using GANs - specifically *Multi-Agent Diverse Generative Adversarial Networks* (MADGANs) [GKN⁺18] - for Generative Data Augmentation. MADGANs aim to aid the first two of the afore mentioned in particular: Mode Collapse and Loss of inter-class Diversity. They, along other modifications, "propose to modify the objective function of the discriminator, in which, along with finding the real and the fake samples, the discriminator also has to correctly predict the generator that generated the given fake sample." [GKN⁺18]. The goal of this adjustment of the discriminator is, that the discriminator has to push the generators towards distinct identifiable modes. While various strategies have been proposed to address mode collapse and inter-class diversity MADGANs explicitly enforce mode separation by introduction of multiple generators and the adjusted discriminator objective. This makes them particularly promising for GDA, as diverse samples and clear distinction of modes is crucial for training robust classifiers. In their paper, they experimentally show, that their architectural adjustment of GANs is generally capable of giving providing assistance for the first two of the mentioned problems.

The experiments in this work are structured into three major parts.

Set 1: Training and Analysis of GANs The first set trains and analyses GANs, explicitly MADGANs and *Conditional GANs* (cGANs). Here, the quality of the resulting images during training will be scored by the *Fréchet Inception Distance* (FID) [HRU⁺18] and the *Inception Score* (IS) [SGZ⁺16].

Set 2: Generating and Classifying Unlabeled Images The second set uses the afore trained generative models to create images. Images without labels—images originating from MADGANs—will be classified using auxiliary classifiers trained with traditional data augmentation techniques.

Set 3: Training and Evaluating Classifiers The third and most significant set of experiments trains classifiers using the generated data. For this, stratified classifiers with differing numbers of real and fake images are trained and evaluated on the respective validation set. Their classification performance will be assessed using standard metrics.¹

All of the above described is executed on the following datasets:

- MNIST [LCB10]
- Fashion MNIST [XRV17]
- CIFAR10 [Kri09]

Aim of the Thesis This thesis evaluates the effectiveness of Multi-Agent Diverse GANs for Generative Data Augmentation. First, the quality of their generated samples is compared to those produced by a Conditional GAN. Next, both sets of generated images are used to augment training datasets for classifiers, which are then assessed on their respective test sets. Classifiers trained on cGAN-augmented data and those trained with traditional augmentation techniques — such as flipping, rotation, and noise addition — serve as baselines for comparison. By doing so, this study examines the impact of MADGAN-based augmentation on classifier performance, highlighting its advantages and limitations relative to conventional methods and cGAN-based augmentation.

¹The set of metrics used to assess the quality of the resulting classifiers is defined in chapter Experiments Setup 4.

2 Related Work

The effectiveness of deep learning models is intrinsically linked to the availability of large and diverse datasets for training. Models with deep and complex architectures require extensive exposure to a wide range of data to learn underlying patterns and generalize well to unseen instances. Insufficient training data can lead to a phenomena called *overfitting*, where a model becomes too specialized to the training data, failing to perform accurately on previously unencountered data [Yin19].

To mitigate the problem of data scarcity and improve generalization capabilities of deep learning models, data augmentation techniques became indispensable. Data augmentation artificially expands the amounts and diversity of training datasets by creating modified versions of existing data or by generating entirely new instances.

Traditional Data Augmentation

Traditional data augmentation on images typically involves applying various transformations to existing data. For image based data, augmentations can take a variety of forms such as² : *Geometric Augmentation*, *Photometric Augmentation*, *Noise-Corruption Augmentation* 3.2.1.

The success of the above mentioned augmentation techniques is established in many papers [PW17], [KSH12a], [Yin19], [SK19], [WZZ⁺13].

Generative Data Augmentation using Deep Convolutional GANs

The basic GAN framework introduced by Goodfellow and colleagues offers a high degree of flexibility and can be adapted for specific augmentation tasks. It can be applied to generate music [DHYY17], speech [LMWN22], text [YZWY17], images [GPAM⁺14] or other instances of data, e.g. tabular data [XSCIV19].

Especially for image data, *Deep Convolutional GANs* (DCGANs) [RMC16] represent a significant advancement in applying GANs to image data augmentation [HFM22]. Their architecture specifically utilizes *Convolutional Neural Network* (CNNs) [LBD⁺89] in both, the generator and the discriminator. The use of CNNs allows DCGANs to learn hierarchical features from the input images and capture the spatial relationship and structure inherent in images. This leads to the generation of more realistic and coherent synthetic images. A study from Zhou et al. [ZCWD23] applied DCGANs, along their adjusted version of those on multiple dataset, including *Fashion MNIST* and *Cifar10*. With their experimental setup, they achieved consistent significant improvements over multiple datasets using the DCGAN-architecture, compared to their baseline.

²More categories of traditional data augmentation techniques exist, such as Occlusion-Based, Composition-Based, Domain-Specific or Adversarial Augmentation. For the purpose of this work, solely the aforementioned are discussed in greater detail.

Inherently in the vanilla version of GANs or the DCGANs realization of using convolutional layers, the generators role is solely to learn the underlying data distribution of the training samples and produce instances of close resemblance to instances from the training data. This however results in unlabeled samples, not to be beneficial to expand data for a supervised classification task.

Generative Data Augmentation using Conditional GANs

The introduction of *Conditional Generative Adversarial Networks* (cGANs) [MO14] allows to condition the generative process by additional information, such as class labels or other modalities. The conditioning acts on both the generator and the discriminator, which means that both models have access to the same conditional information. The generator combines the random vector input and the conditioning information into a joint hidden representation. The discriminator, on the other hand, evaluates the created data from generator, given context of the conditioning information, i.e. the class label passed. This approach enables the generator to create data that adheres to specific inputs, like creating specific digits from the MNIST dataset 1. Multiple papers were able to utilize the advantages of cGANs, to e.g. unify class distributions for a stratified classifier training or generatively increase the number of images and augmenting the training data[JPB22][ZCWD23][RCF25][WM21].

Generative Data Augmentation using MADGANs

Regardless of the mentioned successes using GANs (DCGANs or cGANs) for GDA 2, GANs in general have proven to be notoriously hard to train. "*Among them, mode collapse stands out as one of the most daunting ones.*" [DCLK20], which limits the GANs ability to generate diverse samples, able to be assigned to all classes trained on. Another prominent problem with GANs is the Lack of inter-class diversity between generated samples.

MADGANs [GKN⁺18] emphasis on diversity, achieved through its multi-agent architecture and the modified discriminator objective function, directly addresses these limitations. By encouraging multiple generators to specialize in different modes of the data distribution, MADGAN aims to generate a more comprehensive and diverse set of synthetic samples compared to traditional GANs and potentially other generative data augmentation techniques that might be susceptible to mode collapse. The ability of MADGAN to disentangle different modalities i.e. classes, as suggested by experiments involving diverse-class datasets, indicates its potential to generate augmented data that effectively covers both intra-class and inter-class variations. This comprehensive coverage is crucial for training robust image classifiers that can generalize well to a wide range of real-world scenarios.

3 Theoretical Background

This chapter serves as a reference for the theoretical background necessary to understand the insights gained in the following experimental chapters. Section 3.1 discusses classification models used to train on the extended dataset resulting from the generative augmentation process. In it, *Neural Networks* (NNs) for image classification are introduced and the baselines for later comparisons are examined. Sections 3.2 and 3.2.2 establish the foundation for data augmentation and generative data augmentation. Following sections 3.3, 3.4, 3.5, and 3.6 provide theoretical knowledge necessary to understand the GAN architectures and their differences. The narrative follows their increasing complexity, starting from vanilla GANs, moving through deep convolutional GANs and conditional GANs, before diving into the background of multi-agent diverse GANs. The final section (3.8) explains the theory behind the Inception Score and Fréchet Inception Distance, concluding with an examination of the state-of-the-art *InceptionV3* model used to compute them.

3.1 Image Classification Models

3.1.1 Neural Networks for Classification

Convolutional Neural Networks (CNNs) have become the dominant architecture for image classification tasks due to their inherent ability to automatically learn hierarchical features from raw pixel data. At their core, CNNs are build up by a sequence of convolutional-, pooling- and fully connected layers to extract hierarchical features, and funneling the information, typically into the N classes defined by the training data. Convolutional layers employ learnable filters to detect local patterns in the two-dimensional information - two dimensional in the case of images specifically. Pooling layers reduce the spatial dimensions to small translations. Fully connected layers then map the extracted information into class probabilities, utilizing the *Softmax* activation function. The afore mentioned layers are discussed in greater detail, in the following subsections.

Convolutional Layers TODO: here is a nice place for a ref to [DV18] These layers compute the output from the local regions of the input. Let $(r \times c)$ be the two-dimensional input, e.g., a grayscale image, where r represents the X-coordinate and c the Y-coordinate of a pixel. Thus, $r \cdot c$ denotes the size of the image. Furthermore, let $(a \times b)$ be a filter with kernel size $a \cdot b$, where the filter is smaller than the input. This filter is moved from the top-left to the bottom-right over the input.

In each iteration, the dot product between the respective coefficients of the input region and the coefficients of the filter is computed. This dot product is then processed by the activation function g , which determines how much of the feature is present. If

the activation function is ReLU, for example, only positive values are retained, meaning negative responses are set to zero. The result is written to the subsequent layer.

The stride determines how far the filter is moved after each operation. For a stride of $s = 1$, the filter can be placed in $(r - a + 1)$ positions along the height and $(c - b + 1)$ positions along the width, leading to an output size of $(r - a + 1) \times (c - b + 1)$. In general, the output size in the two-dimensional case is given by:

$$\left(\frac{r - a + s}{s} \right) \times \left(\frac{c - b + s}{s} \right).$$

An image of this process can be found in Figure X in the Appendix (7). This image shows an input of size $[10 \times 10]$ and a filter of size $[3 \times 3]$. With a stride of $s = 1$, the resulting layer has a size of $[8 \times 8]$ (computed as $(10 - 3 + 1) \times (10 - 3 + 1)$).

The stride of the filter can also be greater than 1. Additionally, there is the option to apply padding to the image. There are different ways to implement padding. When padding of size p is applied, the output size for a square input and filter is calculated as follows:

$$\text{Output size} = \left\lfloor \frac{r - a + 2p}{s} \right\rfloor + 1$$

where $\lfloor \cdot \rfloor$ denotes the floor function, which ensures that the output size is an integer.

Pooling Layers A pooling layer compresses the data along the spatial axes to reduce its dimensionality. Similar to the convolutional layer, a pooling layer uses a filter that moves by the stride value. However, instead of summing the covered elements, the pooling operation applies the Max operator, selecting the maximum value within the filter's region.

For example, starting with an input of size $[32 \times 32 \times 10]$, applying a pooling operation with a $[2 \times 2]$ filter and a stride of 2 results in an output size of $[16 \times 16 \times 10]$. This operation reduces the spatial dimensions by half while keeping the depth unchanged.

Max pooling helps retain the most important features, providing some invariance to small translations or distortions in the input, which is crucial for tasks like object recognition in convolutional neural networks (CNNs).

Fully-Connected Layers Fully-Connected (FC), also called *Dense* layer, typically computes the scores for the respective classes. In the case of ten classes, the result is a volume of size $[1 \times 1 \times 10]$ ³. By this stage, all spatial information has been transformed, leaving a quasi-one-dimensional vector containing the ten class scores for the CIFAR-10 dataset.

In a FC layer, each input is connected to each output, meaning every neuron in the

³Typically, the output from the layer before the FC one is "flattened" into a one-dimensional vector, preserving all information but removing spatial structure. For example, a $[2 \times 2]$ layer would become a vector of size $[1 \times 4]$.

previous layer is connected to each neuron in the FC layer. The output is the weighted sum of all inputs, followed by an activation function, leading to the final classification scores that represent the likelihood of the input belonging to each class. The spatial dimensions are collapsed into a single vector of class scores, which are then used for classification.

Batch Normalization Layers With their introduction in "*Batch Normalization: Accelerating Deep Network Training by Reducing Internal Covariate Shift*" by Ioffe et al. [IS15], Batch Normalization (batchnorm) is an integral part of convolutional networks. These layers normalize the inputs to subsequent layers and thereby stabilize the distribution of activations throughout the training process. This reduces the internal covariate shift, allowing for higher learning rates and faster convergence. By normalization of activation, batchnorm helps prevent gradients from vanishing or exploding. Additionally, it can provide regularization benefits and eliminate the need for Dropout, in some cases. With the aforementioned benefits, batchnorm layers are particularly beneficial for deep learning networks with many layers.

Typical Activation Functions for CNNs

- **ReLU (Rectified Linear Unit):**

$$g(x) = \max(0, x) \quad (1)$$

ReLU is the most widely used activation function in CNNs. It introduces non-linearity while maintaining efficiency by outputting zero for negative values and passing positive values unchanged.

- **Leaky ReLU:**

$$f(x) = \begin{cases} 0 & \text{if } x < 0 \\ x & \text{otherwise} \end{cases} \quad (2)$$

A variant of ReLU, Leaky ReLU allows small negative values to flow through, addressing the "dying ReLU" problem where neurons can become inactive.

- **Sigmoid (Logistic):**

$$g(x) = \frac{1}{1 + e^{-x}} \quad (3)$$

The sigmoid function squashes values between 0 and 1, commonly used for binary classification tasks. However, it can suffer from vanishing gradients for very large or small inputs.

- **Tanh (Hyperbolic Tangent):**

$$g(x) = \frac{2}{1 + e^{-2x}} - 1 \quad (4)$$

Tanh outputs values between -1 and 1 and is similar to the sigmoid but with a wider output range, making it more effective in many scenarios compared to sigmoid.

- **Softmax:**

$$g(x_i) = \frac{e^{x_i}}{\sum_j e^{x_j}} \quad (5)$$

Softmax is typically used in the output layer of CNNs for multi-class classification. It converts logits into probabilities, ensuring that the sum of the outputs is 1.

- **Cross-Entropy Loss:**

$$g(y, \hat{y}) = - \sum_i y_i \log(\hat{y}_i) \quad (6)$$

Cross-entropy is a common loss function for classification tasks. It measures the dissimilarity between the true label distribution y and the predicted probability distribution \hat{y} . Lower values indicate a better alignment between the predicted and true classes. For consistency, the cross-entropy function is denoted with g here, although it is more commonly represented in the literature as $H(y, \hat{y})$ or $H(p, q)$, where p refers to the true label distribution and q to the output of the discriminative model.

3.1.2 Classification Models for augmented Training

The classification models, on which the data augmentation is tested, are simple CNN classifiers consisting of the described layers. For each dataset MNIST, Fashion MNIST and CIFAR10 1, a dedicated classifier architecture is created. The main differences between these architectures is the number of blocks, made of two-dimensional convolutional, batchnorm and pooling layers. All three models use a use the ReLU function for activation of the convolutional layers and the Softmax function for the activation at their respective output layer, resulting in probability distribution over the space of classes. More on the specific model architectures and used metrics for evaluation can be found in chapter 4.1.

3.2 Data Augmentation

In this chapter, DA techiques in the context on images are discussed is greater detail. Starting with traditional augmentations e.g. rotating or cropping an image, ending on generative augmentations for which generative models are used to expand the training data of subsequent models.

3.2.1 Traditional Data Augmentation

The need for data augmentation to make classification algorithms more resilient has existed for decades. Early papers mentioning the augmentation of data for classification tasks date back to the 1970s [NS67]. For the context of deep learning, however, the augmentation of images was popularized by Krizhevsky et al. in 2012 [KSH12b], with the introduction of *AlexNet*—a deep CNN used to classify images from the *ImageNet* dataset [DDS⁺09], containing 1.000 classes. This paper also referenced the earlier work of Simard et al. from 2003 [SSP03].

Generally speaking, traditional data augmentation techniques can be described as enlarging the initial training data by applying transformations that preserve the respective labels of individual instances. These techniques solely focus on modifying already existing data without creating entirely new instances (see: 3.2.2). Augmentations are categorized based on the type of transformations applied:

Geometric Augmentation This category modifies the shape, position, and perspective: Rotation, Scaling, Flipping, Cropping, Shearing, Perspective Transform.

Photometric Augmentation Alters pixel values while keeping the spatial structure: Brightness, Contrast, Hue Shift, Blurring.

Noise-Corruption Augmentation Imitates real-world degradations and distortions caused by cameras and sensors: Gaussian Noise, Speckle Noise, Salt-and-Pepper Noise.

Mathematically, let X be an original data sample drawn from the dataset distribution $P(X)$. Traditional data augmentation applies a transformation function $f : X \mapsto \tilde{X}$, where f is a function sampled from a predefined set of augmentation operations \mathcal{F} . The augmented data sample \tilde{X} is then given by:

$$\tilde{X} = f(X), \quad f \sim \mathcal{F}.$$

Since TDA does not create entirely new data points but modifies existing ones, the distribution of augmented samples $P_{\tilde{X}}$ should ideally remain close to the original data distribution:

$$P_{\tilde{X}}(X) \approx P(X).$$

In the context of data augmentation pipelines, this can be generalized as:

$$\text{TDA} : (X, f) \mapsto \tilde{X}, \quad f \in \mathcal{F}.$$

When applying the augmentations shown in Figure 1, it is mandatory to consider domain-specific knowledge and constraints. For example, flipping images from the MNIST dataset to train a generative model may result in an image where a horizontally flipped "9" appears, which, in the domain of Arabic numerals, is semantically incorrect.

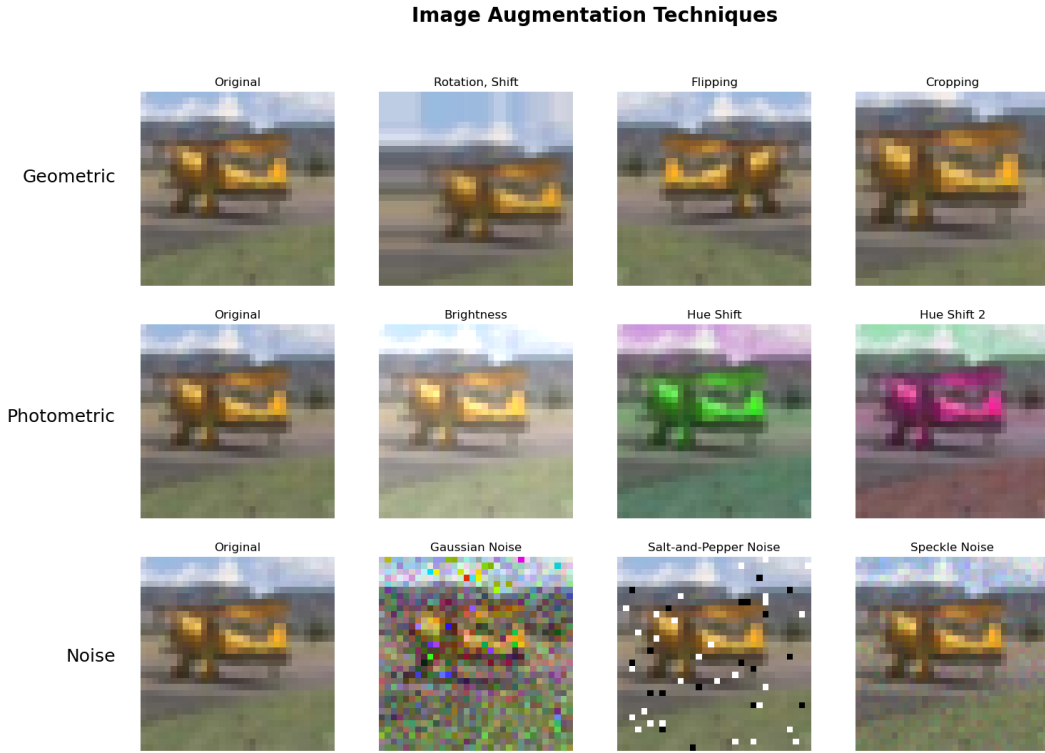


Figure 1: Exemplary use of traditional augmentation techniques from the categories *geometric* (first row), *photometric* (second row), and *noise-corruption* (third row). The image shown is an image from the CIFAR10 dataset, assigned to the class "airplane".

Conversely, when classifying an airplane, which can have varying shapes, colors, three-dimensional orientations in space, and images taken through a dusted lens, applying all of the above augmentations could be beneficial.

3.2.2 Generative Data Augmentation

Differing from the previously mentioned TDA 3.2.1, GDA does not focus on altering existing data instances but rather on creating entirely new samples that match the underlying data distribution of the training data. These generated instances may or may not include labels.

The goal is to train a generative model G that produces instances X_1 , for example, from a noise vector z , such that the distribution of the generated data approximates the true distribution $P(X)$ of the original dataset. In this context, G can be viewed as a function:

$$G : z \mapsto X_1, \quad X_1 \sim P_G(X) \approx P(X),$$

where $P_G(X)$ is the learned distribution of the generative model, aiming to approximate the real data distribution $P(X)$.

In the case of *conditional* generative data augmentation, additional information such

as class labels y is incorporated into the generation process. This allows the model to generate samples corresponding to specific categories within the data. The conditional generative model G then follows:

$$G : (z, y) \mapsto X_1, \quad X_1 \sim P_G(X | y) \approx P(X | y),$$

where $P_G(X | y)$ represents the learned conditional distribution, aiming to approximate the real class-conditioned data distribution $P(X | y)$. This enables targeted data generation for specific categories, enhancing data diversity while maintaining class consistency.

3.3 Generative Adversarial Network

Generative Adversarial Network (GANs) have first been introduced by Goodfellow et al. in 2014 [GPAM⁺14]. GANs are a type of generative models designed to learn the underlying data distribution of their training data and generate new, realistic instances. The core idea of the framework is an adversarial training process between two NNs: the generator G and the *Discriminator* D , competing against one another in a minimax game [Neu28]. The following figure (2) shows a visualization of the vanilla gan architecture.

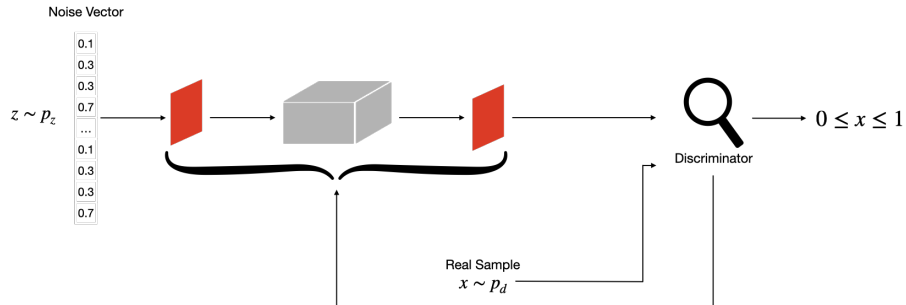


Figure 2: Visualization of the vanilla GAN architecture. The figure shows the noise vector, flowing into the discriminator, as well as the real sample from P_d

3.3.1 Mathematical Formulation

Let $X \sim P_{data}$ be samples drawn from the real data distribution, and let $z \sim P_z$ be random noise sampled from a known prior (e.g., a Gaussian or uniform distribution). The generator G is a function $G : \mathbb{R}^d \rightarrow \mathbb{R}^n$ that maps a noise vector z to a synthetic data instance \tilde{X} , attempting to approximate $P_{data} : \tilde{X} = G(z), \quad z \sim P_z$.

The discriminator D is a function $D : \mathbb{R}^n \rightarrow [0, 1]$ that outputs the probability that a given sample is real rather than generated. It is trained to distinguish between real samples $X \sim P_{data}$ and generated samples $\tilde{X} \sim P_G$, where P_G is the implicit distribution induced by G .

The training objective is formulated as the following minimax game:

$$\mathcal{L}_{adv} = \min_G \max_D \mathbb{E}_{X \sim P_{data}} [\log D(X)] + \mathbb{E}_{z \sim P_z} [\log(1 - D(G(z)))] \quad (7)$$

Here, the discriminator D aims to maximize the probability of correctly classifying real and fake samples \hat{x} , while the generator G aims to generate samples that fool D , minimizing $\log(1 - D(G(z)))$. In an ideal scenario, the game converges to a Nash equilibrium where G produces samples indistinguishable from real data, i.e., $P_G \approx P_{data}$.

3.3.2 Training Process

GAN training follows an alternating optimization approach:

1. Update D : Given a batch of real samples from P_{data} and fake samples generated by G , update D to maximize its ability to discriminate real from fake data.
2. Update G : Generate new fake samples and update G to minimize $\log(1 - D(G(z)))$, effectively pushing G to generate more realistic samples.
3. Repeat the process iteratively, typically using stochastic gradient descent (SGD) or Adam optimization.

3.3.3 Challenges in GAN Training

Following, challenges that can occur during the training of gans are discussed. These have already been mentioned in the introductory section 1. Here, they are described in greater detail.

Mode Collapse Mode collapse occurs when the generator produces only a small subset of the data distribution, leading to a lack of diversity. Instead of generating varied samples, it repeatedly produces similar ones that fool the discriminator. This happens when the generator finds an easy "shortcut" rather than learning the full distribution. More formally, G collapses many values of z to the same value of x [GPAM⁺14]. A common technique to mitigate this issue is minibatch discrimination [SGZ⁺16]. In several studies, experiments have been conducted to enhance diversity of GANs ([CFB⁺24], [HBB21], [HBB22])

Lack of Inter-Class Diversity Even if mode collapse is avoided, GANs may struggle to generate samples that represent all data classes equally. This is a common issue in class-conditional GANs, where samples across different classes may overlap or lack distinct features. Causes include imbalanced datasets, poor class conditioning, or weak discriminator feedback [OOS17].

Failure to Converge Unlike traditional neural networks, GANs follow an adversarial training process, making optimization highly unstable. The loss functions of both the generator and discriminator change dynamically, often leading to non-convergent behavior. Methods like Wasserstein GANs (WGAN) [ACB17] and spectral normalization [MKKY18] improve stability and help achieve better convergence.

Vanishing & unstable Gradients When the discriminator becomes too strong, it perfectly distinguishes real from fake samples, leading to vanishing gradients for the generator. This prevents meaningful updates, stalling progress. On the other hand, unstable gradients cause erratic updates, preventing smooth learning. Alternative loss functions (e.g., LSGANs [MLX⁺17]) and spectral normalization help stabilize training.

Imbalance between Generator and Discriminator A well-balanced GAN requires both models to improve at a similar pace. If the discriminator overpowers the generator, training halts. If it's too weak, the generator receives poor feedback and produces low-quality outputs [GPAM⁺14]. Balancing techniques include adaptive learning rates, gradient penalties, and label smoothing [RMC16].

3.4 Deep Convolutional Generative Adversarial Network

Deep Convolutional Generative Adversarial Networks (DCGANs) were introduced by Radford et al. in 2015 [RMC16] as an improvement over vanilla GANs. While the fundamental adversarial framework remains the same (see 3.3 Mathematical Formulation, 3.3 Training Procecss), DCGANs leverage deep convolutional neural networks to enhance stability and generate higher-quality images.

3.4.1 Architectural Adjustments

To improve training stability and image quality, DCGANs implement the use of convolutional layers.

- **Convolutional Architecture:** Fully connected layers in both G and D are replaced with deep convolutional layers, enabling better spatial feature extraction.
- **Strided Convolutions:** In the discriminator, pooling layers are removed in favor of strided convolutions, reducing the risk of information loss.

- **Transposed Convolutions:** The generator employs transposed convolutions (also known as fractionally-strided convolutions) instead of upsampling layers to improve the quality of generated images.
- **Batch Normalization:** Applied to both G and D , batchnorm helps stabilize training by reducing internal covariate shift 3.1.1. Batchnorm is omitted in the generator’s final layer to allow unrestricted output variability and in the discriminator’s input layer to preserve the original data distribution.
- **LeakyReLU Activation:** The discriminator uses LeakyReLU instead of standard ReLU to prevent dying neurons and allow gradients to flow through negative inputs 3.1.1.
- **No Fully Connected Layers:** Fully connected layers are removed to maintain spatial coherence in generated images, as they discard spatial information by flattening feature maps. Instead, convolutional layers preserve local structures, enabling more realistic image synthesis 3.1.1.

3.5 Conditional Generative Adversarial Network

Conditional Generative Adversarial Networks (cGANs), introduced by Mirza and Osindero in 2014 [MO14], extend the vanilla GAN framework by incorporating additional information y , such as class labels, into both the generator and discriminator. This allows cGANs to generate samples conditioned on specific attributes, enabling controlled generation.

3.5.1 Mathematical Formulation

The core idea of cGANs is to condition both the generator G and the discriminator D on auxiliary information y . Instead of generating data solely from a noise vector z , the generator now takes y as an additional input:

$$\tilde{X} = G(z, y) \quad (8)$$

Similarly, the discriminator receives both the real or generated sample and the corresponding condition:

$$D(X, y) \quad \text{and} \quad D(G(z, y), y) \quad (9)$$

The adversarial objective function for cGANs extends the standard GAN loss to incorporate this conditional dependency:

$$\mathcal{L}_{\text{adv}} = \min_G \max_D \mathbb{E}_{X, y \sim P_{\text{data}}} [\log D(X, y)] + \mathbb{E}_{z \sim P_z, y \sim P_y} [\log(1 - D(G(z, y), y))] \quad (10)$$

This formulation forces to generate samples that align with the given condition , while learns to discriminate between real and generated samples, considering their respective conditions.

3.5.2 Architectural Adjustments

To implement cGANs, architectural adjustments are necessary compared to vanilla GANs:

- **Input Conditioning:** Both the generator and discriminator must receive the conditional information y as input. This is typically achieved by concatenating the condition y with the noise vector z in the generator’s input and with the input image X in the discriminator’s input.
- **Embedding Conditional Information:** For categorical conditions (e.g., class labels), the condition y is often embedded into a lower-dimensional vector before concatenation. This embedding allows the network to learn meaningful representations of the conditions.
- **Concatenation, Addition, or Multiplication:** The conditional information can be incorporated through concatenation, addition, or element-wise multiplication at various layers within the generator and discriminator, depending on the specific application and architecture.
- **Preservation of Conditional Information:** Care must be taken, that the conditional information is preserved throughout the network. This means, that the information must traverse the network, all the way to the output layer.

These architectural modifications ensure that the generator and discriminator can effectively utilize the conditional information to generate and discriminate samples based on the given conditions.

3.6 Multi-Agent Diverse Generative Adversarial Network

MADGAN is proposed as a generalized framework for the GAN architecture [GKN⁺18]. The framework employs multiple generators, one discriminator and an adjusted objective for the discriminator. The adjusted objective aims to enforce the identifications of the generator creating given fake images $G_i\hat{x}$. These changes specifically aim to ease the first two mentioned problems of GANs, namely *Mode Collapse* and *Lack of Inter-Class Diversity* 3.3.3. This chapter delves into the specifics of this framework: integration of multi-agent systems with diversity-promoting techniques, within the GAN framework. The following subsections will detail the architecture, objective function, and training procedure of the MADGAN framework.

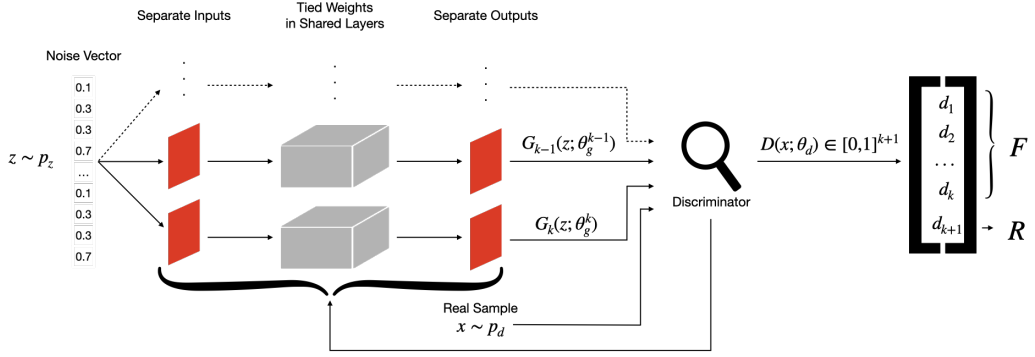


Figure 3: Visualization of the MADGAN architecture. The figure shows the $k + 1$ outputs of the discriminator and the k generators, with tied weights in the middle of the network.

3.6.1 Mathematical Formulation

As afore mentioned, the MADGAN architecture employs multiple generators and one discriminator. The goal the for K generators is to generate samples from different high probability regions of the data P_{data} . In order to guide the generators into their respective direction, the objective of the discriminator has been modified, in which it no longer has to just differentiate between real and fake images, but also identify the generator that produced a given fake instance. Intuitively, the discriminator thereby forces the generators into mostly disjoint regions within the real data distribution. Inspired by the formulation for the discriminator in the paper "*Improved Techniques for Training GANs*" [SGZ⁺16], their discriminator model has an output of $k + 1$, utilizing the *Softmax* activation function 3.1.1, where k sets the number of used generators. The output at $k + 1$ represents the probability that the given samples belongs to the real data distribution P_{data} , whereas the scores at $j \in \{1, \dots, k\}$ describe the probability of said sample originating from either of the generators. The above figure 3 shows a visualization of the architecture. Thus, when learning the discriminators parameters θ_d , the cross-entropy between the softmax outputs and the *Dirac delta distribution* (Ddd) $\delta \in \{0, 1\}^{k+1}$ is optimized. Here, $\delta(j) = 1$ if the sample belongs to the j -th generator, else $\delta(k + 1) = 1$ if the sample originates from P_{data} . Following this definition, the Ddd δ can be understood as a one-hot encoding indicating whether a given sample is real or, and if not, from which generator it originates⁴. The objective function for the optimization of θ_d , with θ_g freezed is therefore:

$$\max_{\theta_d} \mathbb{E}_{x \sim p} H(\delta, D(x; \theta_d)) \quad (11)$$

⁴It is important to point out, that the Dirac delta distribution is actually continuous. Their usage of the Ddd reminds of the Kronecker delta function, which $\delta(i, j) = 1$ for $i = j$; 0 for $i \neq j$.

$H(\dots)$ here represents the negative cross-entropy function. Important to point out here is that, "Intuitively, in order to correctly identify the generator that produced a given fake sample, the discriminator must learn to push different generators towards different identifiable modes." [GKN⁺18], page 4. Figure 2 shows a visualization of the generators being pushed to different modes. The objective for the generators however, remains semantically the same as in the vanilla GAN 7. The difference here is that the objective function is generalized with an indexing i for the number of generators. That is, for the i -th generator, the objective function is to minimize:

$$\mathcal{L}_{Gen_i} = \mathbf{E}_{x \sim P_{data}} [\log D(X; \theta_d)] + \mathbf{E}_{z \sim P_z} \log(1 - D_{k+1}(G_i(z; \theta_g^i); \theta_x)) \quad (12)$$

Enforcing Diverse Modes: The researchers provide a theorem demonstrating that the k generators collectively form a mixture model. In it, each generator represents a mixture component to the global optimum of $-(k+1) \log(k+1) + 1 \log k$. This is achieved, when $p_{data} = \frac{1}{k} \sum_{i=1}^k p_{g_i}$. It is to point out that, for $k = 1$, the case with one generator, one obtains the exact Jensen-Shannon divergence based objective, as shown in the vanilla GAN paper by Goodfellow et al. [GPAM⁺14]. Following their proof, the objective function for all k generators is to minimize:

$$\mathcal{L}_{Gen_{[0 \dots K]}} = \mathbf{E}_{x \sim P_{data}} [\log D_{k+1}(X)] + \sum_{i=1}^k \mathbf{E}_{x \sim p_{g_i}} \log(1 - D_{k+1}(x)) \quad (13)$$

The exact formulation of their theorem, proof and propositions can be found in Ghosh et al. [GKN⁺18], following formulas (3) through (9).

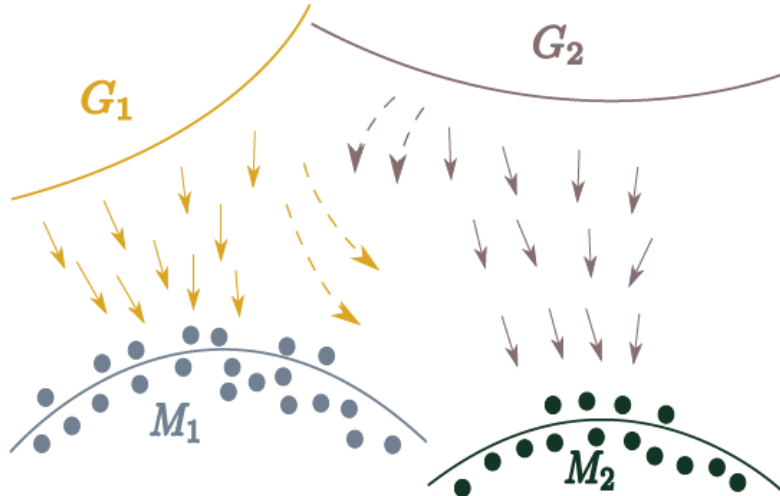


Figure 4: Figure taken from the original paper [GKN⁺18]. The visualization shows how different generators G_1 and G_2 are pushed to different modes M_1 and M_2

3.6.2 Architectural Adjustments

The architecture changes can be summarized into three major changes applied to the vanilla GAN (3.3) architecture:

Multiple Generators: The MADGAN architecture employs multiple generators instead of a single one. Following the intuition behind the adjusted discriminator objective, the respective gans distribute into different, mostly disjoint regions in the real data distribution.

Modified Discriminator Objective: The discriminator in this architecture outputs $k + 1$ instead of 1 utilizing the softmax function 3.1.1. One output for every generator indicating whether an image originates from either one of the generator and one output implying if the discriminator came to the conclusion that the current image is fake or not. As afore described, this encourages the discriminator to push the generators into identifiable distinct outputs.

Parameter Sharing among Generators: Generators in the MADGAN architecture share most of their layers between the k generators. This reduces redundant compute in the initial feature extraction layers capturing high-frequency structures common in many datasets. Especially in single-view data, this is recommended. For multi-view data it is not recommended, to allow each generator to capture mode-specific features.

3.7 Adapting MAD-GAN for Conditional Generation with Explicit Diversity

The initial goal of this research included exploring methods for generating diverse samples in the mentioned datasets 1 to be used for data augmentations. While the multi-agent framework by Ghosh presents a potential approach, experiments revealed significant challenges in achieving stable training and satisfactory results in terms of image quality with the original method. Specifically the CIFAR10 datasets proved to be challenging, which is the only colored dataset used.

Consequently, an alternative framework, termed Conditional Multi-Agent Diverse GAN (cMADGAN), was conceptualized. The adjustment aims to retain the multi-generator diversity principle while simplifying the task of the discriminator. The discriminator model is rolled back to its original objective to differentiate between real and fake images. However, initial experiments indicated that this approach also faced convergence difficulties when applied to the original CIFAR10 dataset. This specific is explained in more detail in the experiments section *todo: reference the correct chapter*

The following sections detail the cMADGAN framework as implemented. This approach utilizes multiple generators (G_1, \dots, G_K), a single conditional discriminator (D) performing standard real/fake classification, and incorporates an explicit diversity loss between generator outputs alongside the adversarial objective.

3.7.1 Mathematical Formulation

Let z be a latent vector sampled from a prior distribution $p(z)$, typically a standard normal distribution. Let c be the condition variable (e.g., class label) sampled from a distribution $p(c)$. The framework also employs K generator networks G_1, \dots, G_K and a single discriminator network D . Each generator G_i maps an input pair (z, c) to the data space, producing a fake sample $\hat{x}_i = G_i(z, c)$. The discriminator D takes an input pair (x, c) (where x can be a real sample from the true data distribution $p_{\text{data}}(x|c)$ or a fake sample \hat{x}_i) and outputs a scalar probability estimating the likelihood that x is real given the condition c .

The training involves optimizing two competing objectives, \mathcal{L}_D for the discriminator and \mathcal{L}_G for the generators:

Discriminator Loss: The discriminator is trained to distinguish real samples from fake samples generated by *any* of the K generators, given the condition c . Using the binary cross-entropy (BCE) loss, the objective is:

$$\begin{aligned} \mathcal{L}_D = & -\mathbb{E}_{x \sim p_{\text{data}}(x|c), c \sim p(c)}[\log D(x, c)] \\ & - \frac{1}{K} \sum_{i=1}^K \mathbb{E}_{z \sim p(z), c \sim p(c)}[\log(1 - D(G_i(z, c), c))] \end{aligned} \quad (14)$$

In practice, techniques like label smoothing might be applied to stabilize training. In its current implementation, it is set to 0.9 for real and 0.1 for fake samples.

Generator Loss: The generators are trained collectively to fool the discriminator and simultaneously produce diverse outputs. The combined loss function includes an adversarial term and an explicit diversity term:

$$\mathcal{L}_G = \mathcal{L}_{\text{adv}} - \lambda_{\text{div}} \mathcal{L}_{\text{sim}} \quad (15)$$

where λ_{div} is a hyperparameter controlling the weight of the diversity component.

The components are defined as:

- **Adversarial Loss (\mathcal{L}_{adv}):** Encourages generators to produce samples that the discriminator classifies as real. The non-saturating formulation based on maximizing the probability of fake samples being classified as real is commonly used:

$$\mathcal{L}_{\text{adv}} = -\frac{1}{K} \sum_{i=1}^K \mathbb{E}_{z \sim p(z), c \sim p(c)}[\log D(G_i(z, c), c)] \quad (16)$$

- **Similarity Loss (\mathcal{L}_{sim}):** This term quantifies the similarity between outputs of different generator pairs for the same input (z, c) . The goal during optimization ($\min \mathcal{L}_G$) is to maximize diversity, which corresponds to minimizing the similarity

term \mathcal{L}_{sim} when $\lambda_{\text{div}} > 0$ due to the negative sign in Eq. 15. Cosine similarity between the flattened outputs is used:

$$\text{CosSim}(a, b) = \frac{\text{vec}(a) \cdot \text{vec}(b)}{\|\text{vec}(a)\|_2 \|\text{vec}(b)\|_2} \quad (17)$$

where $\text{vec}(\cdot)$ denotes flattening the image tensor into a vector. The similarity loss is the average pairwise cosine similarity:

$$\mathcal{L}_{\text{sim}} = \frac{1}{N_p} \sum_{i=1}^K \sum_{j=i+1}^K \mathbb{E}_{z \sim p(z), c \sim p(c)} [\text{CosSim}(G_i(z, c), G_j(z, c))] \quad (18)$$

where $N_p = K(K - 1)/2$ is the number of unique generator pairs. Minimizing the combined \mathcal{L}_G in Eq. 15 thus encourages fooling the discriminator (minimizing \mathcal{L}_{adv}) while discouraging similarity between generator outputs (by minimizing $-\mathcal{L}_{\text{sim}}$).

3.7.2 Architectural Adjustments

The CMADGAN architecture makes specific adjustments compared to both standard conditional GANs and the original MAD-GAN:

- **Multiple Generators:** As the original MADGAN framework proposed, the cMADGAN employs K distinct generator networks. As suggested in the original paper, the generators do not share their weights, due to the selection of datasets (cf. section 4.1 [GKN⁺18]). Each generator takes both the latent vector z and the condition c as input.
- **Conditional Discriminator:** Unlike the original MADGAN discriminator, the task of the cMADGAN discriminator performs the standard conditional GAN task 3.5.2. D receives an image x (real or fake) and its corresponding condition c , and outputs a single probability indicating whether the image is real given the condition.
- **Conditioning Mechanism:** Class conditioning c is integrated into both generator and discriminator networks. There are multiple different ways to encode information 3.5.2.
 - In the generators, this embedding is concatenated with the latent vector z before being processed by the main network layers (e.g., transposed convolutions).
 - In the discriminator, the condition embedding might be concatenated with intermediate feature maps or projected via learned linear layers and combined with image features before the final classification output, following common practices for conditional discriminators [MO14].

- **Explicit Diversity Enforcement:** Diversity is not solely an emergent property of competition but is explicitly encouraged via the \mathcal{L}_{sim} term in the generator objective (Eq. 15), directly penalizing high similarity between the outputs of different generators for the same input (z, c).

The specific convolutional layers, normalization techniques, and activation functions within the generator and discriminator networks follow standard deep convolutional GAN (DCGAN) [RMC16] principles or other relevant architectural patterns suitable, as detailed in the experimental setup section (*TODO: Cross-reference experiments section here*). This cMADGAN structure provides a framework for conditional generation that leverages multiple generators for diversity.

3.8 Image Scores

To quantitatively evaluate the quality and diversity of images generated by generative models, several metrics have been proposed in the literature. These image scores aim to provide an objective measure to compare generative models independently of human evaluation. This section introduces widely-used metrics for evaluating generative models: *Inception Score* (IS), *Fréchet Inception Distance* (FID), and the underlying InceptionV3 model employed for these metrics.q

3.8.1 Inception Score

The Inception Score (IS) [SGZ⁺16] is one of the earliest and most commonly used metrics for evaluating generative models, especially GANs. It leverages a pretrained InceptionV3 classifier to assess two main criteria of generated images:

- **Image Quality (Clarity):** Each generated image should be classified into a specific class with high confidence. This corresponds to a low-entropy conditional label distribution $p(y|x)$.
- **Diversity:** Across the entire set of generated images, the distribution of predicted classes should be diverse and cover many different labels. This corresponds to a high-entropy marginal label distribution $p(y)$.

Mathematically, the Inception Score is computed over a set of generated images x drawn from the generator’s distribution p_g :

$$IS = \exp \left(\mathbb{E}_{x \sim p_g} [D_{\text{KL}}(p(y|x) \| p(y))] \right) \quad (19)$$

where D_{KL} denotes the Kullback-Leibler divergence between the conditional class distribution $p(y|x)$ for a specific image x and the marginal class distribution $p(y)$ estimated over all generated images.

Interpretation: A higher IS indicates that the model generates images that are confidently classified into diverse classes.

Limitations of IS:

- Does not directly compare generated images with real images.
- Insensitive to intra-class diversity (e.g., generating only one type of dog within the 'dog' class).
- Sensitive to the choice and specific training of the pretrained classifier.

3.8.2 Fréchet Inception Distance

The Fréchet Inception Distance (FID) [HRU⁺18] improves upon IS by directly comparing the feature distributions of real and generated images. FID embeds both real (r) and generated (g) images into a lower-dimensional feature space using a pretrained InceptionV3 network (typically using the activations from the final average pooling layer, often referred to as 'pool3'). It then models the distributions of these embeddings as multivariate Gaussians.

Let (μ_r, Σ_r) and (μ_g, Σ_g) denote the means and covariance matrices of the real and generated image Inception feature embeddings, respectively. The FID score is computed as the Fréchet distance (also known as Wasserstein-2 distance) between these two Gaussian distributions:

$$FID = \|\mu_r - \mu_g\|_2^2 + \text{Tr}(\Sigma_r + \Sigma_g - 2(\Sigma_r \Sigma_g)^{1/2}) \quad (20)$$

where $\|\cdot\|_2^2$ is the squared Euclidean norm, $\text{Tr}(\cdot)$ is the trace of a matrix, and $(\Sigma_r \Sigma_g)^{1/2}$ is the matrix square root of the product of the covariance matrices.

Interpretation: Lower FID indicates that the distribution of generated image features is more similar to the distribution of real image features, suggesting better quality and diversity. A score of 0 indicates identical distributions.

Advantages over IS:

- Directly compares the generated image distribution to the real image distribution.
- More sensitive to intra-class mode collapse (lack of diversity within classes) as this affects Σ_g .
- Generally found to correlate better with human judgment of image quality than IS.

Limitations:

- Assumes Gaussian distribution of features, which might be an approximation.

- Sensitive to the choice of feature extractor network and the specific layer used.
- Sensitive to both image quality (affecting feature representations) and diversity (affecting the mean and covariance of features).
- Requires a sufficiently large number of samples (both real and generated) for stable estimation of moments (μ, Σ).

3.8.3 InceptionV3 for Image Evaluation

Both IS and FID commonly rely on the InceptionV3 model [SVI⁺16], a deep convolutional neural network pretrained on the large-scale ImageNet dataset [DDS⁺09]. The InceptionV3 network serves two primary roles in evaluating generative models:

1. **Feature Extractor (for FID):** Intermediate activations, typically from the final average pooling layer ('pool3'), are used as a semantic feature representation of the images. The statistics (mean and covariance) of these features are then compared between real and generated image sets.
2. **Classifier (for IS):** The output layer provides class probabilities for input images. These probabilities are used to calculate the entropy terms required for the Inception Score.

Properties of InceptionV3 relevant for image scoring:

- Trained on the diverse ImageNet dataset, providing a rich semantic feature space capable of capturing complex visual patterns.
- Uses fixed, non-trainable weights during evaluation, ensuring standardization and comparability of scores across different studies (provided the same implementation is used).
- The choice of layer for feature extraction (primarily for FID) impacts sensitivity; earlier layers capture lower-level features like texture, while later layers capture more abstract semantic information. The 'pool3' layer is commonly chosen as a balance.

Limitations of using InceptionV3:

- Domain Gap: The features learned on ImageNet (mostly natural images centered on objects) might not be optimally suited for evaluating images from significantly different domains, such as medical scans, satellite imagery, or abstract art.
- Sensitivity to ImageNet Classes: Performance, particularly for IS, can be less meaningful if the generated images depict objects or scenes vastly different from the 1,000 ImageNet classes.

- Potential Bias: Potential biases present within the ImageNet dataset itself (e.g., representation bias) may be inherited by the features, potentially impacting evaluation fairness or relevance for specific target domains.

4 Experiments Setup

4.1 Preliminary Remarks

Before presenting the specific experiments and corresponding results in Chapter 5, this section outlines essential preliminary remarks. These remarks cover common configurations, definitions, and methodological aspects that apply across the subsequent experimental evaluations, providing necessary context and avoiding repetition later.

4.1.1 Scope Limitation Regarding Standard CIFAR-10

The CIFAR-10 dataset, with its 32x32 pixel color images across 10 classes, represents a significant step up in complexity compared to MNIST or Fashion-MNIST and is a common benchmark in generative modeling. Consequently, initial plans involved evaluating the performance of multi-generator GAN approaches, including the original MAD-GAN [GKN⁺18] and the adapted cMADGAN (Section 3.7), on this standard dataset.

However, preliminary investigations encountered substantial difficulties in achieving stable training and generating samples of sufficient quality and diversity using these frameworks directly on standard CIFAR-10. Extensive efforts were undertaken to address these challenges, spanning a range of common techniques and modifications found in GAN literature. These included, but were not limited to:

- Testing multiple generator and discriminator architectures with varying depths and capacities.
- Experimenting with different normalization layers (e.g., Batch Normalization, Spectral Normalization).
- Adjusting hyperparameters related to the Adam optimizer, particularly the learning rates for the generator(s) and discriminator, including various decay schedules and relative magnitudes.
- Implementing techniques designed to combat mode collapse and improve sample diversity, such as Mini-batch Discrimination.
- Tuning framework-specific hyperparameters like the latent dimension size and the diversity weight (λ_{div}) for cMADGAN.
- Employing standard stabilization methods like label smoothing.

Despite these comprehensive attempts, persistent issues such as training instabilities (e.g., oscillating losses, vanishing or exploding gradients) or consistently poor quantitative results (e.g., low IS, high FID relative to benchmarks or simpler datasets) indicated

that the models did not converge to a satisfactory performance level on the standard CIFAR-10 dataset within the practical constraints of this study.

Given that the primary focus of this thesis is to investigate the comparative effects of different GAN-based data augmentation strategies (including MADGAN and cMADGAN), a pragmatic decision was made to exclude the standard CIFAR-10 dataset from the main comparative experiments presented in the subsequent results chapters. This allows the analysis to focus on datasets (MNIST, Fashion-MNIST, and modified CIFAR-10) where the generative models achieved more stable and interpretable performance, enabling a clearer evaluation of the core research questions related to data augmentation effectiveness. The challenges encountered with standard CIFAR-10, while informative about the limitations of these specific multi-generator approaches on more complex data, are not subjected to further detailed analysis herein.

4.1.2 Datasets

Table 1: Summary of commonly used benchmark datasets for image classification.

Dataset	Samples	Image Size	
MNIST 70.000	28×28	1	Contains grayscale images of handwritten
Fashion- MNIST 70.000	28×28	1	Drop-in replacement for MNIST with grayscale images o

4.1.3 GAN: Architecture, Training and Data Augmentation

Architecture of the GANs In all experiments involving GAN models and their derivatives, the same network architecture has been employed for the *MNIST* and *Fashion MNIST* datasets. For initial experiments targeting the standard *CIFAR-10* dataset (32, 32, 3), deeper architectures were utilized for both the generator and discriminator networks to account for the increased complexity of the data. However, for a specific set of experiments detailed in Section [todo: reference the correct section], where the CIFAR-10 dataset was modified (28, 28, 1) to facilitate analysis, architectures comparable to those used for MNIST/Fashion MNIST were employed. These proofed to result in mostly stable training. The specific architecture relevant to each experiment will be reiterated in its respective section.

Training For training all GAN-based models, including DCGAN, cGAN, MADGAN and cMADGAN, the *Adam* optimizer has been utilized. The learning rate follows an exponentially decaying schedule throughout the training process.

Data Augmentation To increase the diversity of the training data for both generator and discriminator models, several traditional augmentation techniques have been

applied. These include horizontal flips, brightness and contrast adjustments, and the addition of Gaussian noise. Horizontal flips are applied with a probability of 50%, except for the *MNIST* dataset, where flips are omitted due to the semantic relevance of digit orientation. Brightness and contrast adjustments are always applied within a uniform range of $[-0.1, 0.1]$. Gaussian noise is added by sampling from a normal distribution with mean 0 and standard deviation 0.05. Finally, the augmented images are clipped to the valid value range of $[-1, 1]$.

4.1.4 Stratified Classifiers as measure for augmentation Quality

To definitively evaluate the quality of the GDA, the fake images are used to replace and expand the underlying original datasets and train classification models on them. For this, the training datasets are specifically crafted to contain different ratios of real to fake images. To avoid biasing one class in the datasets over another, the datasets are stratified with respect to the number of samples per class.⁵

4.1.5 Labeling unconditioned data

Due to the fact, that multiple experiments using unconditioned GANs were executed (5.1), many images have been created with no corresponding label to them. To classify the unlabeled data, simple CNN classifiers, with adequate TDA, were utilized. The applied augmentations techniques are as follows: horizontal- and vertical shift by 0.1 relative to the absolute size of the image, rotation of up to 15 degree and vertical flipping. As aforementioned, flipping images along the vertical axes is omitted for the *MNIST* dataset, due to semantical invalidity. Graphical depictions of the classifiers used can be found in the appendix (8.1.1). The auxiliary classifiers were optimized for their Accuracy on the held-out test set of the respective dataset.

4.1.6 Utilization of InceptionV3 for FID and IS

It is crucial to note that the significant differences between the ImageNet domain (high-resolution, color, 1000 object classes) and datasets commonly used in GAN research like *MNIST*, *Fashion-MNIST* (low-resolution, grayscale), or *CIFAR-10* (low-resolution, color, 10 simpler classes) represent a substantial domain gap 3.8.3. This gap may limit the effectiveness or absolute interpretability of InceptionV3-based scores for these specific datasets. Furthermore, due to the sensitivity of these scores to implementation details (e.g., image resizing methods, specific InceptionV3 weight versions), a direct comparison of scores calculated here to those from external literature is generally unreliable unless the evaluation methodology is verified to be identical. Therefore, within

⁵Out of the used datasets, only the *MNIST* dataset is not originally stratified.

this thesis, IS and FID scores are primarily utilized for relative comparisons between the different models and experiments conducted herein, rather than for absolute benchmarking against potentially disparate external results. This context warrants careful consideration when analyzing the experimental outcomes presented later.

4.2 Experimental Workflow

The evaluation of each generative model adhered to a consistent experimental workflow, outlined below:

1. **GAN Training:** The specific generative model (e.g., DCGAN, cGAN, MADGAN, cMADGAN) was trained on the target dataset. Model performance during training was monitored using predefined metrics such as FID and IS.
2. **Synthetic Sample Generation (Per Generator):** After training, the individual generators $G_i / G_{i,j}$ within the trained model (where $i = 1$ for single-generator models like DCGAN/cGAN, and $i = 1 \dots K, j = 0 \dots (K - 1)$ for multi-generator models MADGAN/cMADGAN with $K \in \{3, 5, 7, 10\}$) are used to create a distinct set of synthetic images, denoted as $S_{\text{fake},i}$. For each class in the original dataset, at least 6.000 images were generated by each generator G_i , resulting in K separate datasets of synthetic samples for each trained multi-generator model.
 - *Labeling Unconditional Samples:* For samples generated by unconditional models or generators (DCGAN, MADGAN generators), class labels were assigned to the images within each respective set $S_{\text{fake},i}$ using the pre-trained classifiers detailed in Section 4.1.5.
3. **Downstream Classifier Training (GDA Evaluation - Per Generator):** The effectiveness of Generative Data Augmentation (GDA) was evaluated separately for each generator $G_i / G_{i,j}$ of a trained GAN-based model, using its corresponding synthetic sample set $S_{\text{fake},i} / S_{\text{fake},i,j}$. For single-generator models, this step was performed once using $S_{\text{fake},1}$. Using a fixed classifier architecture specific to each dataset trained for 50 epochs, classifiers were trained under two distinct augmentation scenarios for each sample set $S_{\text{fake},i}$:
 - *Replacement Scenario:* This assessed the utility of synthetic data from generator G_i as a substitute for real data. Training commenced with a baseline classifier using 5.000 real images per class. In subsequent steps, the number of real images per class was decreased by 1.000 while the number of synthetic images per class (drawn from $S_{\text{fake},i}$) was increased by 1.000, maintaining a constant dataset size of 5.000 images per class. This process continued until the final classifier was trained solely on 5.000 synthetic images per class from $S_{\text{fake},i}$.

- *Expansion Scenario:* This evaluated synthetic data from generator G_i as a supplement to real data. Training started with the same baseline (5.000 real images per class). The real dataset was then augmented by adding synthetic images from $S_{\text{fake},i}$ in increments of 1.000 per class per step, reaching a maximum of 5.000 synthetic images per class. The final classifier in this scenario was trained on a combined dataset of 5.000 real and 5.000 synthetic images per class from $S_{\text{fake},i}$.

Note that for each trained MADGAN or cMADGAN model with K generators, the full set of Replacement and Expansion classifier training experiments was performed K times, once for each generator’s synthetic dataset.

4. **Downstream Classifier Evaluation:** The performance of all trained classifiers (baseline and those from the replacement and expansion scenarios for each generator set $S_{\text{fake},i}$) was evaluated using predefined classification metrics [TODO: Add reference to metrics definition, e.g., Section X.Y on Evaluation Metrics]. Results for multi-generator models may be presented as averages across the K generators or by selecting representative examples of specific generators with specified ratios between real and fake images.

In total, this setup results in 44 (datasets (2) * augmentation types (4) * experiment setup (2) * n-generators trained ([3, 5, 7, 10])) experiment sets. Taking the different ratios of real to fake images in the expansion / replacement scenarios into account, a total of 1.166 separate classifiers were trained to evaluate the potential of multi-agent architecture for GDA.

4.3 Comparison of Classifier Performance

Due to the fact that the MADGAN and cMADGAN architectures apply a multi-agent strategy i.e., training multiple generators for one model, only the best run is selected for direct comparison to others. For example, when comparing MADGAN to cMADGAN in 5.2.4, the best performing subset of the respective GAN architecture is used for comparison. The rest of the experiments not discussed explicitly or only mentioned can be seen in the appendix 8.3.

4.4 Hardware and Software Environment

4.4.1 Hardware

All models trained in the context of this thesis were trained utilizing the *DeepLearning Cluster* provided by the *Hochschule der Medien - Stuttgart*. The cluster provides 8 nodes that with dedicated graphics cards supporting the *CUDA* framework. The

specific machines deployed in the cluster can be seen here Deeplearn cluster Documentation⁶.

4.4.2 Software

The code for the experiments was developed with the programming language python, using version 3.9. Models are based on the tensorflow ecosystem. The exact packages and their respective version can be found here Aanconda environment⁷.

⁶Link to the documentation for print versions: <https://deeplearn.pages.mi.hdm-stuttgart.de/docs/>.

⁷Link to the environment file for print versions: https://github.com/N10100010/mad_gan_thesis/blob/main/code/server_env.yml.

5 Experiments Results

Motivation The primary motivation for investigating multi-generator GAN architectures for Generative Data Augmentation (GDA) stems from a suggestion by Ian Goodfellow on the Lex Fridman Podcast [FG19]. He proposed leveraging the diversity inherent in multiple generative models trained on the same data to potentially improve downstream classifiers:

So one thing I think is worth trying [...] is, what if you trained a whole lot of different generative models on the same training set, create samples from all of them and then train a classifier on that. Because each of the generative models might generalize in a slightly different way, they might capture different axes of variation, that one individual model wouldn't and then the classifier can capture all of those ideas, by training on all of their data.

[FG19, 50:37]

Goodfellow's concept resonates strongly with the principles of Multi-Agent Diverse GANs (MADGANs) [GKN⁺18]. The MADGAN architecture, with its explicit diversity-promoting objective and use of multiple generators, provides a suitable framework for realizing this augmentation strategy. Therefore, the work by Ghosh et al. laid the conceptual groundwork for this thesis.

5.1 Key Research Questions

This chapter investigates the following questions regarding MADGANs for data augmentation:

- **Question 1:** How do the FID- and Inception Score compare between the generative methods?
- **Question 2:** Does Generative Data Augmentation (GDA) with MADGANs enhance downstream classifier performance more effectively than Traditional Data Augmentation (TDA)?
- **Question 3:** How does the performance enhancement achieved with MADGAN-based GDA compare to that of GDA using standard GANs or conditional GANs?
- **Question 4:** How does the performance enhancement achieved with MADGAN-based GDA compare to that of cMADGAN-GDA?
- **Question 5:** What is the impact of varying the number of MADGAN generators on downstream classifier performance?

5.2 Key Research Question Answers

As mentioned in the subchapter about the experimental workflow, four sets of multi-agent generators models were trained for the MADGAN and cMADGAN architectures (4.2). The four sets differ by K , the number of generators trained, with $K \in [3, 5, 7, 10]$. Onward, the generator of a discussion is identified explicitly by a suffix referencing the generator of a trained set $G_{i,j}$ with $i = K, j = 0 \dots (K - 1)$ (e.g., MADGAN_{5,0} for the first generator in the architecture trained with five generators). The set of generators however, is referenced via the notation: MADGAN $K = 5$ (e.g., if a discussion talks about the average performance of the generators 0...4). Throughout this chapter, the experiment will be viewed with respect to afore mentioned differentiation between expansion and replacement scenarios 3. The comparisons of FID- and Inception Score are excluded from this differentiation. Experiment not directly discussed in greater detail can be seen in the appendix 8.3. The generated graphs contain all respective runs of a given experimental setup for which, best, worst, average, median, and baseline are explicitly highlighted. Each gray line in a graph, that is not highlighted represents every other combination of the setup. Especially for the multi-agent generator setups, this results in many graphs, up to 60 per figure. Therefore, a colorful highlighting of specific graphs is omitted as this would not benefit the overall readability of the respective graphs. This however removes the potential for interesting insights. TODO: maaah, important sentence... Could be phrased better

5.2.1 Comparison of FID- and Inception Scores

In order to compare the FID-Score and the means and standard deviations of the IS, 10.000 generated samples are chosen by random selection. These fake images are drawn from the entirety of the generated data for a given generator, regardless of their assigned class. The comparison is being based on the respective datasets used (MNIST, Fashion-MNIST) for data generation.

MNIST Dataset

Generator Type	Generators trained	FID	IS	IS-std
DCGAN	1	122.097	2.611	0.056
cGAN	1	28.721	2.553	0.022
MADGAN	K=3 (avg)	23.177	2.511	0.04
MADGAN	K=5 (avg)	22.656	2.471	0.044
MADGAN	K=7 (avg)	21.599	2.533	0.051
MADGAN	K=10 (avg)	20.973	2.474	0.037
cMADGAN	K=3 (avg)	25.578	2.398	0.036
cMADGAN	K=5 (avg)	29.071	2.35	0.039
cMADGAN	K=7 (avg)	30.645	2.354	0.039
cMADGAN	K=10 (avg)	110.553	2.062	0.018

Table 2: FID and IS results for GAN models on MNIST, comparing single-generator (DCGAN, cGAN) and multi-generator (MADGAN, cMADGAN; K=3-10) approaches.

Interpretation: Table 2 presents the Fréchet Inception Distance (FID, lower is better) and Inception Score (IS, higher is better) for various GAN models evaluated on the MNIST dataset. The results reveal a trade-off between the two metrics across different architectures.

The baseline DCGAN achieved the highest IS (2.611) but performed poorly in terms of FID (122.097). Introducing conditioning via cGAN significantly improved the FID to 28.721 while maintaining a high IS (2.553). The results for the DCGAN point to an eventual mode collapse. A histogram of the resulting labels from this data generation can confirm the mode collapse⁸.

For unconditional models, the multi-generator MADGAN framework consistently yielded better FID scores than the baselines. Furthermore, MADGAN’s FID improved monotonically as the number of generators increased, achieving the best overall FID of 20.973 with 10 generators. However, its IS scores (2.5) were slightly lower than the single-generator baselines.

The conditional multi-generator adaptation, cMADGAN, showed a more complex relationship with the number of generators (K). It performed very poorly for K=3 (FID 110.553) but improved substantially at K=5, achieving a competitive FID (25.578) - better than cGAN - albeit with a lower IS (2.398). Contrary to MADGAN, increasing generators beyond K=5 resulted in worse FID scores for cMADGAN (29.071 for K=7, 30.645 for K=10). Consequently, for K>=5, the unconditional MADGAN consistently outperformed cMADGAN in FID within these experiments.

In summary, on MNIST, standard conditioning (cGAN) greatly enhances baseline FID. The unconditional MADGAN framework effectively improves FID further, benefiting from more generators. The conditional cMADGAN variant demonstrates potential (peaking at K=5) but exhibits non-monotonic FID performance with increasing generator count in this setup, suggesting a more complex optimization landscape com-

⁸A histogram of the resulting labels originating from the generation process of the DCGAN on MNIST can be found [here](#) 23.

pared to its unconditional counterpart.

Fashion-MNIST Dataset

Generator Type	Generators trained	FID	IS	IS-std
DCGAN	1	25.56	4.21	0.099
cGAN	1	123.349	3.573	0.117
MADGAN	K=3 (avg)	26.202	4.496	0.099
MADGAN	K=5 (avg)	24.218	4.497	0.098
MADGAN	K=7 (avg)	23.875	4.523	0.094
MADGAN	K=10 (avg)	21.587	4.534	0.097
cMADGAN	K=3 (avg)	25.555	4.623	0.105
cMADGAN	K=5 (avg)	160.082	3.346	0.038
cMADGAN	K=7 (avg)	154.115	2.929	0.034
cMADGAN	K=10 (avg)	159.067	3.317	0.035

Table 3: FID and IS results for GAN models on Fashion-MNIST, comparing single-generator (DCGAN, cGAN) and multi-generator (MADGAN, cMADGAN; K=3-10) approaches.

Interpretation: The evaluation metrics for the various GAN models on the Fashion-MNIST dataset, presented in Table 3, reveal distinct performance patterns. The baseline DCGAN provided a reasonable starting point with an FID of 25.56 and an IS of 4.21. However, unlike observations on MNIST, standard conditioning via cGAN proved detrimental on this dataset within this setup, resulting in significantly degraded FID (123.35) and IS (3.57) compared to the unconditional DCGAN.

In contrast, the unconditional MADGAN framework demonstrated robust and consistently improving performance. Its FID score, initially comparable to DCGAN at K=3 (26.20), improved monotonically as the number of generators increased, achieving the table’s best FID of 21.59 at K=10. Notably, MADGAN also maintained high IS scores (around 4.5), which showed a slight tendency to increase with more generators.

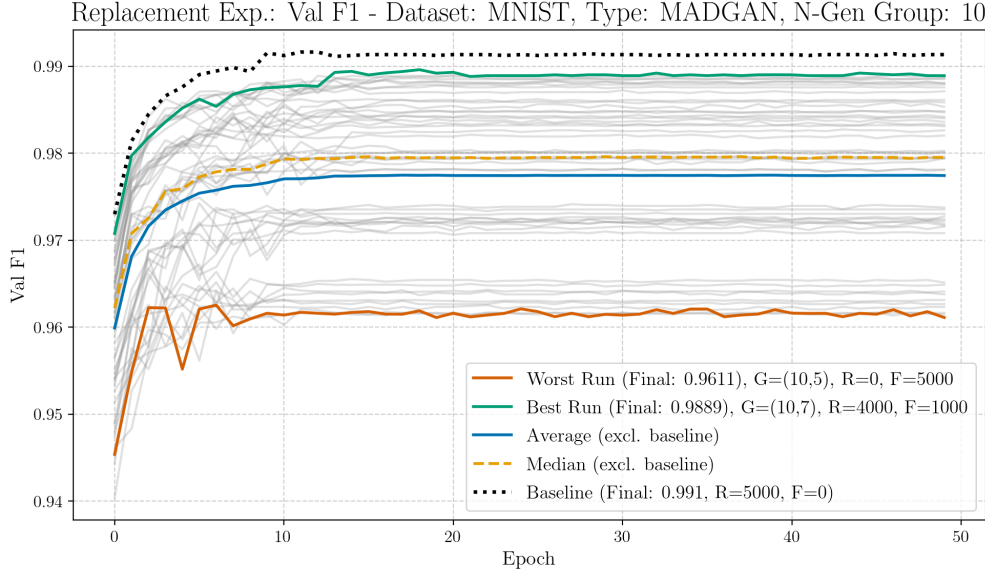
The conditional adaptation, cMADGAN, exhibited highly sensitive and divergent behavior on Fashion-MNIST compared to MNIST. Only the $K = 3$ configuration yielded strong results, achieving a competitive FID (25.56) while registering the table’s highest IS (4.62). However, increasing the generator count further to $K = 5, 7$, or 10 led to a dramatic performance collapse, characterized by extremely high FID scores (approximately 154–160) and substantially lower IS scores (around 2.9–3.3).

Overall, while cMADGAN K=3 achieved the best IS score, MADGAN K=10 attained the best FID score and offered a strong combination of both metrics. In conclusion, for Fashion-MNIST under these experimental conditions, standard conditioning failed to provide benefits, whereas the unconditional MADGAN framework scaled effectively, improving FID and IS with more generators. The conditional cMADGAN approach was only viable with a small number of generators (K=3) and did not exhibit the positive scaling or peak performance characteristics observed on MNIST.

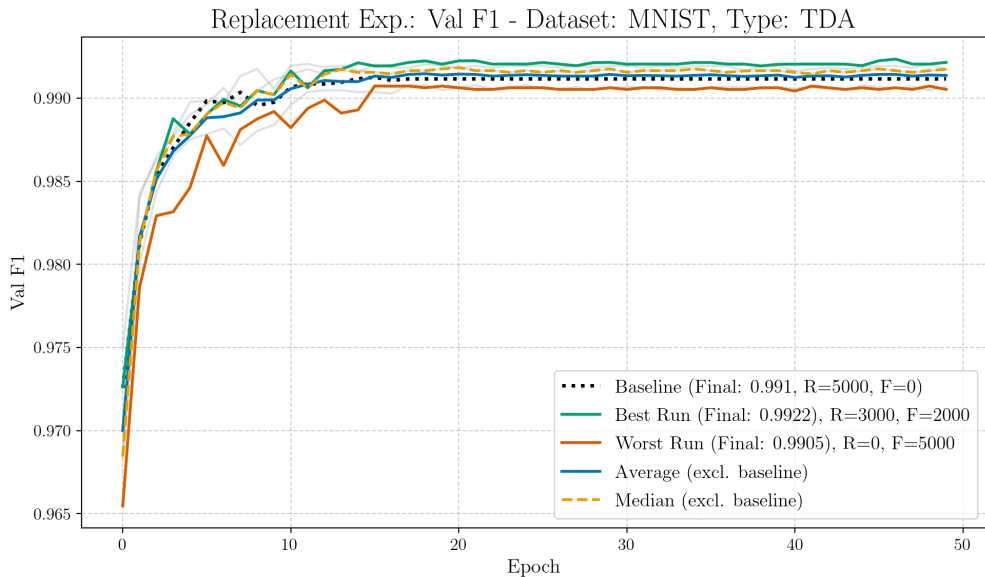
5.2.2 Question 2: Effectiveness of MADGAN GDA vs. TDA

As mentioned in the beginning of this chapter, four sets of generators with different numbers for K were trained, with $K \in [3, 5, 7, 10]$, for the multi-agent architectures. For comparison against other GDA methods, the best performing set (e.g., MADGAN $K = 3$) or the best performing generator (e.g., $G_{3,2}$) is used. All other experiments are present in the appendix 8.3. From here onward, the differentiation between replacement and expansion experiments will be used.

Replacement Experiment, Dataset: MNIST



(a) F1 Score on MNIST over 50 epochs. Augmentation technique: MADGAN (K=10)



(b) F1 Score on MNIST over 50 epochs. Augmentation Technique: TDA

Run Type	Experiment	Val F1
best	$G_{10,7}$, R:4000, F:1000	0.9889
worst	$G_{10,5}$, R:0, F:5000	0.9611
median	-	0.9795
average	-	0.9774

Table 4: Final F1 Scores after 50 epochs. Augmentation technique: MADGAN

Run Type	Metric	Performance
best	TDA (R:3000, F:2000)	0.9922
worst	TDA (R:0, F:5000)	0.9905
median	TDA	0.9917
average	TDA	0.9914

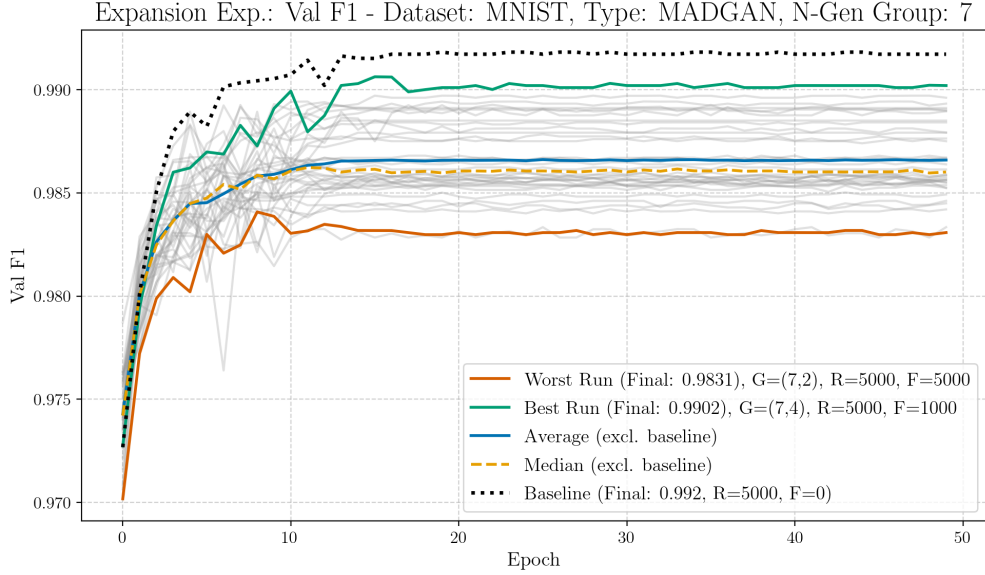
Table 5: Final F1 Scores after 50 epochs. Augmentation technique: TDA

The results for TDA, shown in figure 9b and summarized in table 13. The graphs in the corresponding figure show all out rapid convergence and a stable training over the 50 epochs. With a small spread of the results, all replacement ratios $[(R : 5000, F : 0), \dots, (R : 0, F : 5000)]$ consistently result in excellent performance with an average F1 score of 0.9914. The best and worst results are close to the average and both are over 0.99, only differing in the third decimals. This leads to the conclusion that replacing training images for a classifier with modified images via traditional methods had minimal negative impact on the classifiers' performance, measured on the validation set via the F1 score. It is to point out, that the best, average and median performance surpassed the baseline allowing the conclusion that the replacement of real images with their augmented counterpart had a positive impact on average.

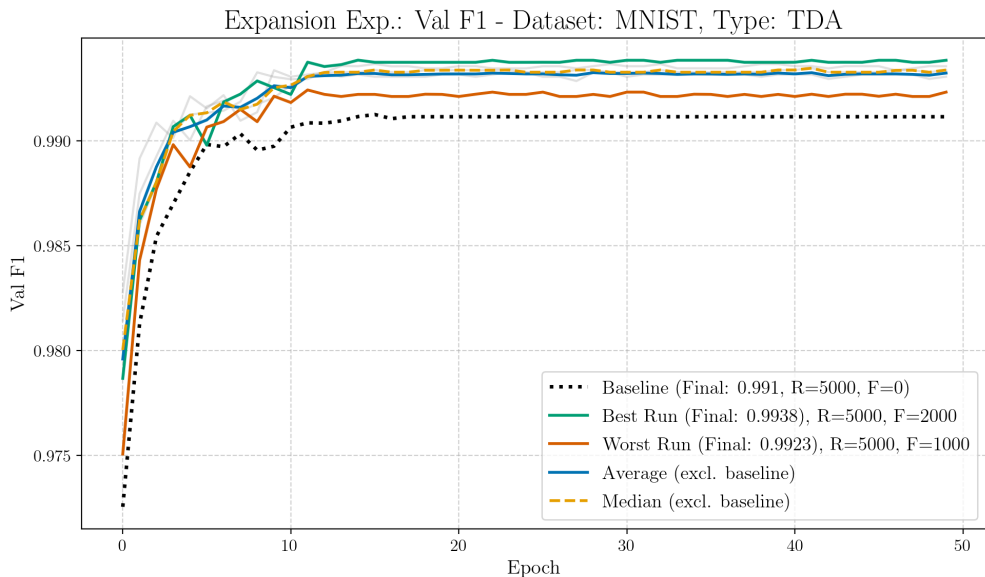
The performance using GDA with samples form MADGAN ($K=10$) model is presented in Figure 9a and Table 12. It is important to note again, that the figure and the summary statistics encompass results across the 10 individual generators and across all replacement ratios resulting in a total of 60 total classifiers. The graph shows convergence to a slightly lower F1 scores, compared to those from TDA. Here, the conclusion can be drawn that the replacement of real with augmented images resulted in an overall negative impact. The summary table quantifies this fact: the average final F1 score across ratios and generators is 0.9775, which is significantly lower than the average of the traditional augmentation. While the best setup ($G_{10,7}, R : 4000, F : 1000$) reached a good score: 0.9889; it is lower than the average performance across the different ratios in the TDA experiment. Even the worst performing classifier in the TDA experiment is better than the best score for GDA in this case.

In direct comparison, the TDA consistently outperforms GDA (with its best resulting setting, MADGAN ($K=10$)) in this replacement scenario. Replacing the real data with synthetic lead to a noticeable degradation of the classifiers' performance on the validation set. Taking the results from question 1 into account (5.2.1), even the MADGAN setup resulting in the best FID score are not as effective as traditional augmented real data, when substituting the real samples in the training set.

Expansion Experiment, Dataset: MNIST



(a) F1 Score on MNIST over 50 epochs. Augmentation technique: MADGAN (K=7)



(b) F1 Score on MNIST over 50 epochs. Augmentation Technique: TDA

Run Type	Experiment	Val F1
best	$G_{7,4}$, R:5000, F:1000	0.9902
worst	$G_{7,2}$, R:5000, F:5000	0.9831
median	-	0.9860
average	-	0.9866

Table 6: Final F1 Scores after 50 epochs. Augmentation technique: MADGAN

Run Type	Experiment	Performance
best	TDA (R:5000, F:2000)	0.9938
worst	TDA (R:5000, F: 1000)	0.9923
median	TDA	0.9934
average	TDA	0.9932

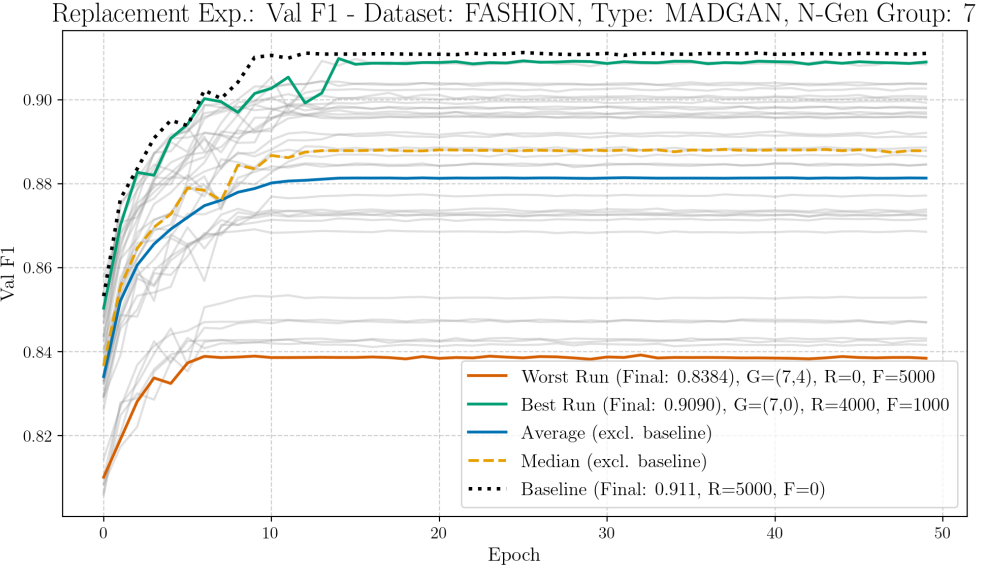
Table 7: Final F1 Scores after 50 epochs. Augmentation technique: TDA

The results using TDA (Table 7) show consistently high performance. The average final F1 score across all expansion levels (adding 0 to 5,000 augmented samples per class) is 0.9932, with minimal variation between the best (0.9938, achieved when adding 2,000 augmented samples) and worst (0.9923) cases. This indicates that expanding the dataset with traditionally augmented samples maintains, and perhaps very slightly improves, the already high baseline performance on MNIST.

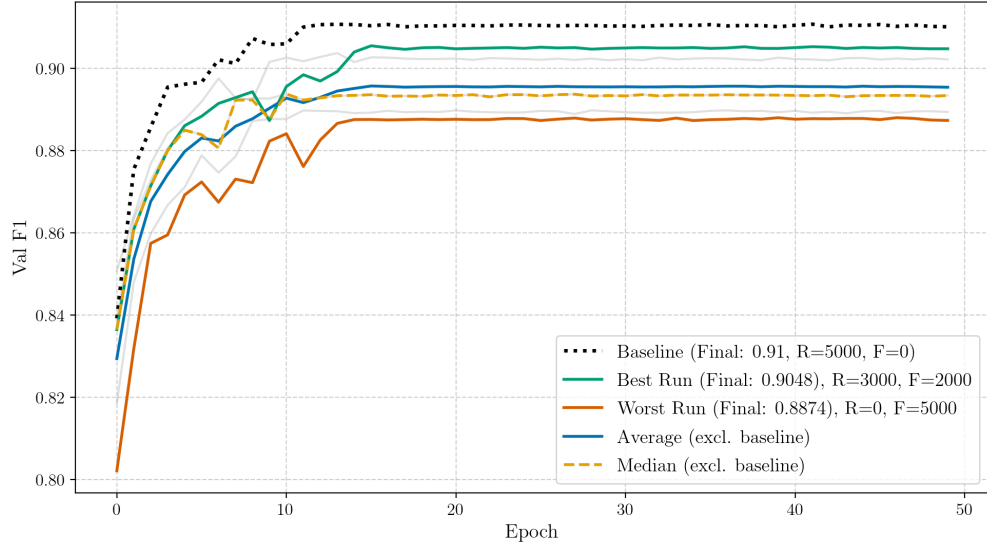
In contrast, using GDA with samples generated by the MADGAN ($K=7$) model did not yield performance improvements over the baseline trained only on real data. To be noted explicitly, none of the expansion experiments using MADGAN GDA surpassed the baseline performance level (see: 8.3.1). The summary statistics in Table 6, which cover results across all 7 generators and all expansion ratios, confirm this. The average final F1 score is 0.9866, noticeably lower than the TDA results. The best-performing run across all generators and expansion levels only reached 0.9902 (using generator $G_{7,4}$ when adding 1,000 synthetic samples), which is below even the worst TDA result. Performance tended to decrease as more synthetic data was added, with the lowest score (0.9831) occurring when the maximum of 5,000 synthetic samples per class were added (using generator $G_{7,2}$).

Comparing the two augmentation strategies in the expansion scenario, TDA is clearly superior on MNIST in this setup. Expanding the dataset with traditionally augmented data maintains excellent performance, whereas expanding with MADGAN-generated synthetic data fails to improve over the real-data baseline and leads to lower overall performance. This suggests that the synthetic samples from MADGAN ($K=7$), despite the model potentially having good generative scores, dilute rather than enhance the training data quality when added to the real MNIST dataset for this downstream classification task.

Replacement Experiment, Dataset: Fashion-MNIST



(a) F1 Score on FASHION over 50 epochs. Augmentation tech.: MADGAN (K=7)
Replacement Exp.: Val F1 - Dataset: FASHION, Type: TDA



(b) F1 Score on FASHION over 50 epochs. Augmentation Technique: TDA

Run Type	Experiment	Val F1
best	$G_{7,2}$, R:4000, F:1000	0.9079
worst	$G_{7,0}$, R:0, F:5000	0.3419
median	-	0.8927
average	-	0.7993

Table 8: Final F1 Scores after 50 epochs. Augmentation tech.: MADGAN (K=7)

Run Type	Experiment	Val F1
best	TDA (R:3000, F:2000)	0.9048
worst	TDA (R:0, F:5000)	0.8874
median	TDA	0.8934
average	TDA	0.8955

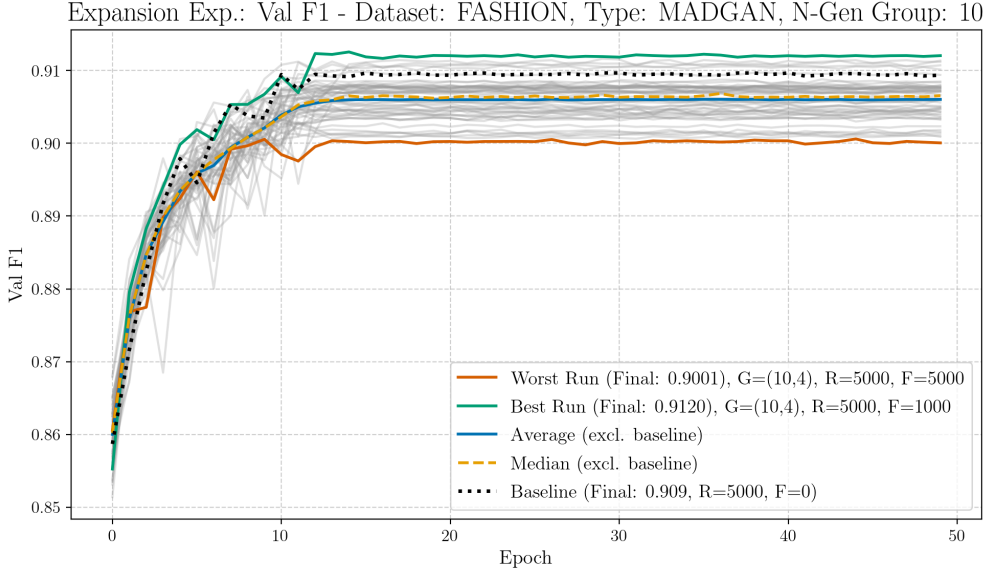
Table 9: Final F1 Scores after 50 epochs. Augmentation technique: TDA

For TDA (Table 9), the results indicate reasonably strong and relatively stable classifier performance as real data is replaced by traditionally augmented samples. The average final F1 score across all replacement ratios is 0.8955. Performance degrades moderately as more real data is substituted, with the best score (0.9048) observed at a mix of 3000 real and 2000 augmented samples per class, and the worst score (0.8874) occurring when using only augmented data (0 real, 5000 augmented). The overall range is narrow, suggesting TDA provides consistent results.

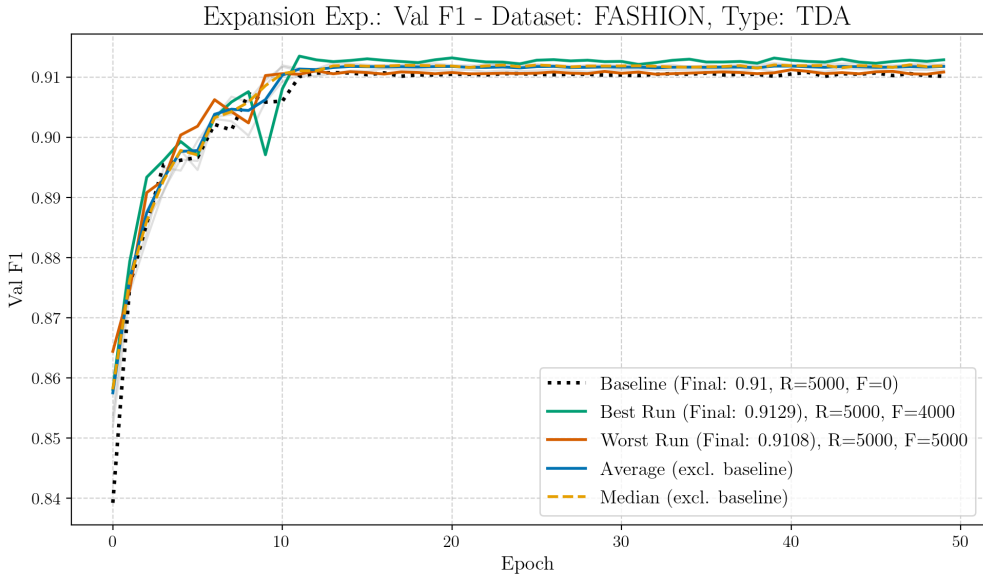
The MADGAN (K=7) GDA results (Table 8) reveal a much higher degree of variability. These summary statistics encompass results across all 7 individual generators and all replacement ratios. Notably, the best-performing run (generator $G_{7,2}$ with 4000 real / 1000 fake samples) achieved an F1 score of 0.9079, slightly surpassing the best TDA result. However, extreme inconsistency offsets this potential advantage. The worst-performing run (generator $G_{7,0}$ using only synthetic data) yielded a drastically low F1 score of 0.3419, far below the worst TDA score. This disparity heavily impacts the average F1 score for MADGAN GDA, bringing it down to 0.7993, significantly lower than the TDA average. Interestingly, the median F1 score for MADGAN GDA (0.8927) is quite close to the TDA median (0.8934), suggesting that while the average is poor due to outliers, typical performance might be closer to TDA.

In direct comparison for the replacement scenario on Fashion-MNIST, TDA offers more reliable and consistent performance. While MADGAN GDA demonstrates the potential to slightly exceed TDA’s peak performance under specific optimal conditions (best generator, limited replacement), it suffers from extreme variability. Relying solely on synthetic data from weaker generators leads to a catastrophic performance drop, making MADGAN GDA a much less robust strategy on average compared to TDA when replacing real data in this setup.

Expansion Experiment, Dataset: Fashion-MNIST



(a) F1 Score on FASHION over 50 epochs. Augmentation tech.: MADGAN (K=10)



(b) F1 Score on FASHION over 50 epochs. Augmentation Technique: TDA

Run Type	Experiment	Val F1
best	$G_{10,4}$, R:5000, F:1000	0.9120
worst	$G_{10,4}$, R:5000, F:5000	0.9001
median	-	0.9066
average	-	0.9060

Table 10: Final F1 Scores after 50 epochs. Augmentation tech.: MADGAN (K=X)

Run Type	Experiment	Val F1
best	TDA (R:5000, F:4000)	0.9129
worst	TDA (R:5000, F:5000)	0.9108
median	TDA	0.9119
average	TDA	0.9118

Table 11: Final F1 Scores after 50 epochs. Augmentation technique: TDA

The results indicate that data expansion is beneficial on Fashion-MNIST for both augmentation techniques, unlike the observations on MNIST where MADGAN GDA did not surpass the baseline. Using TDA (Table 11), adding augmented samples improves performance over baseline (R:5000/F:0), achieving a peak F1 score of 0.9129 when adding 4.000 augmented samples per class. Performance remains very high and stable across different expansion levels, with an average F1 of 0.9118 and even the worst case (adding 5.000 samples) scoring 0.9108.

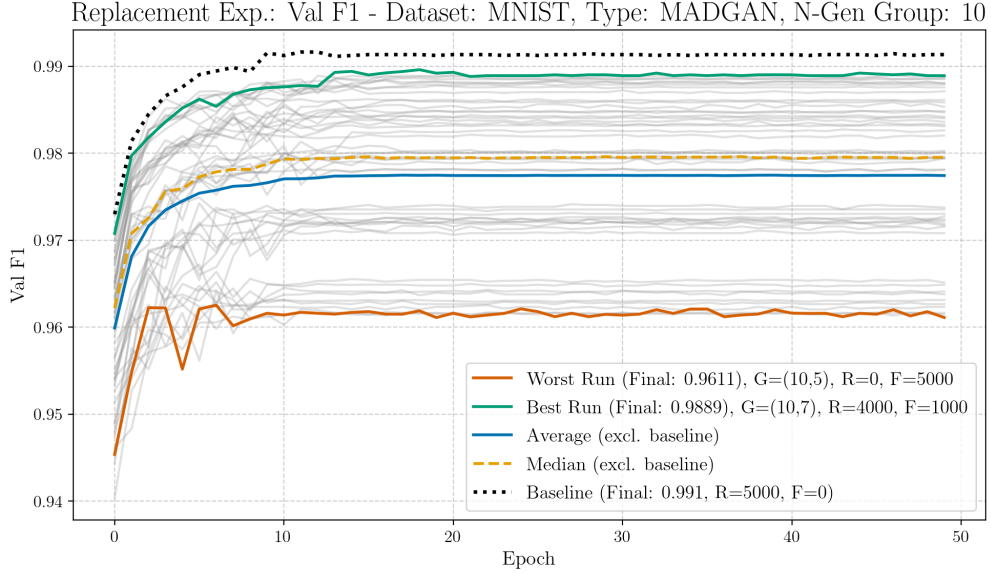
Similarly, expansion using MADGAN ($K=10$) GDA also demonstrates the potential to improve performance over the baseline. The summary statistics in Table 10, covering results across all 10 generators and expansion ratios, show a best-case F1 score of 0.9120 (achieved by generator $G_{10,4}$ when adding 1.000 synthetic samples). This peak performance is very close to the TDA peak and suggests GDA can be effective in this scenario. However, MADGAN GDA performance is slightly less consistent than TDA. The average F1 score (0.9060) and median (0.9066) are marginally lower than TDA’s averages. Furthermore, performance degrades more noticeably when adding the maximum number of synthetic samples, with the worst run dropping to 0.9001, below TDA’s worst case. The variability across generators and ratios, while present, is considerably less extreme than observed in the Fashion-MNIST replacement experiment.

In direct comparison for the expansion scenario on Fashion-MNIST, both TDA and MADGAN GDA ($K=10$) show benefits over using only the original real data. TDA maintains a slight edge, providing marginally higher peak performance and greater stability, especially when large amounts of augmented data are added. MADGAN GDA is highly competitive, achieving a peak performance nearly identical to TDA’s, but exhibiting slightly lower average scores and greater performance degradation when maximally expanded. This suggests MADGAN GDA is a viable expansion technique on Fashion-MNIST, though TDA remains slightly more robust.

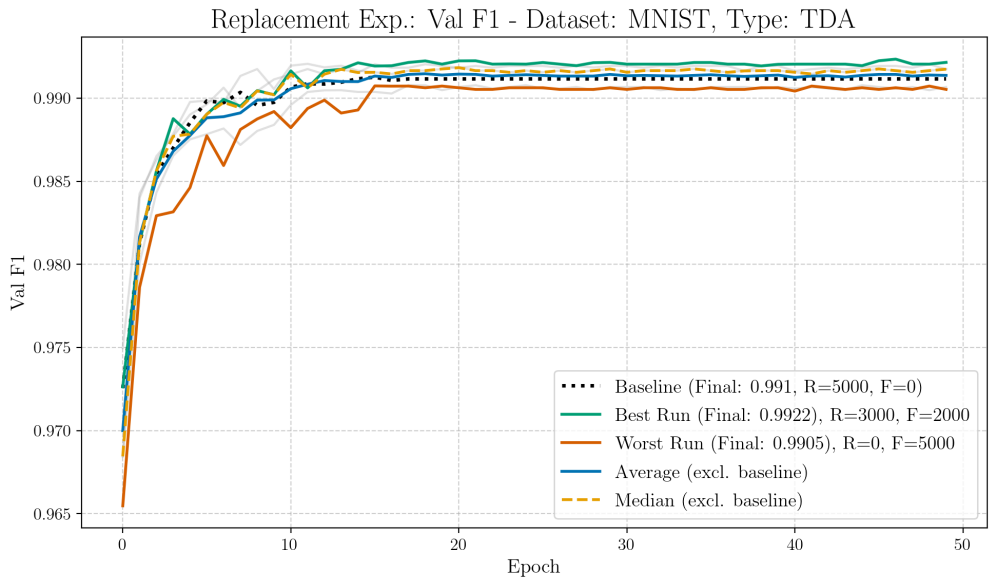
5.2.3 MADGAN GDA vs. Deep Convolutional/Conditional GAN GDA

In the foregoing chapter (5.2.2), the most successful setting for the MADGAN architecture has been set. Following, the same settings for the respective dataset and the corresponding experimental setup (replacement, expansion) will be used to compare against deep convolutional and conditional GANs

Replacement Experiment, Dataset: MNIST



(a) F1 Score on MNIST over 50 epochs. Augmentation technique: MADGAN (K=10)



(b) F1 Score on MNIST over 50 epochs. Augmentation Technique: TDA

Run Type	Experiment	Val F1
best	$G_{10,7}$, R:4000, F:1000	0.9889
worst	$G_{10,5}$, R:0, F:5000	0.9611
median	-	0.9795
average	-	0.9774

Table 12: Final F1 Scores after 50 epochs. Augmentation technique: MADGAN

Run Type	Metric	Performance
best	TDA (R:3000, F:2000)	0.9922
worst	TDA (R:0, F:5000)	0.9905
median	TDA	0.9917
average	TDA	0.9914

Table 13: Final F1 Scores after 50 epochs. Augmentation technique: TDA

5.2.4 MADGAN GDA vs. cMADGAN GDA Performance**5.2.5 Impact of MADGAN Generator Count**

6 Remarks

Is Weight Sharing Mandatory in MAD-GAN?

No, weight sharing is not strictly mandatory to implement the general idea of having multiple generators aiming for diversity and fooling a single discriminator. You could implement K completely independent generator networks.

However, the weight-sharing strategy proposed by Ghosh et al. is a key architectural feature and contribution of their specific MAD-GAN formulation. In their paper, they propose sharing the parameters of the initial, deeper layers across all generators and only having separate (unshared) parameters for the final few layers of each generator.

So, while not theoretically mandatory for any multi-generator setup, it's central to the design and efficiency benefits highlighted in the original MAD-GAN paper. Deviating significantly from it means you are implementing a different variant of a multi-generator diverse GAN.

Advantages of Weight Sharing (as proposed in MAD-GAN):

Parameter Efficiency: This is a major advantage. Instead of storing and training K full generator networks, you store one large shared network base and K smaller "heads" (the final unshared layers). This drastically reduces the total number of parameters.

Lower Memory Footprint: Requires less GPU memory, making it feasible to train more generators or use larger base networks.

Faster Training (Potentially): Fewer parameters typically mean fewer computations per training step, potentially leading to faster epochs, although the overall training dynamic is complex.

Improved Training Stability and Sample Efficiency: The shared base learns common low-level and mid-level features more effectively because it receives gradient updates influenced by the learning objectives of all generators. It essentially gets a stronger, more averaged learning signal for shared features. This shared learning can prevent individual generators from collapsing early or diverging drastically, potentially leading to more stable training.

Generators benefit from features learned via the experiences of other generators through the shared base. Knowledge Transfer: Useful features learned by the shared base (e.g., basic shapes, textures common to the dataset) are immediately available to all generators, promoting faster learning of complex structures.

Implicit Regularization: Sharing weights constrains the generators, acting as a form of regularization that might prevent individual generators from overfitting noise or specific data points too quickly.

Limited Diversity Potential: Because a significant portion of the network is shared, the fundamental feature extraction process is common to all generators. The diversity is primarily introduced by the final few unshared layers. This might impose a ceiling on the maximum achievable diversity compared to completely independent generators, which could potentially learn radically different internal representations from scratch.

Optimization Complexity: Training the shared parameters involves backpropagating

gradients derived from multiple generator heads, each with its adversarial loss and influenced by the diversity loss relative to others. Balancing these potentially conflicting gradient signals flowing into the shared base can be tricky and might require careful tuning of learning rates and the diversity weight (λ). Poor tuning could lead to suboptimal learning in the shared base. Architectural Constraint: The fixed structure (shared base + separate heads) might not be the optimal architecture for every problem or dataset. Completely independent generators offer more flexibility in exploring different architectures for each one. Potential Bottleneck: If the shared base fails to learn good representations or gets stuck in a poor local minimum, it negatively impacts all generators simultaneously. With independent generators, there's a chance that at least one might find a better solution path independently. In summary, the weight-sharing strategy in the original MAD-GAN paper is a clever design choice offering significant efficiency and stability benefits, making it practical to train multiple generators. However, this comes at the cost of potentially limiting the absolute maximum diversity achievable and introducing specific optimization challenges compared to using fully independent generator networks. The choice depends on the trade-off between efficiency, stability, and the desired level/type of diversity for a specific application.

7 Outlook

repair networks [TFNL22]

Measure the resulting diversity between the generated samples using the MS-SSIM scores [OOS17]; they did that as well

8 Conclusion

Data generated by a GAN, may it be a cGAN or a MADGAN, may not fully capture the distribution characteristics of its training data. Though, generated images do visually appear realistic, they may only partially reflect the statistical characteristics of the original data. This can lead to synthetic images that appear *good* to a human inspector, but may contain amounts of noise that may interfere with a subsequent classifier.

from an information theoretical standpoint, a generative model G trained on data X , distilling knowledge into a classifier C should not offer more information than what was already present in X .

Future research could focus on directly evaluating the impact of using MAD-GAN generated samples for augmenting various image classification datasets across different domains and comparing the resulting performance gains with those achieved by traditional and other generative augmentation techniques. Exploring methods to exert more control over the types of variations generated by MAD-GAN to specifically target weaknesses or improve the robustness of classifiers against particular types of noise or adversarial attacks would also be a valuable direction. Additionally, investigating the computational efficiency and scalability of training MAD-GAN for very large and complex datasets in the context of practical data augmentation pipelines would be crucial for its wider adoption. Finally, exploring the applicability of the MAD-GAN framework to generate diverse augmented data for other computer vision tasks beyond image classification, as well as for other data modalities such as natural language processing or audio processing, could further broaden its impact. The work by Ghosh et al. on Multi-Agent Diverse GANs represents a promising step towards leveraging the power of generative models for more effective and robust data augmentation in image classification and beyond.

after all, we tested an augmentation technique and maybe it should be treated as such. Augmentations should be drawn from a number of different techniques. Braughly speaking, across different domains, types of classifiers, etc. there might not be a single best kind of augmentation technique. Ultimately, this is an optimization problem in and of itself and can and should be treated as such.

List of References

- [ACB17] ARJOVSKY, Martin ; CHINTALA, Soumith ; BOTTOU, Léon: *Wasserstein GAN*. <https://arxiv.org/abs/1701.07875>. Version: 2017
- [BNI⁺23] BISWAS, Angona ; NASIM, MD Abdullah A. ; IMRAN, Al ; SEJUTY, Anika T. ; FAIROOZ, Fabliha ; PUPPALA, Sai ; TALUKDER, Sajedul: *Generative Adversarial Networks for Data Augmentation*. <https://arxiv.org/abs/2306.02019>. Version: 2023
- [CFB⁺24] CHANG, A. ; FONTAINE, M. C. ; BOOTH, S. ; MATARIĆ, M. J. ; NIKOLAIDIS, S.: Quality-Diversity Generative Sampling for Learning with Synthetic Data. In: *Proceedings of the AAAI Conference on Artificial Intelligence* 38 (2024), Nr. 18, S. 19805–19812
- [DCLK20] DURALL, Ricard ; CHATZIMICHAILIDIS, Avraam ; LABUS, Peter ; KEPUPER, Janis: *Combating Mode Collapse in GAN training: An Empirical Analysis using Hessian Eigenvalues*. <https://arxiv.org/abs/2012.09673>. Version: 2020
- [DDS⁺09] DENG, Jia ; DONG, Wei ; SOCHER, Richard ; LI, Li-Jia ; LI, Kai ; FEI-FEI, Li: ImageNet: A large-scale hierarchical image database. In: *2009 IEEE Conference on Computer Vision and Pattern Recognition*, 2009, S. 248–255
- [DHYY17] DONG, Hao-Wen ; HSIAO, Wen-Yi ; YANG, Li-Chia ; YANG, Yi-Hsuan: *MuseGAN: Multi-track Sequential Generative Adversarial Networks for Symbolic Music Generation and Accompaniment*. <https://arxiv.org/abs/1709.06298>. Version: 2017
- [DV18] DUMOULIN, Vincent ; VISIN, Francesco: *A guide to convolution arithmetic for deep learning*. <https://arxiv.org/abs/1603.07285>. Version: 2018
- [FG19] FRIDMAN, Lex ; GOODFELLOW, Ian: *Ian Goodfellow: Generative Adversarial Networks (GANs) / Lex Fridman Podcast #19*. Audio podcast episode, *Lex Fridman Podcast*, YouTube. <https://www.youtube.com/watch?v=Z6rxFNMGdn0&t=3037s>. Version: apr 2019. – Accessed: 2025-03-14
- [Gav20] GAVRIKOV, Paul: *visualkeras*. <https://github.com/paulgavrikov/visualkeras>, 2020
- [GKN⁺18] GHOSH, Arnab ; KULHARIA, Viveka ; NAMBOODIRI, Vinay ; TORR, Philip H. S. ; DOKANIA, Puneet K.: *Multi-Agent Diverse Generative Adversarial Networks*. <https://arxiv.org/abs/1704.02906>. Version: 2018
- [GPAM⁺14] GOODFELLOW, Ian J. ; POUGET-ABADIE, Jean ; MIRZA, Mehdi ; XU, Bing ; WARDE-FARLEY, David ; OZAIR, Sherjil ; COURVILLE, Aaron ; BENGIO, Yoshua: *Generative Adversarial Networks*. <https://arxiv.org/abs/1406.2661>. Version: 2014

- [HBB21] HUMAYUN, A. I. ; BALESTRIERO, R. ; BARANIUK, R.: MaGNET: Uniform Sampling from Deep Generative Network Manifolds without Retraining. In: *arXiv preprint arXiv:2110.08009* (2021)
- [HBB22] HUMAYUN, A. I. ; BALESTRIERO, R. ; BARANIUK, R.: Polarity Sampling: Quality and Diversity Control of Pre-Trained Generative Networks via Singular Values. In: *Proceedings of the IEEE/CVF Conference on Computer Vision and Pattern Recognition (CVPR)*, 2022, S. 10641–10650
- [HFM22] HUANG, Y. ; FIELDS, K. G. ; MA, Y.: A Tutorial on Generative Adversarial Networks with Application to Classification of Imbalanced Data. In: *Statistical Analysis and Data Mining* 15 (2022), Nr. 5, S. 543–552. <http://dx.doi.org/10.1002/sam.11570>. – DOI 10.1002/sam.11570
- [HRU⁺18] HEUSEL, Martin ; RAMSAUER, Hubert ; UNTERTHINER, Thomas ; NESSLER, Bernhard ; HOCHREITER, Sepp: *GANs Trained by a Two Time-Scale Update Rule Converge to a Local Nash Equilibrium*. <https://arxiv.org/abs/1706.08500>. Version: 2018
- [IS15] IOFFE, Sergey ; SZEGEDY, Christian: *Batch Normalization: Accelerating Deep Network Training by Reducing Internal Covariate Shift*. <https://arxiv.org/abs/1502.03167>. Version: 2015
- [IZZE18] ISOLA, Phillip ; ZHU, Jun-Yan ; ZHOU, Tinghui ; EFROS, Alexei A.: *Image-to-Image Translation with Conditional Adversarial Networks*. <https://arxiv.org/abs/1611.07004>. Version: 2018
- [JLR25] JUN LI, Wei Z. Chenyang Zhang Z. Chenyang Zhang ; REN, Yawei: A Comprehensive Survey of Image Generation Models Based on Deep Learning. In: *Annals of Data Science* 12 (2025), February, 141–170. <http://dx.doi.org/10.1007/s40745-024-00544-1>. – DOI 10.1007/s40745-024-00544-1
- [JLY20] JI, Shulei ; LUO, Jing ; YANG, Xinyu: *A Comprehensive Survey on Deep Music Generation: Multi-level Representations, Algorithms, Evaluations, and Future Directions*. <https://arxiv.org/abs/2011.06801>. Version: 2020
- [JPB22] JEONG, Jason ; PATEL, B. ; BANERJEE, I.: GAN augmentation for multiclass image classification using hemorrhage detection as a case-study. In: *Journal of Medical Imaging (Bellingham, Wash.)* 9 (2022), Nr. 3, S. 035504. <http://dx.doi.org/10.1117/1.JMI.9.3.035504>. – DOI 10.1117/1.JMI.9.3.035504
- [Kri09] KRIZHEVSKY, Alex: *Learning Multiple Layers of Features from Tiny Images*. Technical Report, University of Toronto. <https://www.cs.toronto.edu/~kriz/learning-features-2009-TR.pdf>. Version: 2009
- [KSH12a] KRIZHEVSKY, Alex ; SUTSKEVER, Ilya ; HINTON, Geoffrey E. ; PEREIRA, F. (Hrsg.) ; BURGES, C.J. (Hrsg.) ; BOTTOU, L. (Hrsg.) ; WEINBERGER, K.Q. (Hrsg.): *ImageNet Classification with Deep Convolutional Neural Networks*. https://proceedings.neurips.cc/paper_files/

- paper/2012/file/c399862d3b9d6b76c8436e924a68c45b-Paper.pdf.
Version: 2012
- [KSH12b] KRIZHEVSKY, Alex ; SUTSKEVER, Ilya ; HINTON, Geoffrey E.: ImageNet Classification with Deep Convolutional Neural Networks. In: *Communications of the ACM* 60 (2012), Nr. 6, S. 84–90. <http://dx.doi.org/10.1145/3065386>. – DOI 10.1145/3065386
- [LBD⁺89] LECUN, Y. ; BOSER, B. ; DENKER, J. S. ; HENDERSON, D. ; HOWARD, R. E. ; HUBBARD, W. ; JACKEL, L. D.: Backpropagation Applied to Handwritten Zip Code Recognition. In: *Neural Computation* 1 (1989), Nr. 4, S. 541–551. <http://dx.doi.org/10.1162/neco.1989.1.4.541>. – DOI 10.1162/neco.1989.1.4.541
- [LCB10] LECUN, Yann ; CORTES, Corinna ; BURGES, CJ: MNIST handwritten digit database. In: *ATT Labs [Online]*. Available: <http://yann.lecun.com/exdb/mnist> 2 (2010)
- [LMWN22] LI, Xiaomin ; METSIS, Vangelis ; WANG, Huangyingrui ; NGU, Anne Hee H.: *TTS-GAN: A Transformer-based Time-Series Generative Adversarial Network*. <https://arxiv.org/abs/2202.02691>. Version: 2022
- [LTH⁺17] LEDIG, Christian ; THEIS, Lucas ; HUSZAR, Ferenc ; CABALLERO, Jose ; CUNNINGHAM, Andrew ; ACOSTA, Alejandro ;AITKEN, Andrew ; TEJANI, Alykhan ; TOTZ, Johannes ; WANG, Zehan ; SHI, Wenzhe: *Photo-Realistic Single Image Super-Resolution Using a Generative Adversarial Network*. <https://arxiv.org/abs/1609.04802>. Version: 2017
- [MKKY18] MIYATO, Takeru ; KATAOKA, Toshiki ; KOYAMA, Masanori ; YOSHIDA, Yuichi: *Spectral Normalization for Generative Adversarial Networks*. <https://arxiv.org/abs/1802.05957>. Version: 2018
- [MLX⁺17] MAO, Xudong ; LI, Qing ; XIE, Haoran ; LAU, Raymond Y. K. ; WANG, Zhen ; SMOLLEY, Stephen P.: *Least Squares Generative Adversarial Networks*. <https://arxiv.org/abs/1611.04076>. Version: 2017
- [MO14] MIRZA, Mehdi ; OSINDERO, Simon: *Conditional Generative Adversarial Nets*. <https://arxiv.org/abs/1411.1784>. Version: 2014
- [Neu28] NEUMANN, John von: Zur Theorie der Gesellschaftsspiele. In: *Mathematische Annalen* 100 (1928), Nr. 1, S. 295–320
- [NS67] NAGY, George ; SHELTON, Henry: Self-Corrective Character Recognition System. In: *IBM Journal of Research and Development* 11 (1967), Nr. 6, S. 612–628. <http://dx.doi.org/10.1147/rd.116.0612>. – DOI 10.1147/rd.116.0612
- [OOS17] ODENA, Augustus ; OLAH, Christopher ; SHLENS, Jonathon: Conditional image synthesis with auxiliary classifier GANs. In: *Proceedings of the 34th International Conference on Machine Learning - Volume 70*, JMLR.org, 2017 (ICML'17), S. 2642–2651

- [PKD⁺16] PATHAK, Deepak ; KRAHENBUHL, Philipp ; DONAHUE, Jeff ; DARRELL, Trevor ; EFROS, Alexei A.: *Context Encoders: Feature Learning by In-painting.* <https://arxiv.org/abs/1604.07379>. Version: 2016
- [PW17] PEREZ, Luis ; WANG, Jason: *The Effectiveness of Data Augmentation in Image Classification using Deep Learning.* <https://arxiv.org/abs/1712.04621>. Version: 2017
- [RAY⁺16] REED, Scott ; AKATA, Zeynep ; YAN, Xinchen ; LOGESWARAN, Lajanugen ; SCHIELE, Bernt ; LEE, Honglak: *Generative Adversarial Text to Image Synthesis.* <https://arxiv.org/abs/1605.05396>. Version: 2016. – arXiv:1605.05396
- [RCF25] RIBAS, Lucas C. ; CASACA, Wallace ; FARES, Ricardo T.: Conditional Generative Adversarial Networks and Deep Learning Data Augmentation: A Multi-Perspective Data-Driven Survey Across Multiple Application Fields and Classification Architectures. In: *AI* 6 (2025), Nr. 2. <http://dx.doi.org/10.3390/ai6020032>. – DOI 10.3390/ai6020032. – ISSN 2673–2688
- [RMC16] RADFORD, Alec ; METZ, Luke ; CHINTALA, Soumith: Unsupervised Representation Learning with Deep Convolutional Generative Adversarial Networks, 2016
- [SGZ⁺16] SALIMANS, Tim ; GOODFELLOW, Ian ; ZAREMBA, Wojciech ; CHEUNG, Vicki ; RADFORD, Alec ; CHEN, Xi: *Improved Techniques for Training GANs.* <https://arxiv.org/abs/1606.03498>. Version: 2016
- [SK19] SHORTEN, Connor ; KHOSHGOFTAAR, Taghi M.: A survey on Image Data Augmentation for Deep Learning. In: *Journal of Big Data* 6 (2019), July, Nr. 1, 60. <http://dx.doi.org/10.1186/s40537-019-0197-0>. – DOI 10.1186/s40537-019-0197-0. – ISSN 2196–1115
- [SSP03] SIMARD, Patrice Y. ; STEINKRAUS, Dave ; PLATT, John C.: Best Practices for Convolutional Neural Networks Applied to Visual Document Analysis. In: *Seventh International Conference on Document Analysis and Recognition*, 2003, S. 958–963
- [SVI⁺16] SZEGEDY, Christian ; VANHOUCKE, Vincent ; IOFFE, Sergey ; SHLENS, Jon ; WOJNA, Zbigniew: Rethinking the Inception Architecture for Computer Vision. In: *Proceedings of the IEEE Conference on Computer Vision and Pattern Recognition (CVPR)*, 2016, S. 2818–2826
- [TFNL22] TANNO, Ryutaro ; F.PRADIER, Melanie ; NORI, Aditya ; LI, Yingzhen: Repairing Neural Networks by Leaving the Right Past Behind. (2022), 07, S. 19. <http://dx.doi.org/10.48550/arXiv.2207.04806>. – DOI 10.48550/arXiv.2207.04806
- [WM21] WICKRAMARATNE, S. D. ; MAHMUD, M. S.: Conditional-GAN Based Data Augmentation for Deep Learning Task Classifier Improvement Using fNIRS Data. In: *Frontiers in Big Data* 4 (2021), S. 659146. <http://dx.doi.org/10.3389/fdata.2021.659146>. – DOI 10.3389/fdata.2021.659146

- [WWR⁺23] WANG, Hanyu ; WU, Pengxiang ; ROSA, Kevin D. ; WANG, Chen ; SHRIVASTAVA, Abhinav: *Multimodality-guided Image Style Transfer using Cross-modal GAN Inversion*. <https://arxiv.org/abs/2312.01671>. Version: 2023
- [WZZ⁺13] WAN, Li ; ZEILER, Matthew ; ZHANG, Sixin ; LE CUN, Yann ; FERGUS, Rob ; DASGUPTA, Sanjoy (Hrsg.) ; MCALLESTER, David (Hrsg.): *Regularization of Neural Networks using DropConnect*. <https://proceedings.mlr.press/v28/wan13.html>. Version: 17–19 Jun 2013 (Proceedings of Machine Learning Research)
- [XRV17] XIAO, Han ; RASUL, Kashif ; VOLLMGRAF, Roland: *Fashion-MNIST: a Novel Image Dataset for Benchmarking Machine Learning Algorithms*. 2017
- [XSCIV19] XU, Lei ; SKOULARIDOU, Maria ; CUESTA-INFANTE, Alfredo ; VEERA-MACHANENI, Kalyan: *Modeling Tabular data using Conditional GAN*. <https://arxiv.org/abs/1907.00503>. Version: 2019
- [Yin19] YING, Xue: An Overview of Overfitting and its Solutions. In: *Journal of Physics: Conference Series* 1168 (2019), feb, Nr. 2, 022022. <http://dx.doi.org/10.1088/1742-6596/1168/2/022022>. – DOI 10.1088/1742-6596/1168/2/022022
- [YZWY17] YU, Lantao ; ZHANG, Weinan ; WANG, Jun ; YU, Yong: *SeqGAN: Sequence Generative Adversarial Nets with Policy Gradient*. <https://arxiv.org/abs/1609.05473>. Version: 2017
- [ZCWD23] ZHAO, Gaochang ; CAI, Zhao ; WANG, Xin ; DANG, Xiaohu: GAN Data Augmentation Methods in Rock Classification. In: *Applied Sciences* 13 (2023), Nr. 9, S. 5316. <http://dx.doi.org/10.3390/app13095316>. – DOI 10.3390/app13095316

Appendix

8.1 Network Architectures

The following section includes graphical representations of NN referenced throughout the thesis.

8.1.1 Classifiers

The graphical representations of the network architectures are created with the tool *visual keras*, by Paul Gavrikov ([Gav20]).

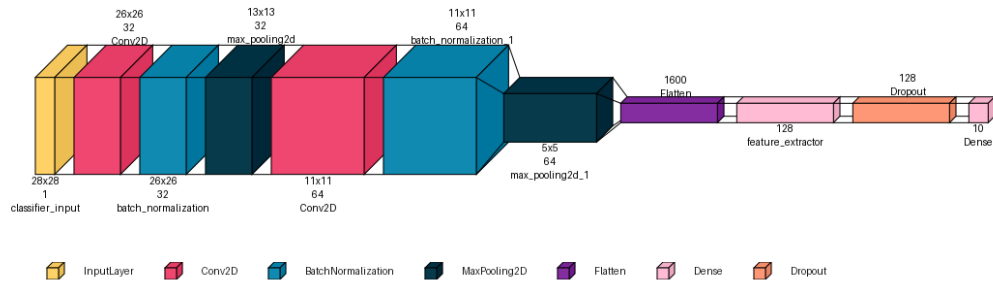


Figure 10: Depiction of the CNN achritecture used to classify unlabeled images from the MNIST GDA experiments and judge the effectiveness of said GDA. (Image created with [Gav20])

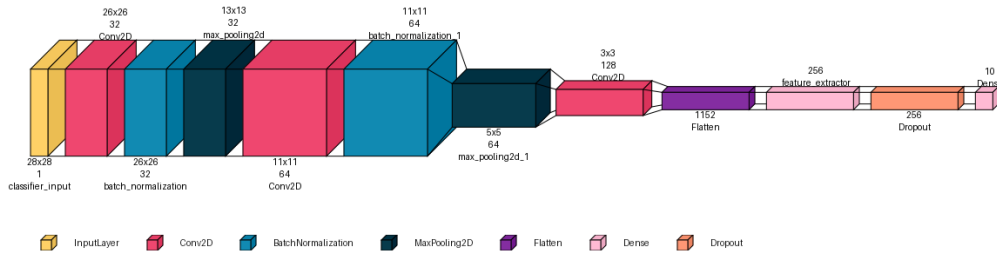


Figure 11: Depiction of the CNN achritecture used to classify unlabeled images from the FashionMNIST GDA experiments and judge the effectiveness of said GDA. (Image created with [Gav20])

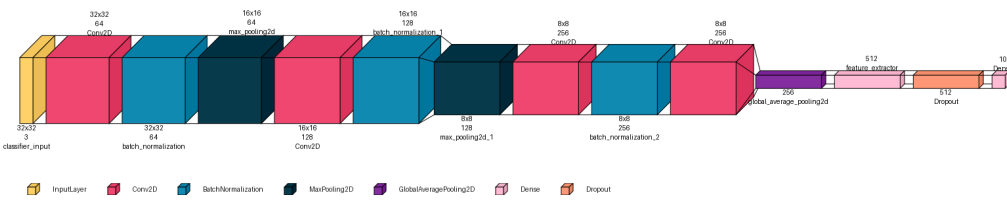


Figure 12: Depiction of the CNN achritecture used to classify unlabeled images from the CIFAR10 GDA experiments and judge the effectiveness of said GDA. (Image created with)

8.1.2 Generator Model Architectures

The graphical representations of the network architectures are created with the tool *visual keras*, by Paul Gavrikov ([Gav20]).

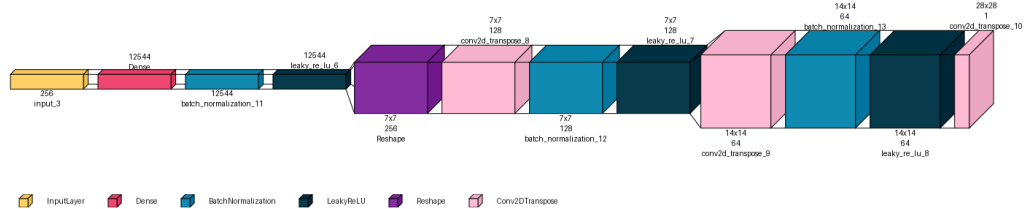


Figure 13: Depiction of the generator used in the deep convolutional GAN dependent experiments. Used to train a generator and create fake image data based on the MNIST dataset.

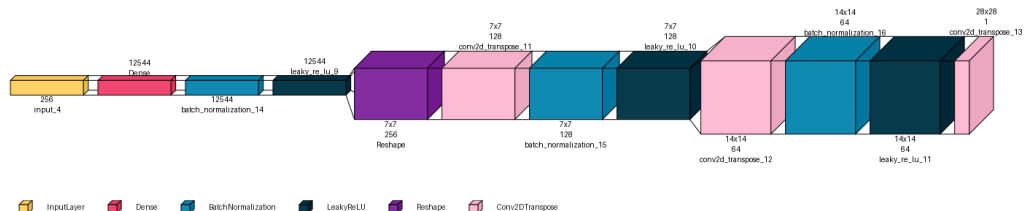


Figure 14: Depiction of the generator used in the deep convolutional GAN dependent experiments. Used to train a generator and create fake image data based on the Fashion-MNIST dataset.

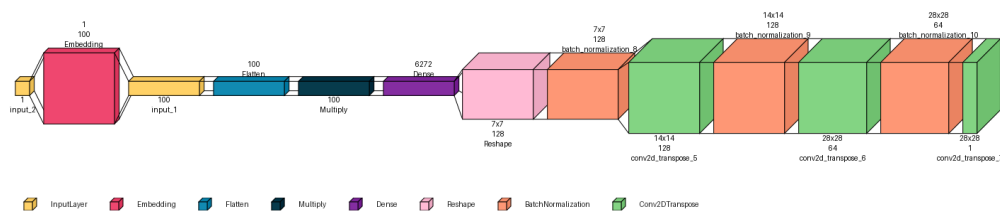


Figure 15: Depiction of the generator used in the Conditional GAN dependent experiments. Used to train a generator and create fake image data based on the MNIST and Fashion-MNIST datasets.

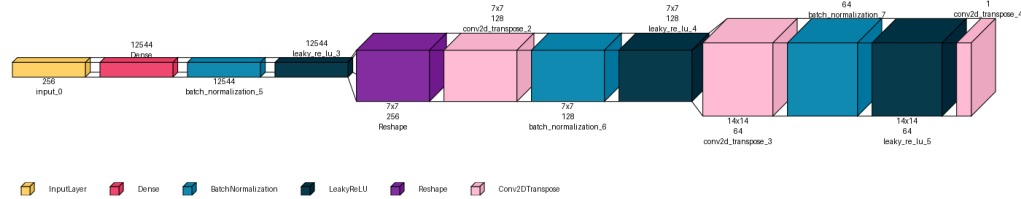


Figure 16: Depiction of the generators used in the MADGAN dependent experiments. Used to train a generator and create fake image data based on the MNIST and Fashion-

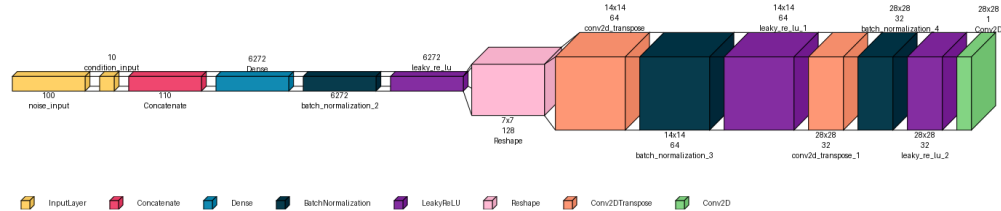


Figure 17: Depiction of the generators used in the cMADGAN dependent experiments. Used to train a generator and create fake image data based on the MNIST and Fashion-MNIST datasets.

8.1.3 Discriminator Model Architectures

The graphical representations of the network architectures are created with the tool *visual keras*, by Paul Gavrikov ([Gav20]).

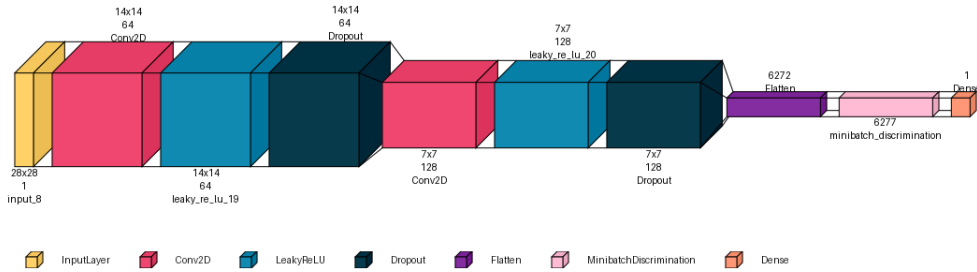


Figure 18: Depiction of the discriminator used in the deep convolutional GAN dependent experiments. Used to train a generator based on the MNIST dataset.

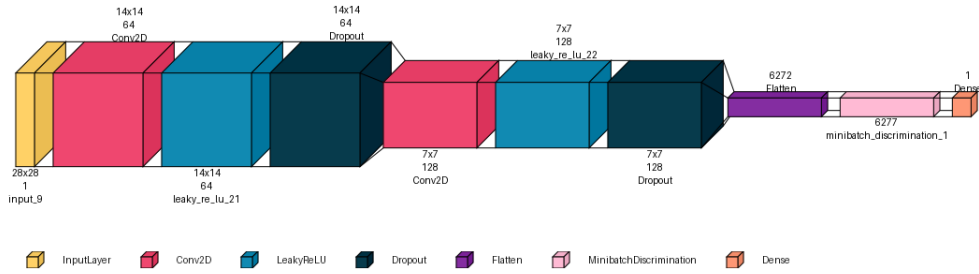


Figure 19: Depiction of the discriminator used in the deep convolutional GAN dependent experiments. Used to train a generator based on the Fashion-MNIST dataset.

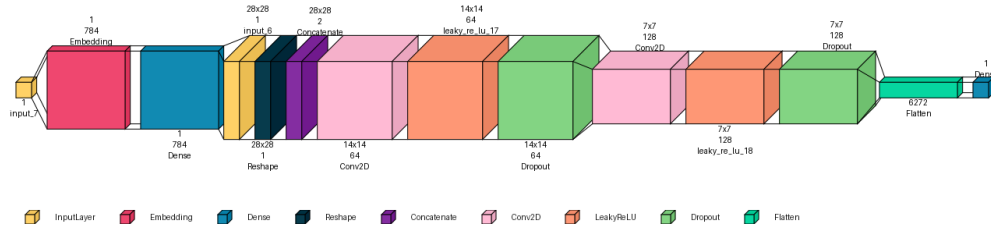


Figure 20: Depiction of the discriminator used in the Conditional GAN dependent experiments. Used to train a generator based on the MNIST and Fashion-MNIST datasets.

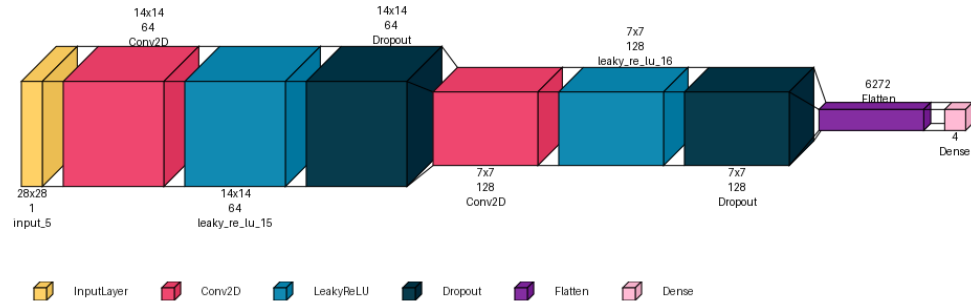


Figure 21: Depiction of the discriminator used in the MADGAN dependent experiments. Used to train a generator based on the MNIST and Fashion-MNIST datasets.

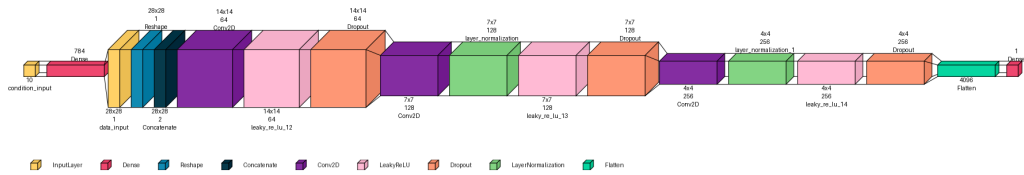


Figure 22: Depiction of the discriminator used in the cMADGAN dependent experiments. Used to train a generator based on the MNIST and Fashion-MNIST datasets.

8.2 FID and Inception Scores from MADGAN Architectures

8.2.1 MADGAN MNIST

N Generators	Index	FID	IS	IS-std
<i>Baseline</i>		-0.004	2.549	0.036
3	0	23.597	2.519	0.050
	1	22.682	2.506	0.027
	2	23.252	2.509	0.045
5	0	23.304	2.467	0.030
	1	22.020	2.446	0.040
	2	23.076	2.497	0.046
	3	22.265	2.467	0.060
	4	22.614	2.479	0.045
7	0	22.487	2.513	0.031
	1	21.076	2.548	0.087
	2	20.941	2.530	0.056
	3	22.250	2.520	0.035
	4	21.557	2.530	0.051
	5	21.297	2.545	0.035
	6	21.582	2.541	0.059
10	0	21.338	2.456	0.045
	1	20.872	2.462	0.040
	2	20.680	2.477	0.028
	3	21.315	2.470	0.030
	4	21.158	2.484	0.027
	5	20.655	2.473	0.037
	6	21.090	2.452	0.039
	7	20.689	2.508	0.048
	8	21.471	2.480	0.044
	9	20.459	2.477	0.036

Table 14: Effect of varying the number of generators ($N = 3, 5, 7, 10$) in the MADGAN model on FID and Inception Score (IS \pm Std Dev) for the **MNIST** dataset. Results for each generator index are presented alongside baseline metrics.

8.2.2 MADGAN Fashion MNIST

N Generators	Index	FID	IS	IS-std
<i>Baseline</i>		-0.004	4.723	0.056
3	0	26.086	4.463	0.103
	1	25.884	4.487	0.099
	2	26.637	4.538	0.094
5	0	23.393	4.467	0.119
	1	24.756	4.520	0.107
	2	25.663	4.506	0.123
	3	23.614	4.487	0.082
	4	23.665	4.504	0.061
7	0	22.370	4.558	0.111
	1	21.838	4.536	0.087
	2	21.923	4.508	0.101
	3	25.403	4.517	0.112
	4	31.493	4.372	0.087
	5	22.158	4.595	0.075
	6	21.942	4.577	0.087
10	0	22.454	4.534	0.117
	1	21.914	4.524	0.121
	2	21.327	4.494	0.089
	3	21.630	4.455	0.063
	4	20.851	4.575	0.097
	5	21.268	4.561	0.048
	6	22.324	4.566	0.127
	7	21.633	4.542	0.084
	8	21.503	4.533	0.127
	9	20.963	4.552	0.100

Table 15: Effect of varying the number of generators ($N = 3, 5, 7, 10$) in the MADGAN model on FID and Inception Score (IS \pm Std Dev) for the **Fashion MNIST** dataset. Results for each generator index are presented alongside baseline metrics.

8.2.3 cMADGAN MNIST

N Generators	Index	FID	IS	IS-std
<i>Baseline</i>		-0.004	2.549	0.036
3	0	30.105	2.494	0.034
	1	23.875	2.317	0.041
	2	22.753	2.384	0.032
5	0	37.638	2.460	0.039
	1	26.614	2.378	0.052
	2	26.739	2.356	0.025
	3	27.642	2.309	0.034
	4	26.722	2.246	0.043
7	0	23.141	2.418	0.037
	1	28.071	2.363	0.036
	2	33.490	2.340	0.033
	3	28.333	2.347	0.031
	4	35.599	2.296	0.050
	5	36.075	2.389	0.047
	6	29.807	2.326	0.036
10	0	108.079	2.076	0.011
	1	82.478	2.250	0.022
	2	153.369	2.124	0.023
	3	126.574	1.846	0.005
	4	110.012	2.005	0.013
	5	130.054	1.861	0.009
	6	103.016	2.010	0.011
	7	74.926	2.383	0.035
	8	110.265	2.086	0.014
	9	106.762	1.975	0.033

Table 16: Effect of varying the number of generators ($N = 3, 5, 7, 10$) in the cMADGAN model on FID and Inception Score (IS \pm Std Dev) for the **MNIST** dataset. Results for each generator index are presented alongside baseline metrics.

8.2.4 cMADGAN Fashion MNIST

N Generators	Index	FID	IS	IS-std
<i>Baseline</i>		-0.004	4.723	0.056
3	0	25.874	4.750	0.132
	1	27.235	4.068	0.090
	2	23.556	5.049	0.093
5	0	170.120	2.938	0.020
	1	167.446	3.430	0.052
	2	221.934	3.325	0.032
	3	187.293	3.269	0.029
	4	53.616	3.770	0.057
7	0	156.601	2.392	0.016
	1	172.054	3.325	0.033
	2	171.505	2.754	0.024
	3	97.514	3.273	0.058
	4	155.474	3.157	0.063
	5	151.494	2.623	0.018
	6	174.161	2.976	0.028
10	0	147.670	3.650	0.037
	1	167.407	2.816	0.026
	2	109.349	3.914	0.068
	3	160.305	3.674	0.040
	4	181.778	2.961	0.023
	5	154.633	3.297	0.022
	6	166.511	2.759	0.034
	7	156.135	3.173	0.027
	8	155.758	3.853	0.036
	9	191.126	3.073	0.034

Table 17: Effect of varying the number of generators ($N = 3, 5, 7, 10$) in the cMADGAN model on FID and Inception Score (IS \pm Std Dev) for the **Fashion MNIST** dataset. Results for each generator index are presented alongside baseline metrics.

8.2.5 DC MNIST

N Generators	FID	IS	IS-std
<i>Baseline</i>	-0.004	2.549	0.036
1	122.097	2.611	0.056

Table 18: FID and Inception Score (Mean \pm Std Dev) for a single DCGAN generator ($N = 1$) trained on the **MNIST** dataset. Baseline scores are included for reference.

8.2.6 DC Fashion MNIST

N Generators	FID	IS	IS-std
<i>Baseline</i>	-0.004	4.723	0.056
1	123.349	3.573	0.117

Table 19: FID and Inception Score (Mean \pm Std Dev) for a single DCGAN generator ($N = 1$) trained on the **Fashion MNIST** dataset. Baseline scores are included for reference.

8.2.7 Conditional MNIST

N Generators	FID	IS	IS-std
<i>Baseline</i>	-0.004	2.549	0.036
1	28.721	2.553	0.022

Table 20: FID and Inception Score (Mean \pm Std Dev) for a single Conditional GAN generator ($N = 1$) trained on the **MNIST** dataset. Baseline scores are included for reference.

8.2.8 Conditional Fashion MNIST

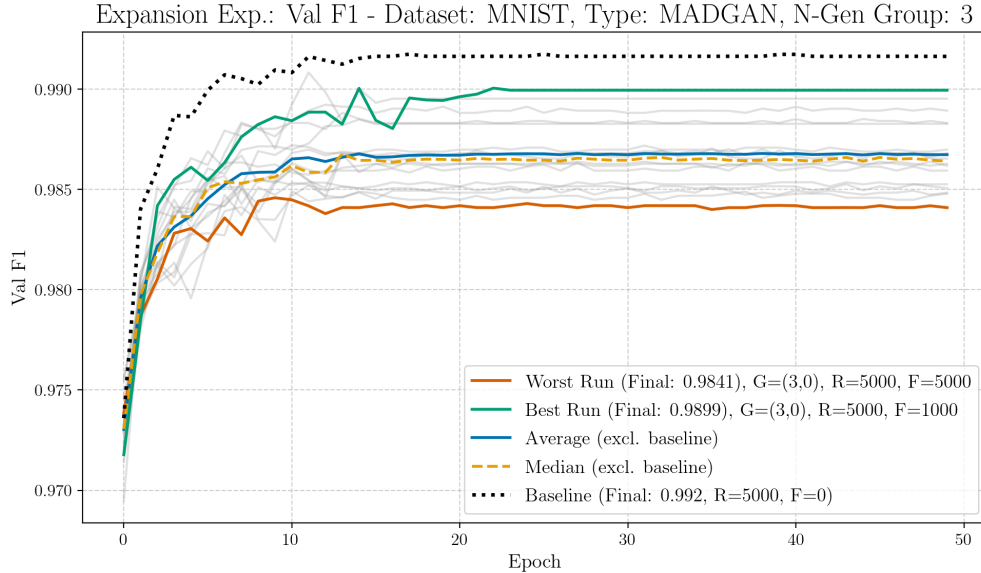
N Generators	FID	IS	IS-std
<i>Baseline</i>	-0.004	4.723	0.056
1	25.560	4.210	0.099

Table 21: FID and Inception Score (Mean \pm Std Dev) for a single Conditional GAN generator ($N = 1$) trained on the **Fashion MNIST** dataset. Baseline scores are included for reference.

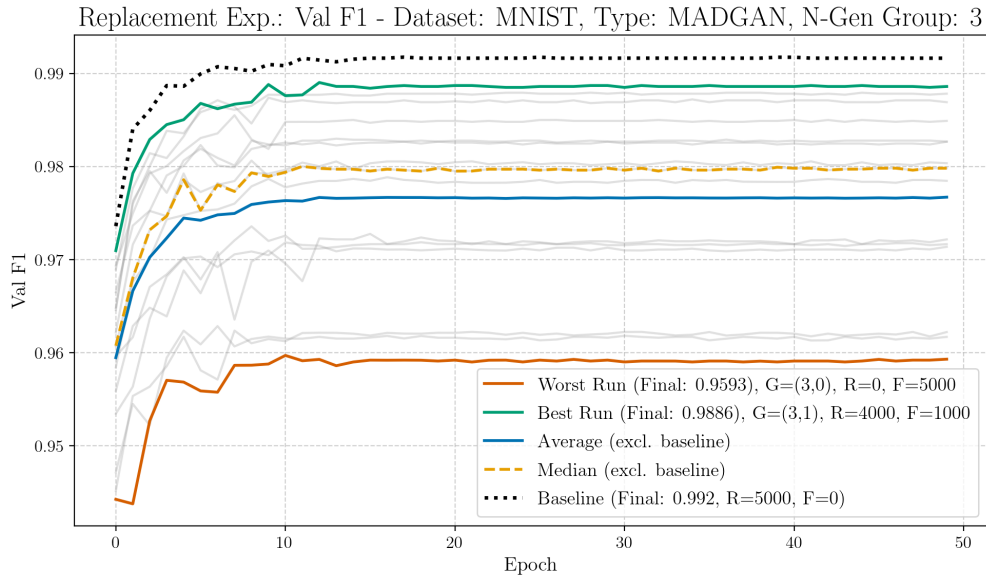
8.3 Stratified Classifier Performances and Graphs

8.3.1 Dataset: MNIST, Architecture: MADGAN

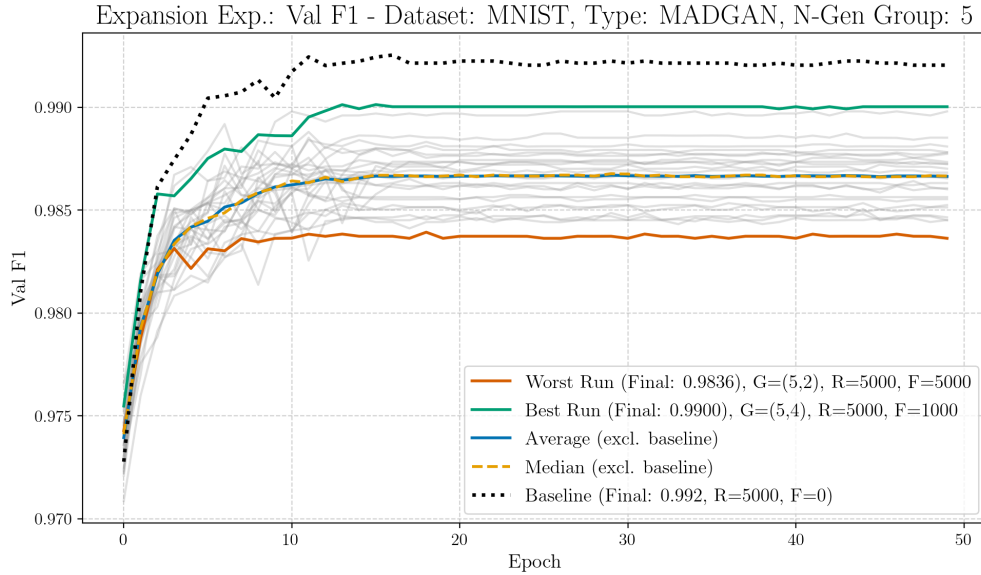
Expansion Experiment: K=3



Replacement Experiment: K=3

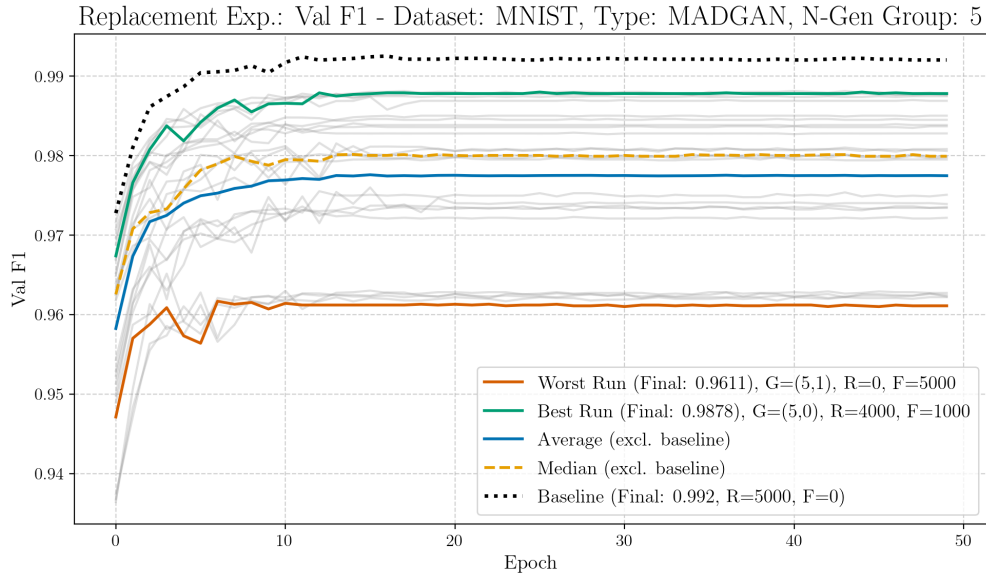


Expansion Experiment: K=5



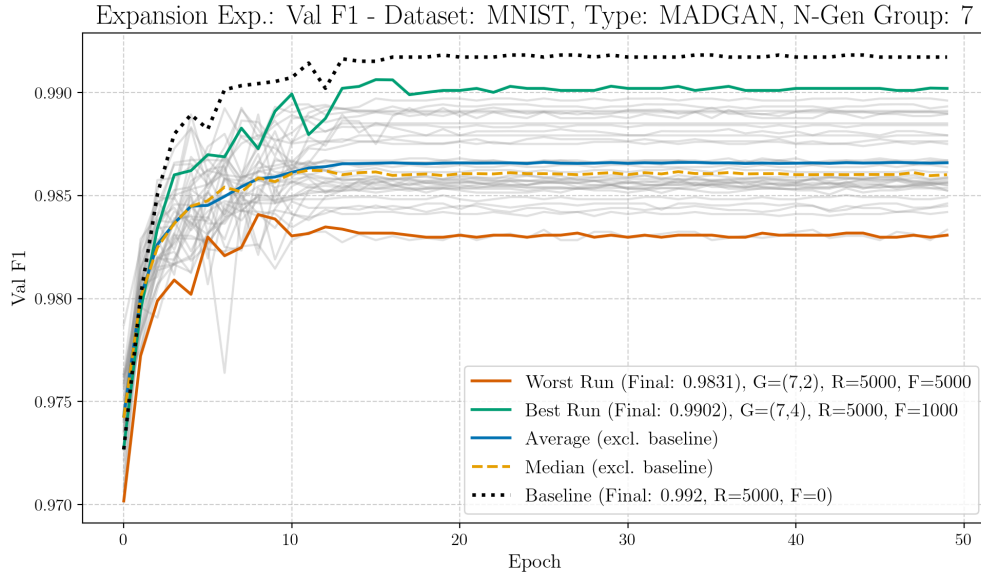
Run Type	Experiment	Val F1
best	$G_{5,4}$, R:5000, F:1000	0.9900
worst	$G_{5,2}$, R:5000, F:5000	0.9836
median	G (K=5)	0.9867
average	G (K=5)	0.9866

Replacement Experiment: K=5



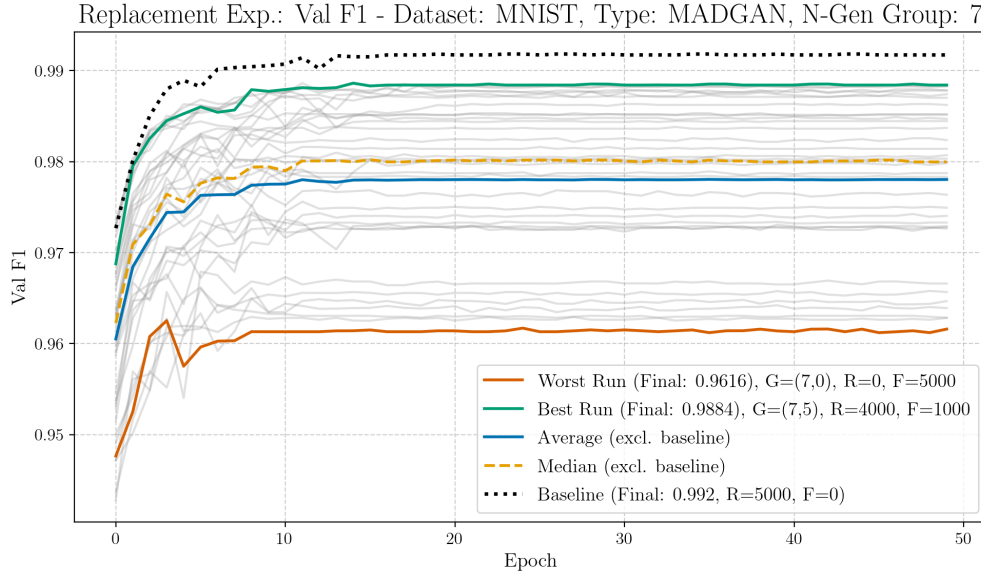
Run Type	Experiment	Val F1
best	$G_{5,0}$, R:4000, F:1000	0.9878
worst	$G_{5,1}$, R:0, F:5000	0.9611
median	G (K=5)	0.9799
average	G (K=5)	0.9775

Expansion Experiment: K=7



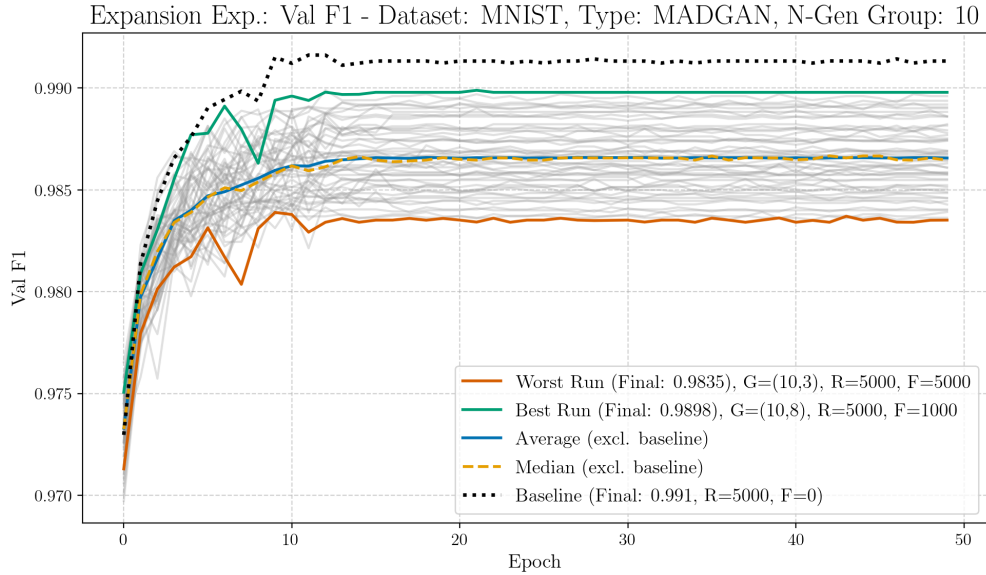
Run Type	Experiment	Val F1
best	$G_{7,4}$, R:5000, F:1000	0.9902
worst	$G_{7,2}$, R:5000, F:5000	0.9831
median	G (K=7)	0.9860
average	G (K=7)	0.9866

Replacement Experiment: K=7



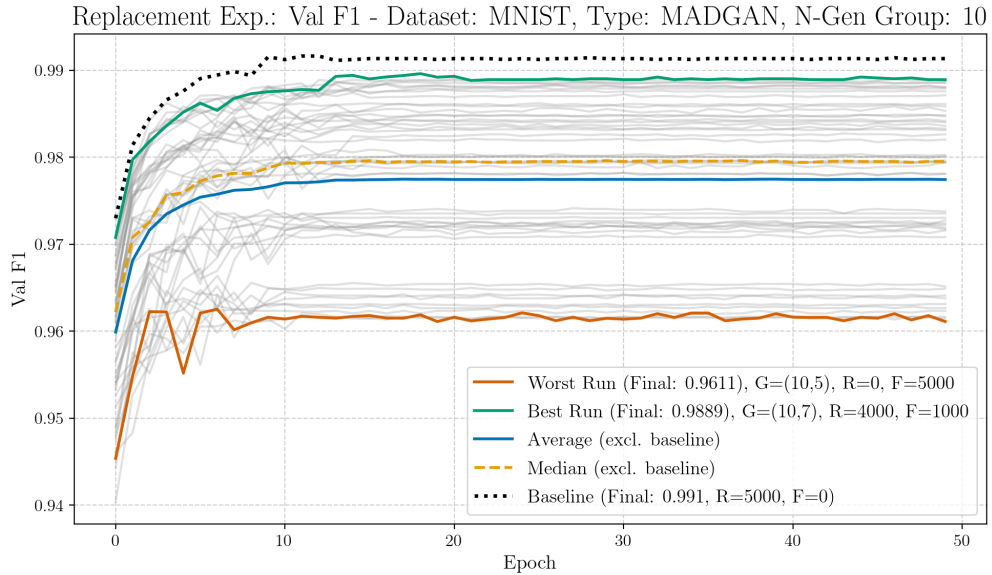
Run Type	Experiment	Val F1
best	$G_{7,5}$, R:4000, F:1000	0.9884
worst	$G_{7,0}$, R:0, F:5000	0.9616
median	G (K=7)	0.9800
average	G (K=7)	0.9780

Expansion Experiment: K=10



Run Type	Experiment	Val F1
best	$G_{10,8}$, R:5000, F:1000	0.9898
worst	$G_{10,3}$, R:5000, F:5000	0.9835
median	G (K=10)	0.9865
average	G (K=10)	0.9866

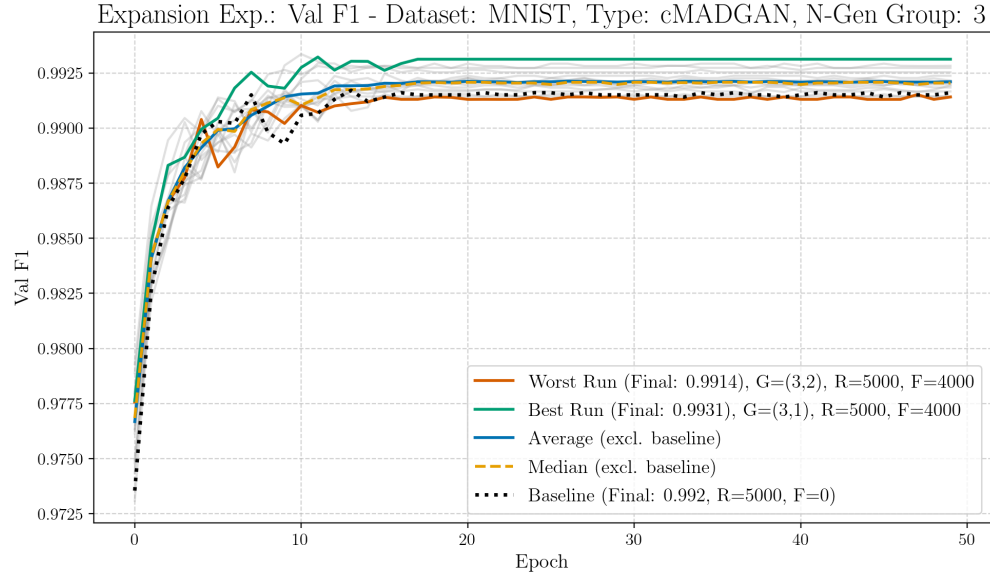
Replacement Experiment: K=10



Run Type	Experiment	Val F1
best	$G_{10,7}$, R:4000, F:1000	0.9889
worst	$G_{10,5}$, R:0, F:5000	0.9611
median	G (K=10)	0.9795
average	G (K=10)	0.9774

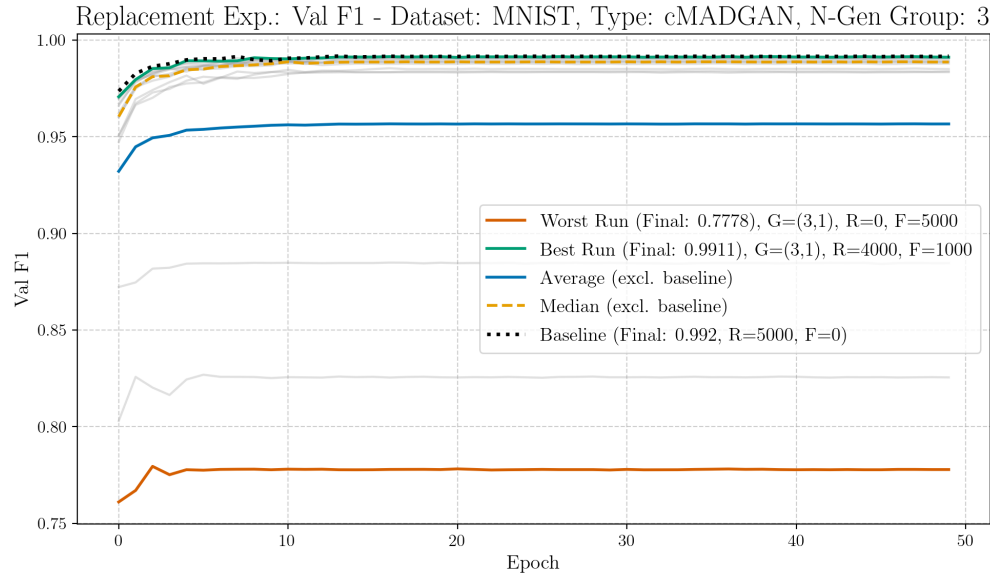
8.3.2 Dataset: MNIST, Architecture: cMADGAN

Expansion Experiment: K=3



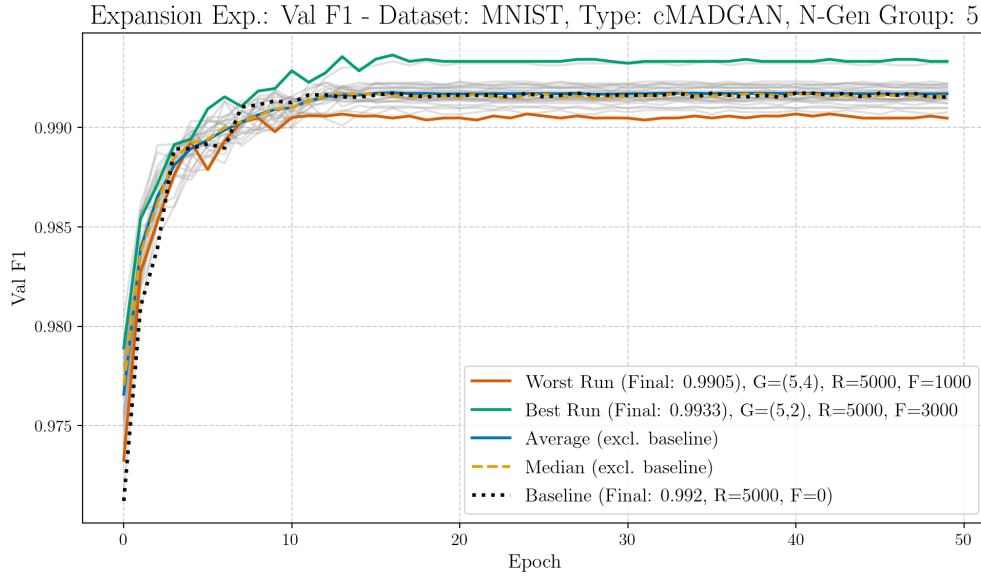
Run Type	Experiment	Val F1
best	$G_{3,1}$, R:5000, F:4000	0.9931
worst	$G_{3,2}$, R:5000, F:4000	0.9914
median	G (K=3)	0.9920
average	G (K=3)	0.9921

Replacement Experiment: K=3



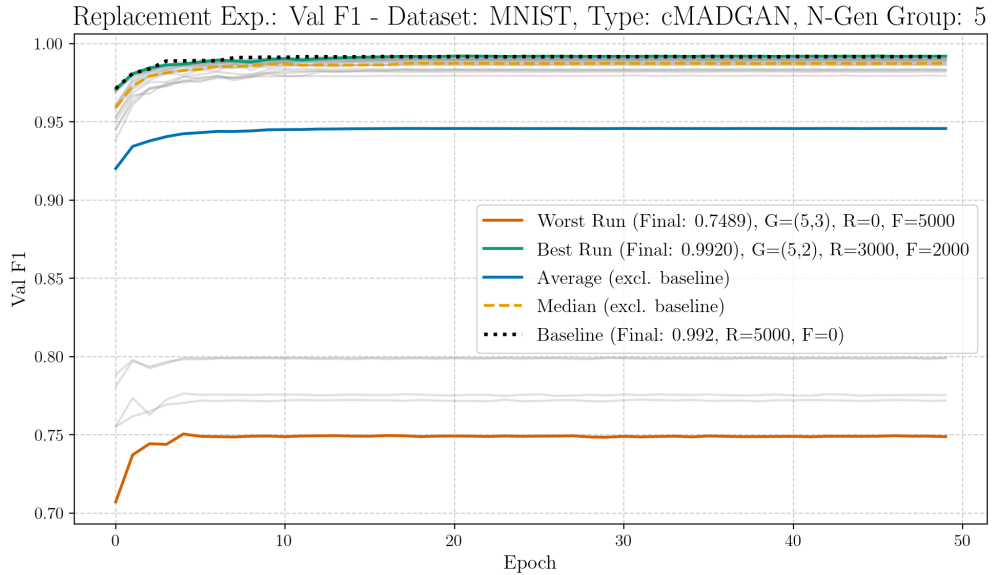
Run Type	Experiment	Val F1
best	$G_{3,1}$, R:4000, F:1000	0.9911
worst	$G_{3,1}$, R:0, F:5000	0.7778
median	G (K=3)	0.9886
average	G (K=3)	0.9566

Expansion Experiment: K=5



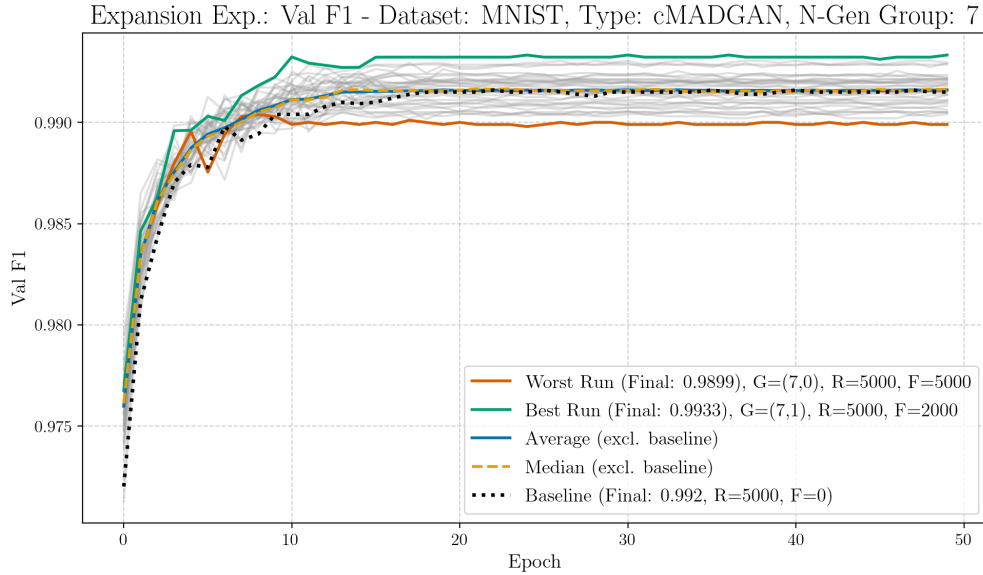
Run Type	Experiment	Val F1
best	$G_{5,2}$, R:5000, F:3000	0.9933
worst	$G_{5,4}$, R:5000, F:1000	0.9905
median	G (K=5)	0.9916
average	G (K=5)	0.9917

Replacement Experiment: K=5



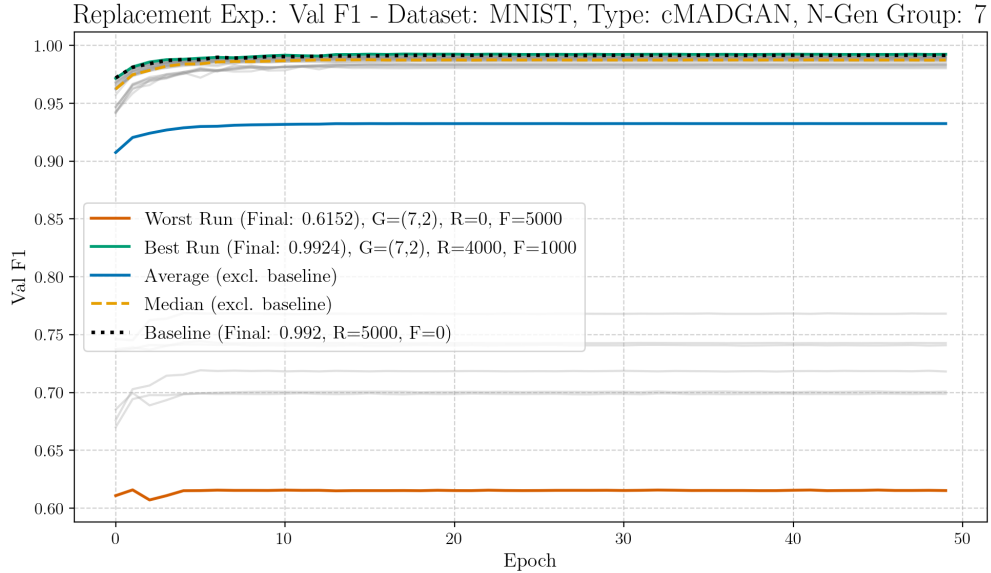
Run Type	Experiment	Val F1
best	$G_{5,2}$, R:3000, F:2000	0.9920
worst	$G_{5,3}$, R:0, F:5000	0.7489
median	G (K=5)	0.9874
average	G (K=5)	0.9458

Expansion Experiment: K=7



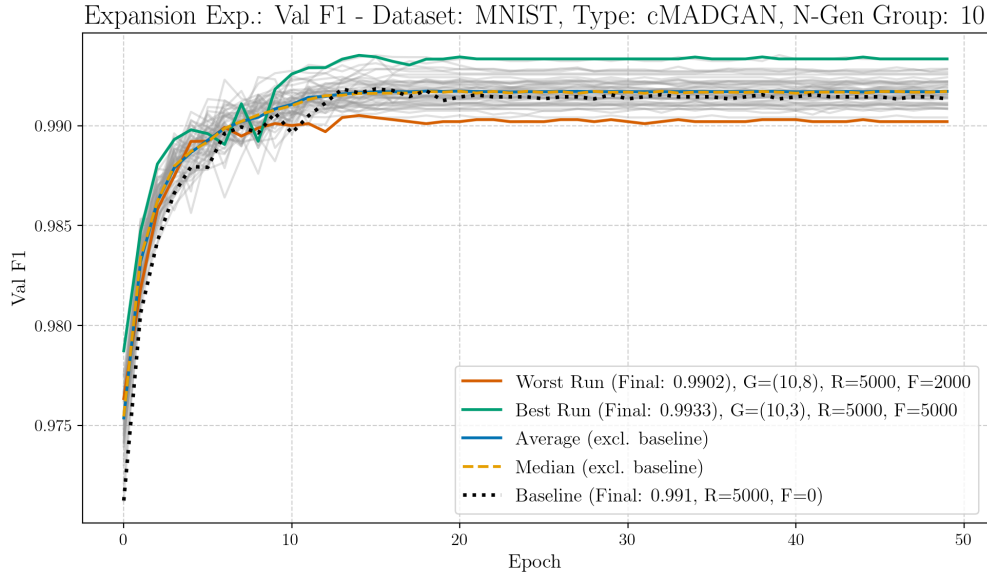
Run Type	Experiment	Val F1
best	$G_{7,1}$, R:5000, F:2000	0.9933
worst	$G_{7,0}$, R:5000, F:5000	0.9899
median	G (K=7)	0.9916
average	G (K=7)	0.9916

Replacement Experiment: K=7



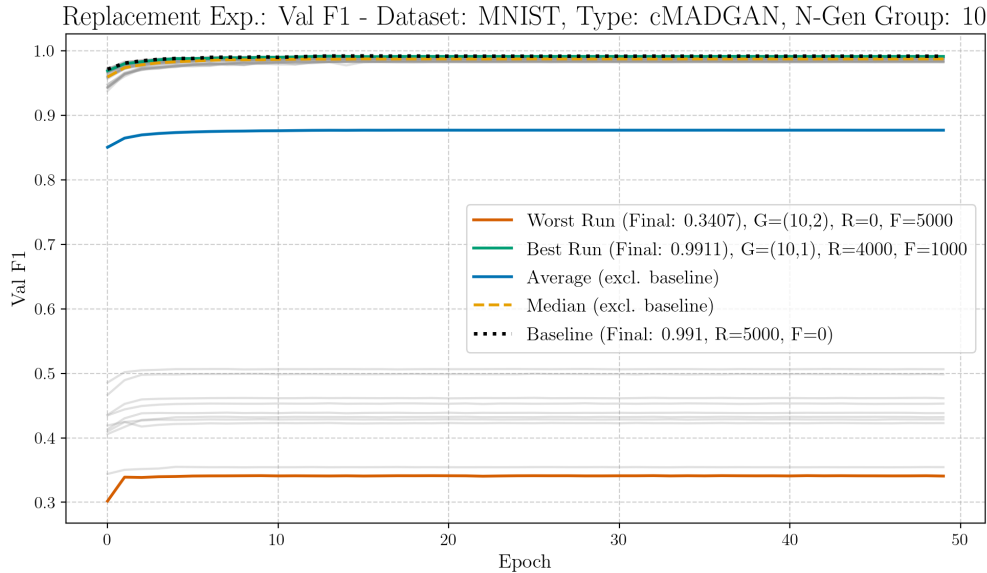
Run Type	Experiment	Val F1
best	$G_{7,2}$, R:4000, F:1000	0.9924
worst	$G_{7,2}$, R:0, F:5000	0.6152
median	G (K=7)	0.9874
average	G (K=7)	0.9325

Expansion Experiment: K=10



Run Type	Experiment	Val F1
best	$G_{10,3}$, R:5000, F:5000	0.9933
worst	$G_{10,8}$, R:5000, F:2000	0.9902
median	G (K=10)	0.9917
average	G (K=10)	0.9917

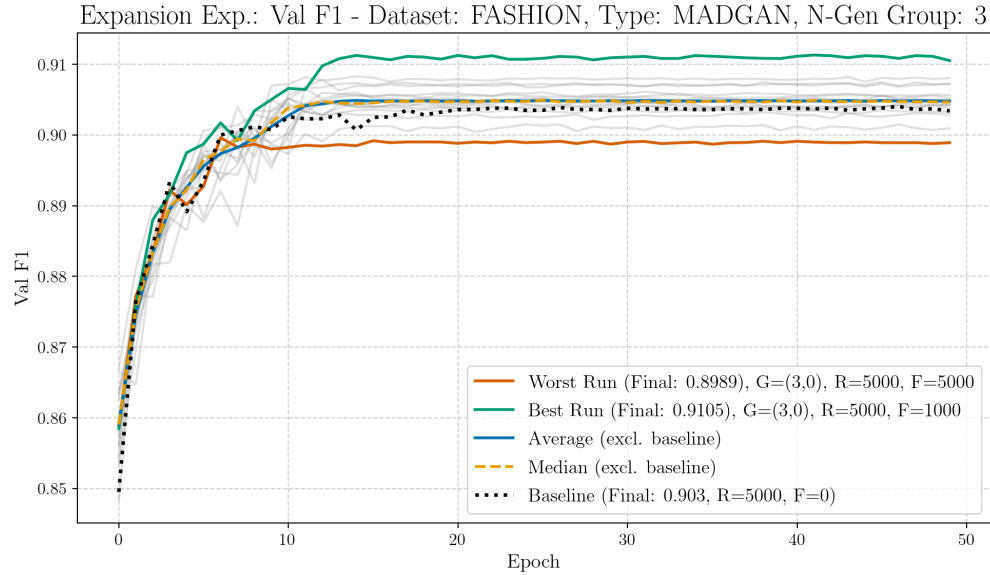
Replacement Experiment: K=10



Run Type	Experiment	Val F1
best	$G_{10,1}$, R:4000, F:1000	0.9911
worst	$G_{10,2}$, R:0, F:5000	0.3407
median	G (K=10)	0.9872
average	G (K=10)	0.8768

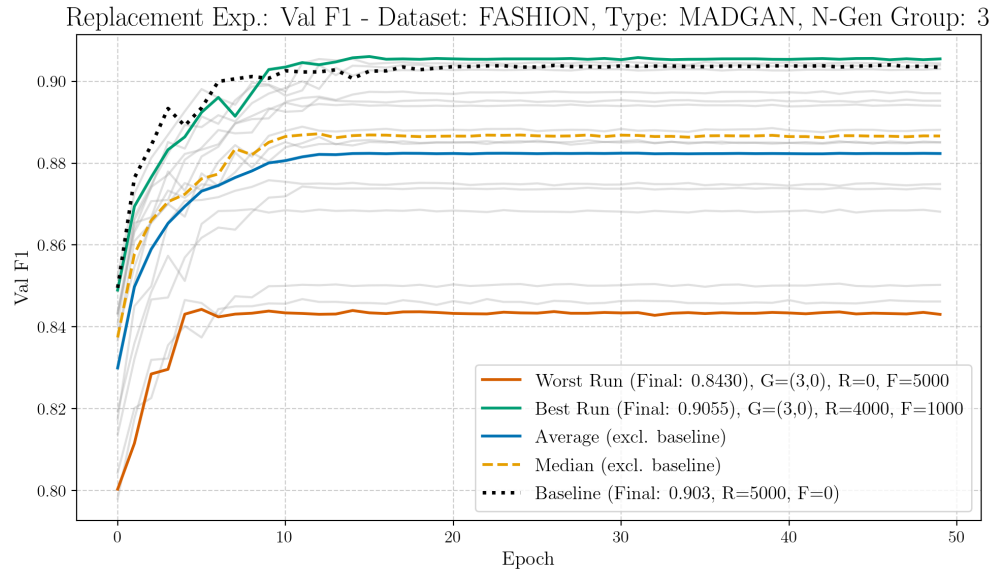
8.3.3 Dataset: FASHION, Architecture: MADGAN

Expansion Experiment: K=3



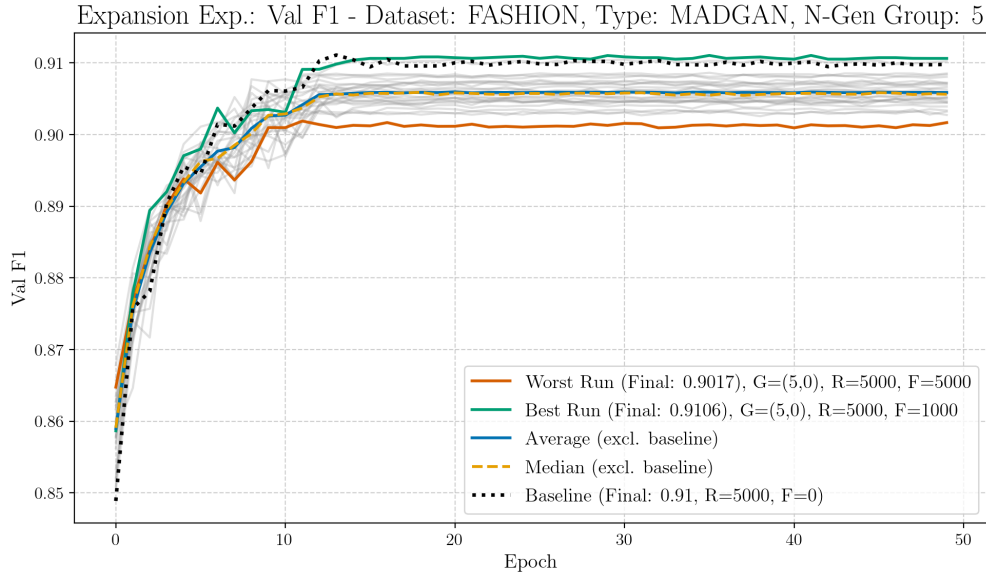
Run Type	Experiment	Val F1
best	$G_{3,0}$, R:5000, F:1000	0.9105
worst	$G_{3,0}$, R:5000, F:5000	0.8989
median	G (K=3)	0.9046
average	G (K=3)	0.9048

Replacement Experiment: K=3



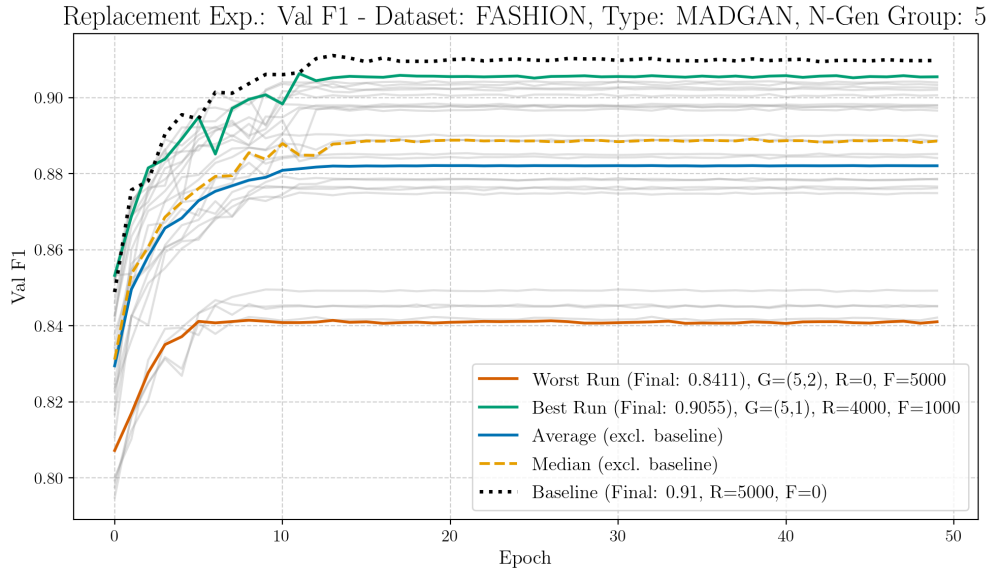
Run Type	Experiment	Val F1
best	$G_{3,0}$, R:4000, F:1000	0.9055
worst	$G_{3,0}$, R:0, F:5000	0.8430
median	G (K=3)	0.8866
average	G (K=3)	0.8824

Expansion Experiment: K=5



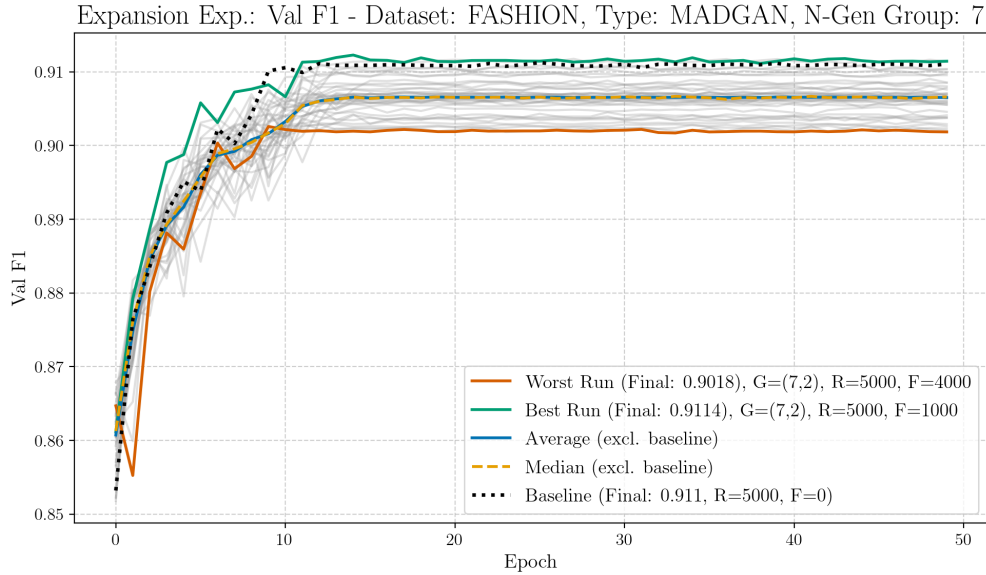
Run Type	Experiment	Val F1
best	$G_{5,0}$, R:5000, F:1000	0.9106
worst	$G_{5,0}$, R:5000, F:5000	0.9017
median	G (K=5)	0.9056
average	G (K=5)	0.9059

Replacement Experiment: K=5



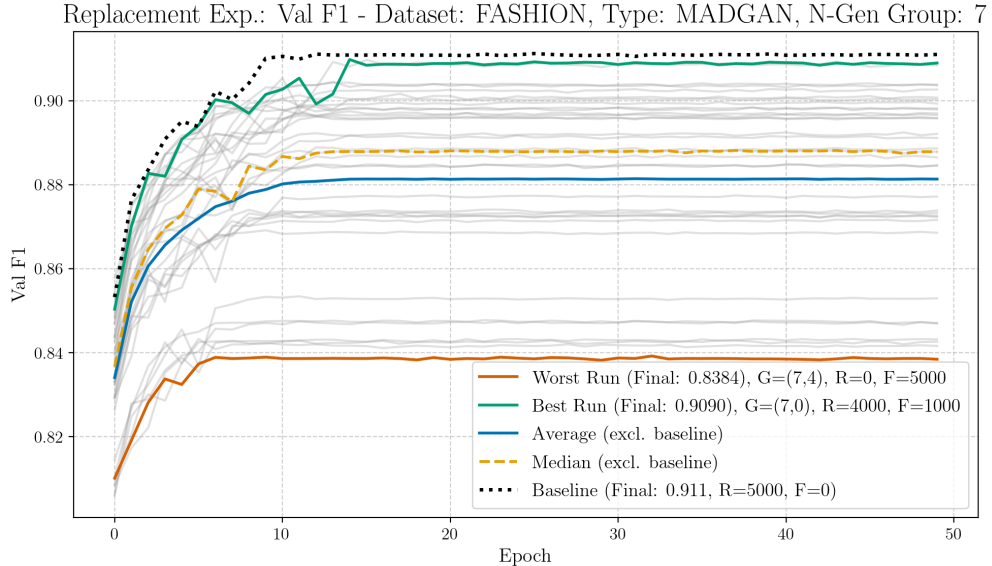
Run Type	Experiment	Val F1
best	$G_{5,1}$, R:4000, F:1000	0.9055
worst	$G_{5,2}$, R:0, F:5000	0.8411
median	G (K=5)	0.8886
average	G (K=5)	0.8821

Expansion Experiment: K=7



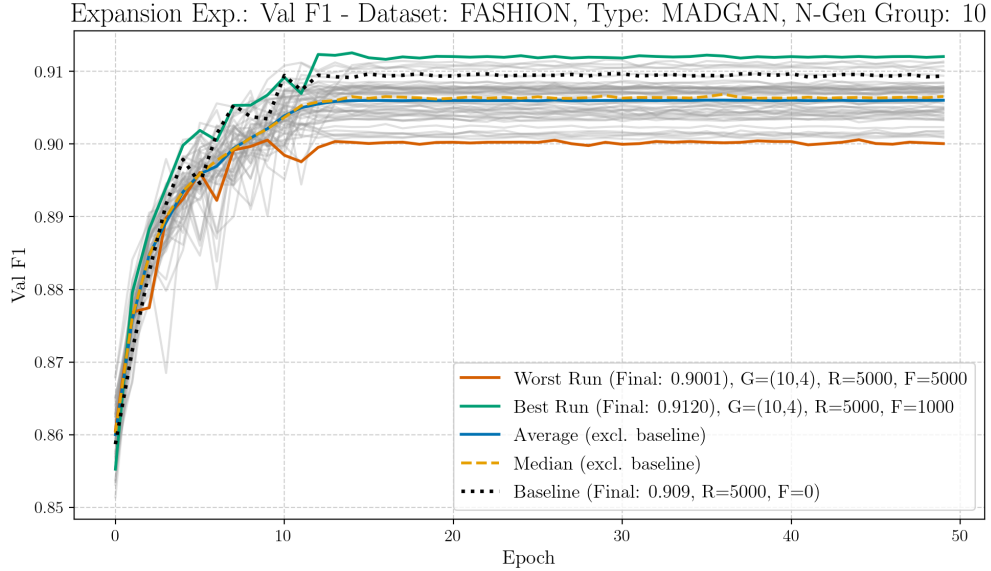
Run Type	Experiment	Val F1
best	$G_{7,2}$, R:5000, F:1000	0.9114
worst	$G_{7,2}$, R:5000, F:4000	0.9018
median	G (K=7)	0.9066
average	G (K=7)	0.9065

Replacement Experiment: K=7



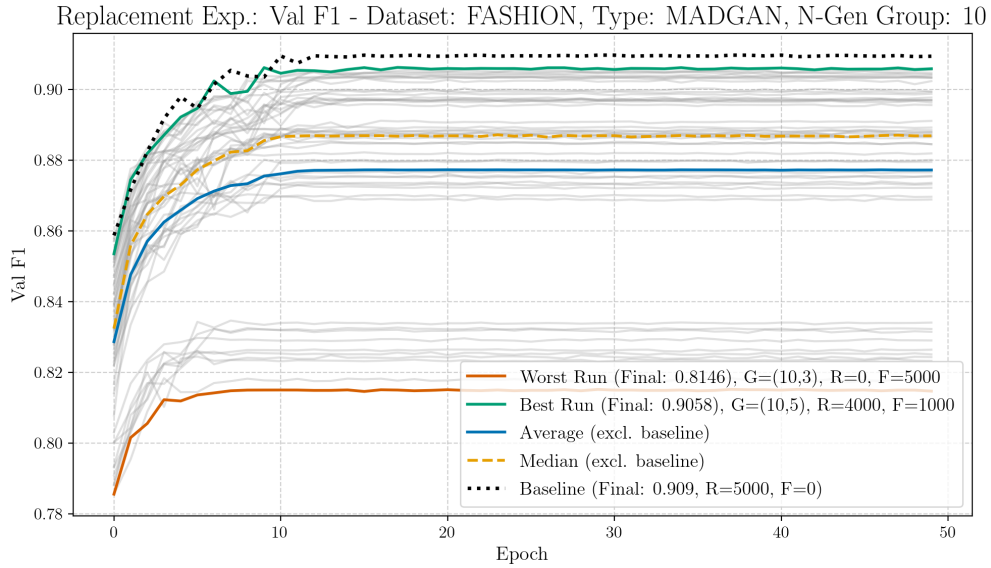
Run Type	Experiment	Val F1
best	$G_{7,0}$, R:4000, F:1000	0.9090
worst	$G_{7,4}$, R:0, F:5000	0.8384
median	G (K=7)	0.8879
average	G (K=7)	0.8813

Expansion Experiment: K=10



Run Type	Experiment	Val F1
best	$G_{10,4}$, R:5000, F:1000	0.9120
worst	$G_{10,4}$, R:5000, F:5000	0.9001
median	G (K=10)	0.9066
average	G (K=10)	0.9060

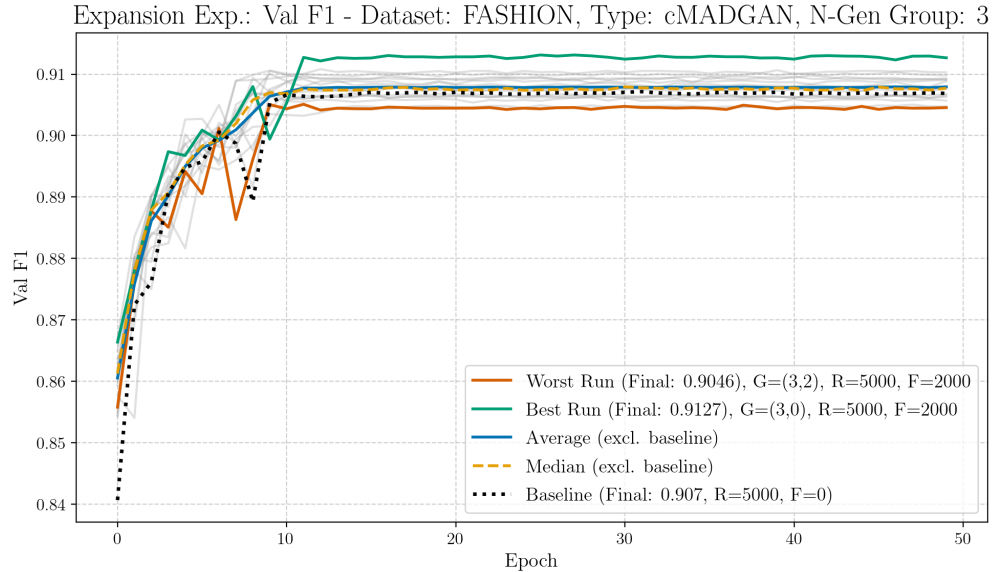
Replacement Experiment: K=10



Run Type	Experiment	Val F1
best	$G_{10,5}$, R:4000, F:1000	0.9058
worst	$G_{10,3}$, R:0, F:5000	0.8146
median	G (K=10)	0.8869
average	G (K=10)	0.8772

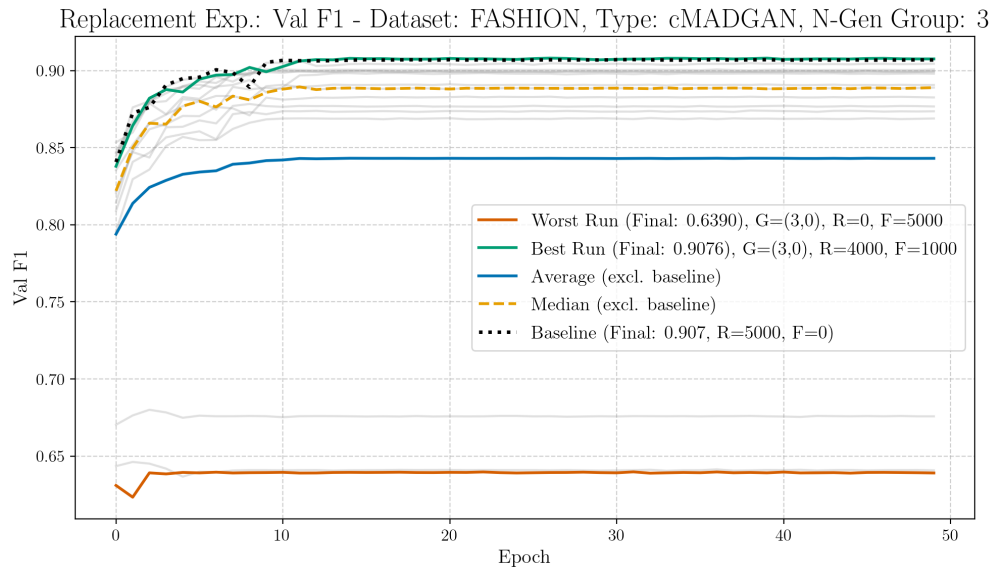
8.3.4 Dataset: FASHION, Architecture: cMADGAN

Expansion Experiment: K=3



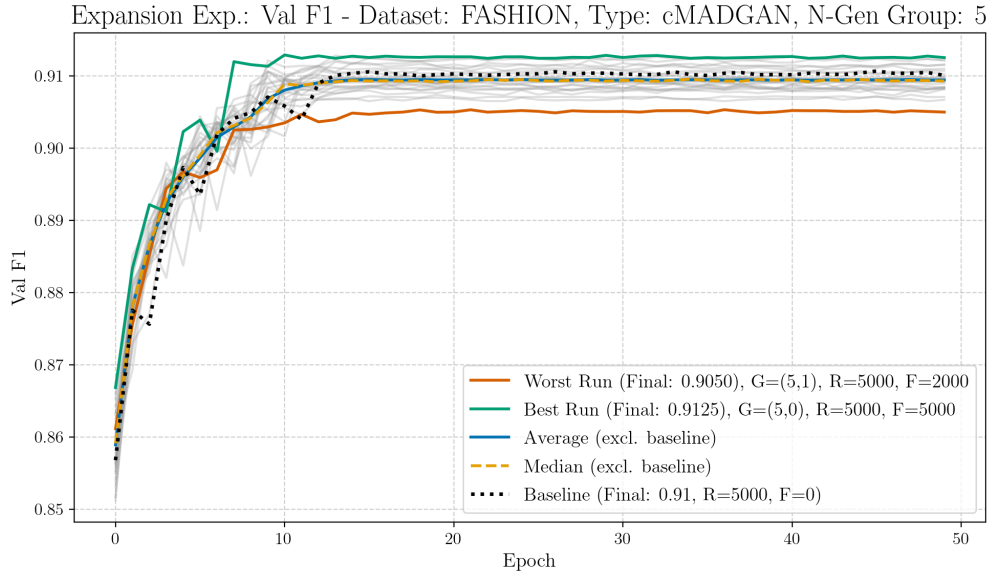
Run Type	Experiment	Val F1
best	$G_{3,0}$, R:5000, F:2000	0.9127
worst	$G_{3,2}$, R:5000, F:2000	0.9046
median	G (K=3)	0.9077
average	G (K=3)	0.9079

Replacement Experiment: K=3



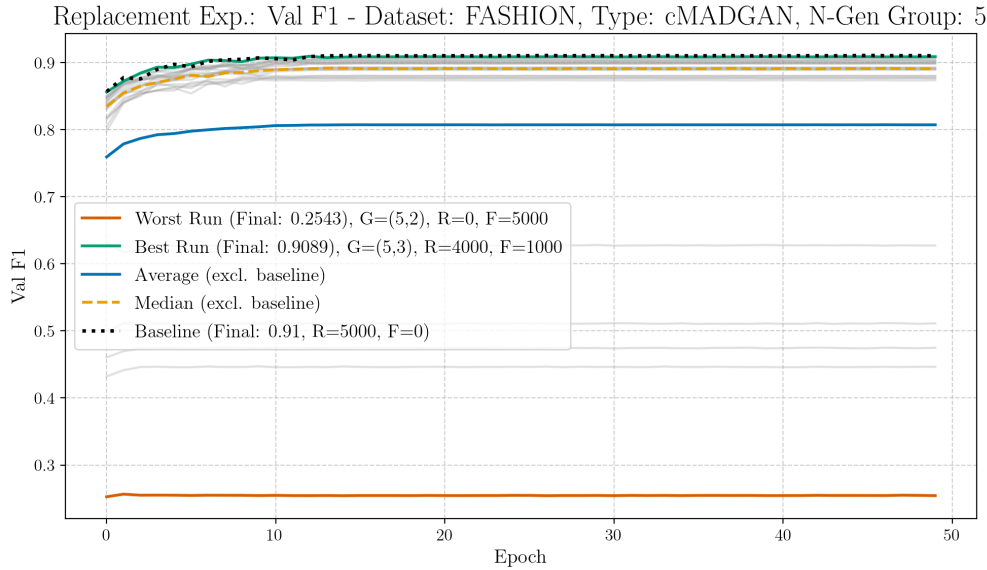
Run Type	Experiment	Val F1
best	$G_{3,0}$, R:4000, F:1000	0.9076
worst	$G_{3,0}$, R:0, F:5000	0.6390
median	G (K=3)	0.8890
average	G (K=3)	0.8431

Expansion Experiment: K=5



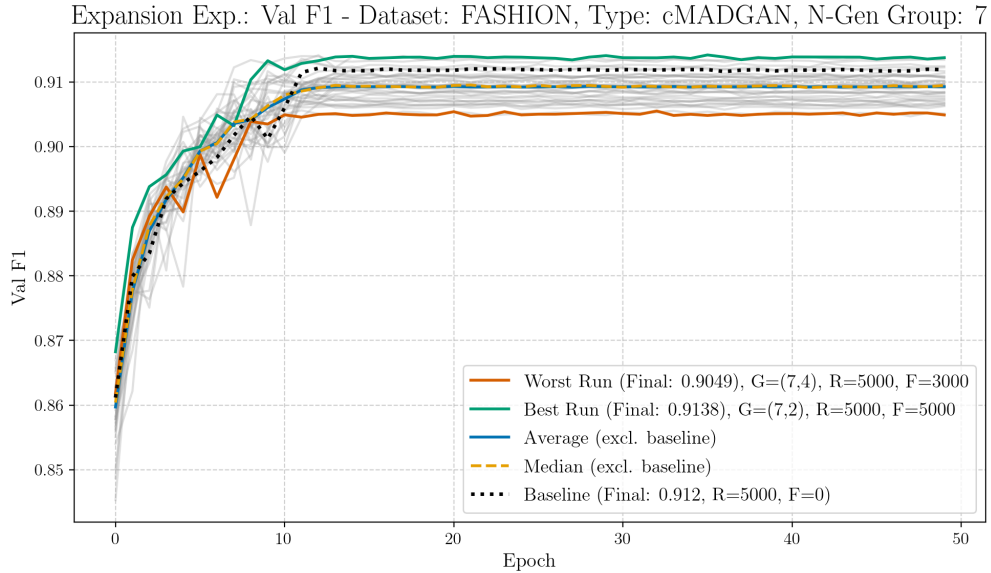
Run Type	Experiment	Val F1
best	$G_{5,0}$, R:5000, F:5000	0.9125
worst	$G_{5,1}$, R:5000, F:2000	0.9050
median	G (K=5)	0.9093
average	G (K=5)	0.9094

Replacement Experiment: K=5



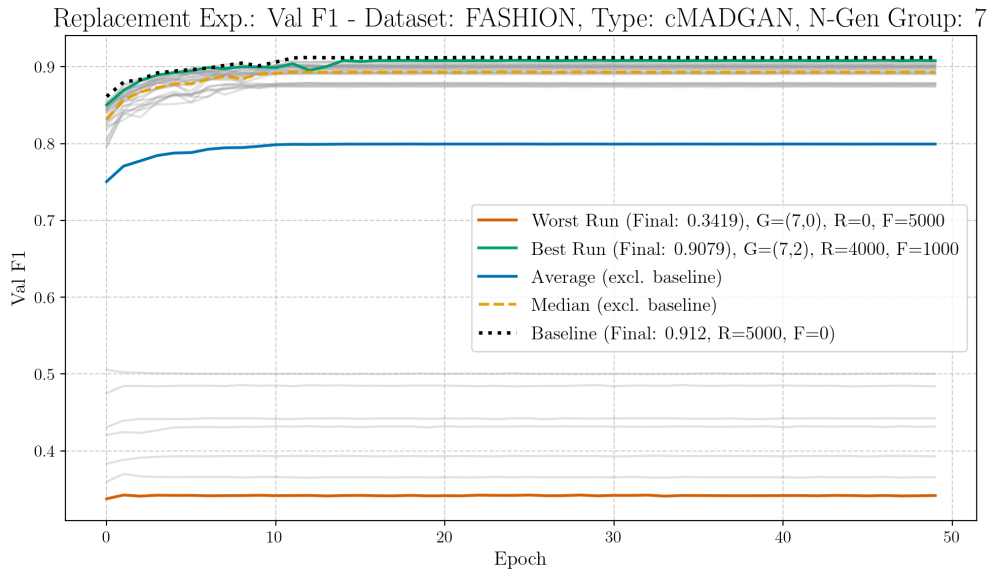
Run Type	Experiment	Val F1
best	$G_{5,3}$, R:4000, F:1000	0.9089
worst	$G_{5,2}$, R:0, F:5000	0.2543
median	G (K=5)	0.8909
average	G (K=5)	0.8072

Expansion Experiment: K=7



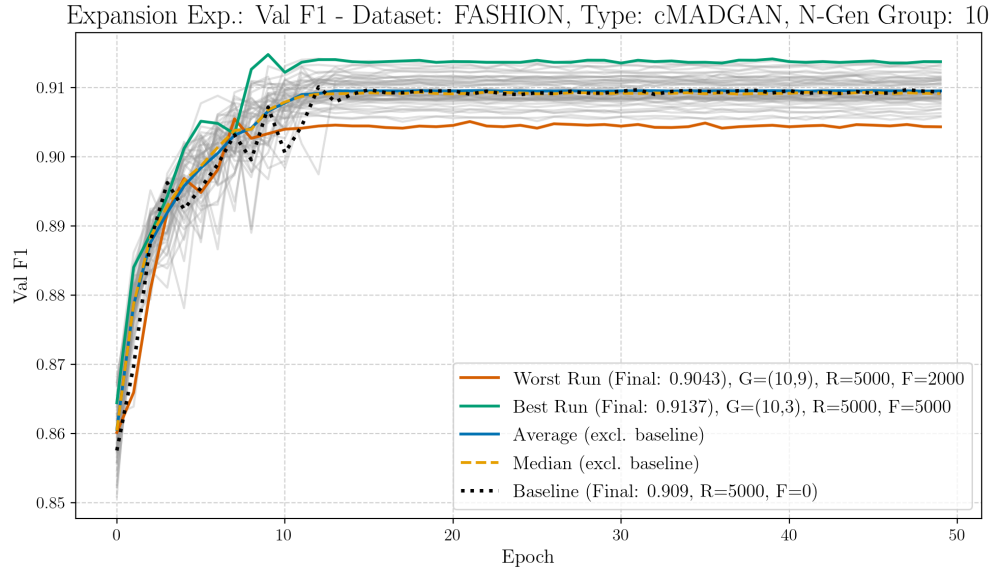
Run Type	Experiment	Val F1
best	$G_{7,2}$, R:5000, F:5000	0.9138
worst	$G_{7,4}$, R:5000, F:3000	0.9049
median	G (K=7)	0.9095
average	G (K=7)	0.9093

Replacement Experiment: K=7



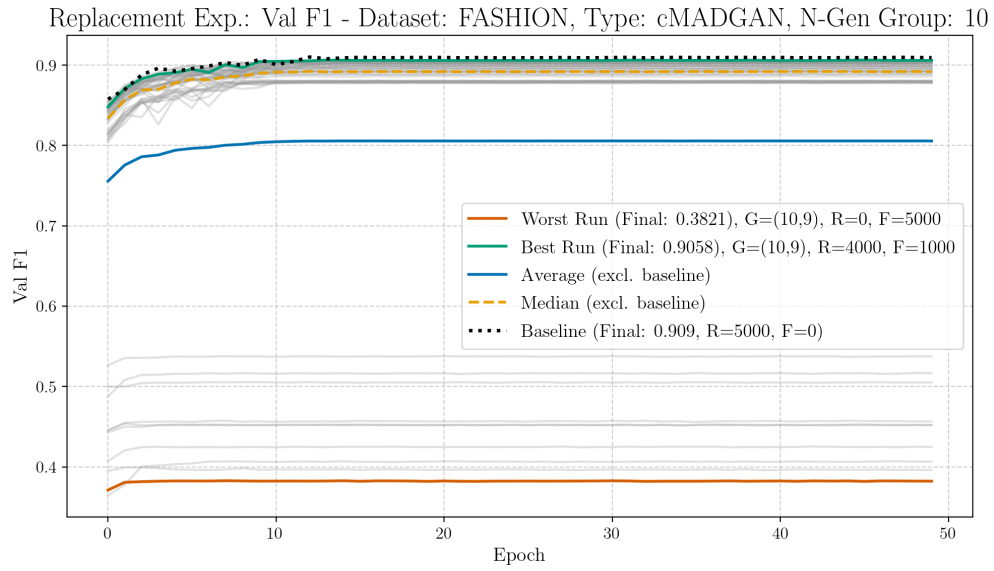
Run Type	Experiment	Val F1
best	$G_{7,2}$, R:4000, F:1000	0.9079
worst	$G_{7,0}$, R:0, F:5000	0.3419
median	G (K=7)	0.8927
average	G (K=7)	0.7993

Expansion Experiment: K=10



Run Type	Experiment	Val F1
best	$G_{10,3}$, R:5000, F:5000	0.9137
worst	$G_{10,9}$, R:5000, F:2000	0.9043
median	G (K=10)	0.9091
average	G (K=10)	0.9095

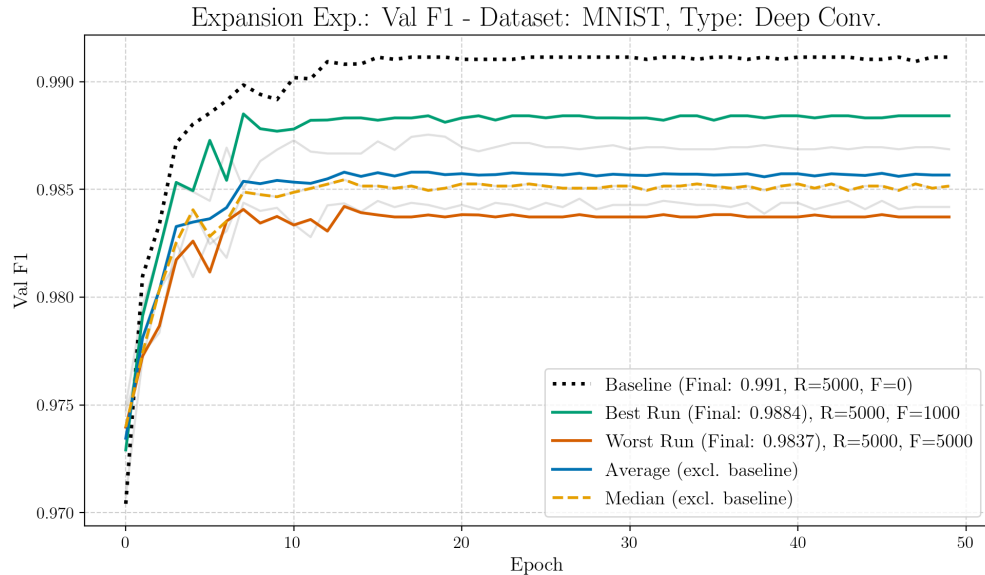
Replacement Experiment: K=10



Run Type	Experiment	Val F1
best	$G_{10,9}$, R:4000, F:1000	0.9058
worst	$G_{10,9}$, R:0, F:5000	0.3821
median	G (K=10)	0.8920
average	G (K=10)	0.8056

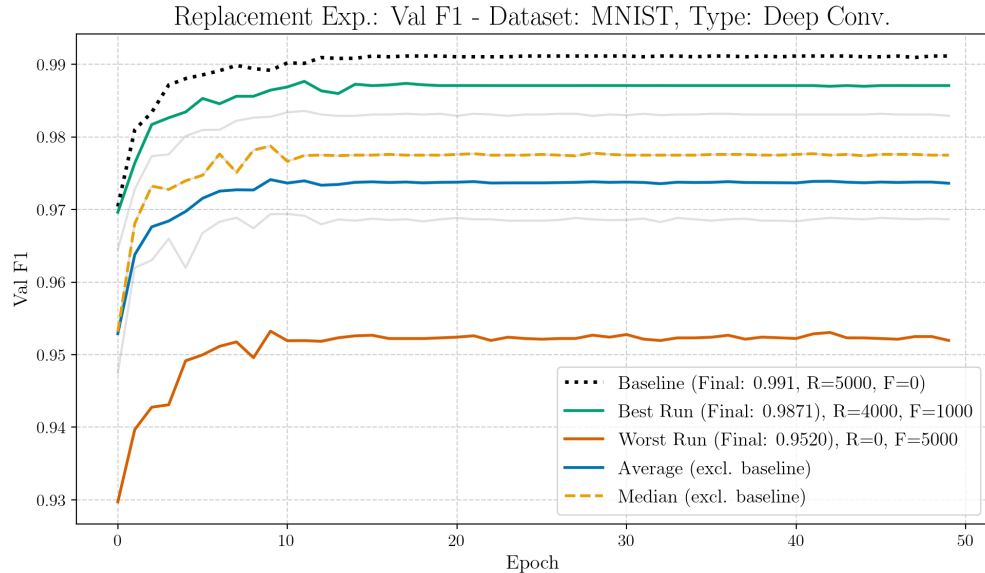
8.3.5 Dataset: MNIST, Architecture: Deep Convolutional GAN

Expansion Experiment:



Run Type	Experiment	Val F1
best	DC (R:5000, F:1000)	0.9884
worst	DC (R:5000, F:5000)	0.9837
median	DC	0.9852
average	DC	0.9857

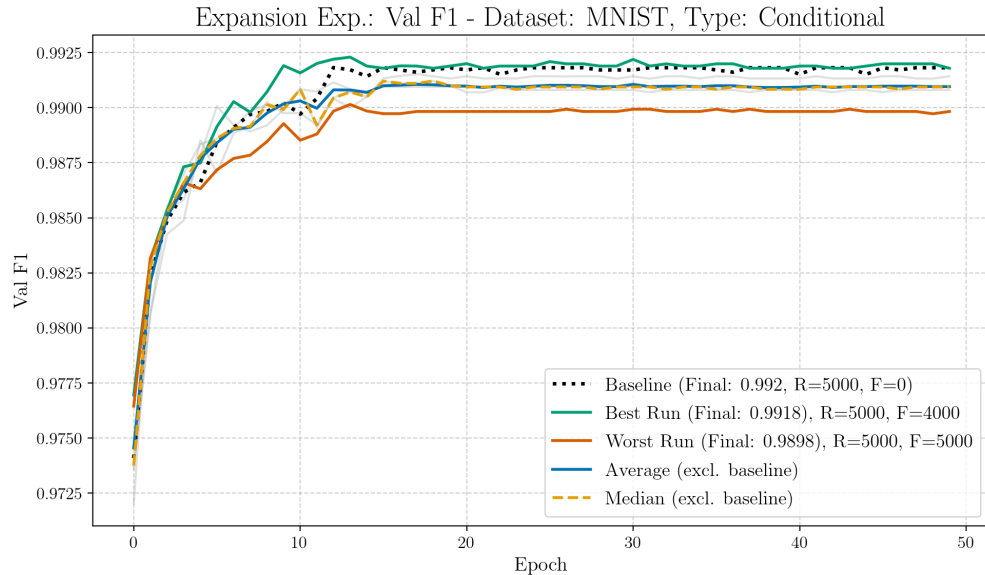
Replacement Experiment:



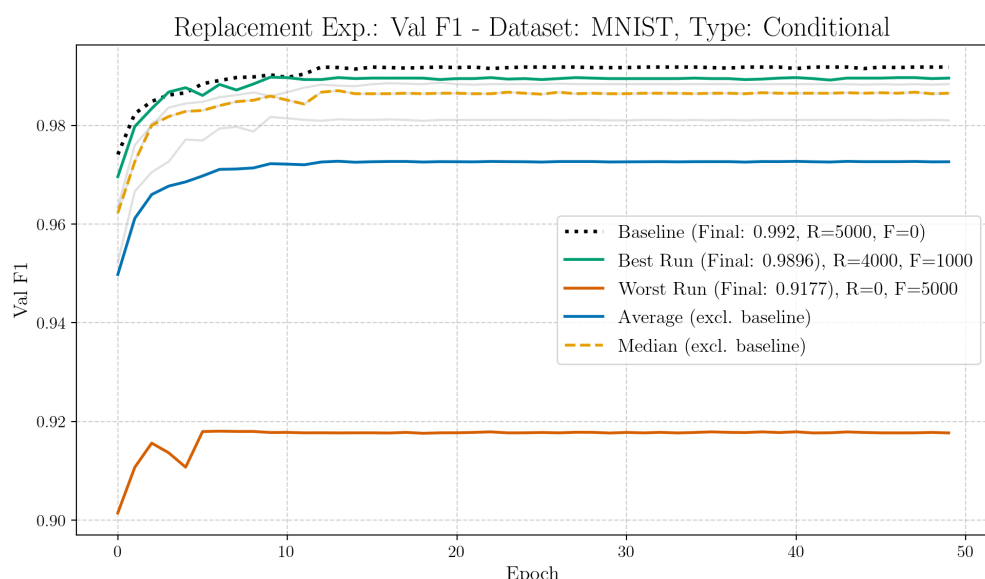
Run Type	Experiment	Val F1
best	DC (R:4000, F:1000)	0.9871
worst	DC (R:0, F:5000)	0.9520
median	DC	0.9775
average	DC	0.9736

8.3.6 Dataset: MNIST, Architecture: COND GAN

Expansion Experiment:



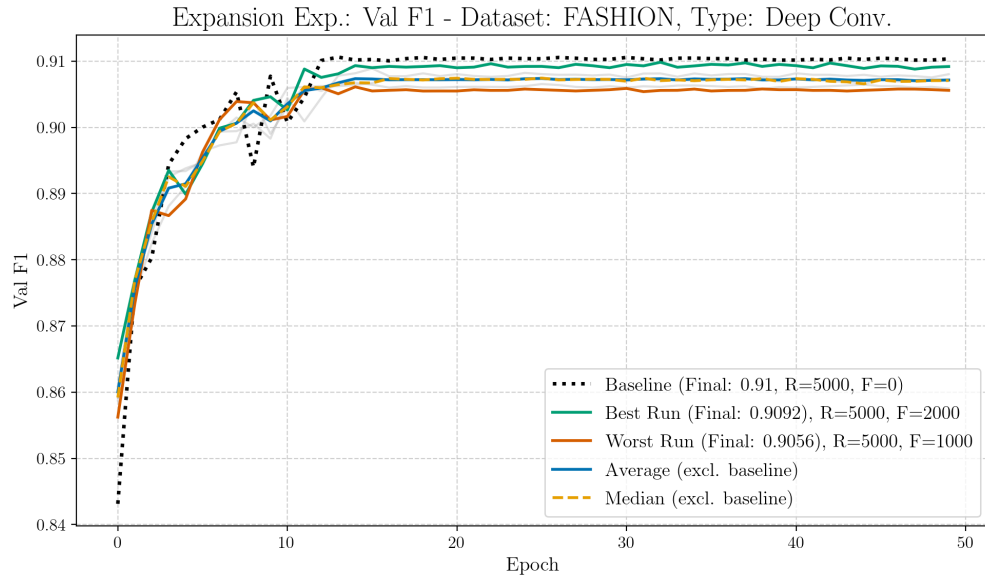
Replacement Experiment:



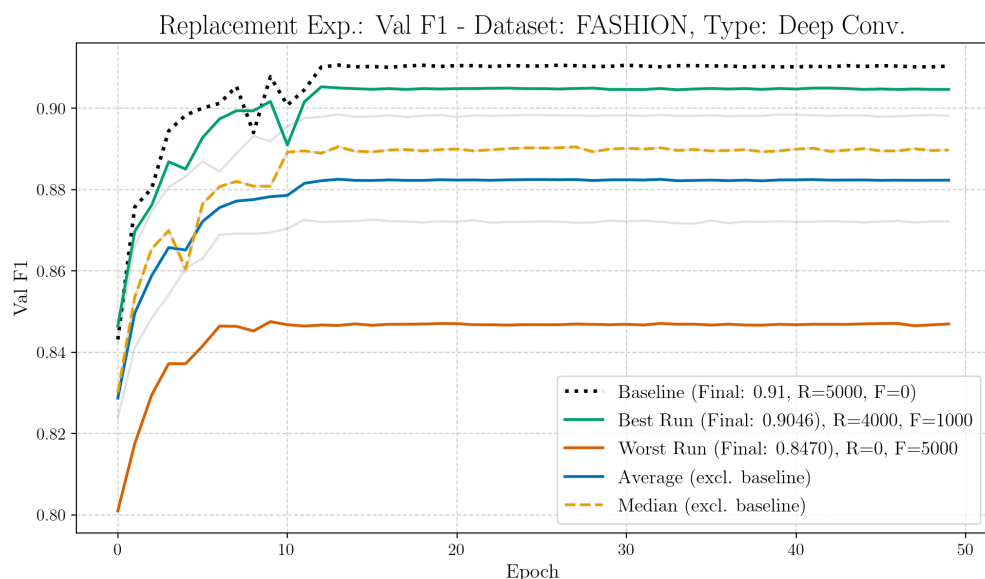
Run Type	Experiment	Val F1
best	Conditional (R:4000, F:1000)	0.9896
worst	Conditional (R:0, F:5000)	0.9177
median	Conditional	0.9865
average	Conditional	0.9726

8.3.7 Dataset: FASHION, Architecture: DC GAN

Expansion Experiment:



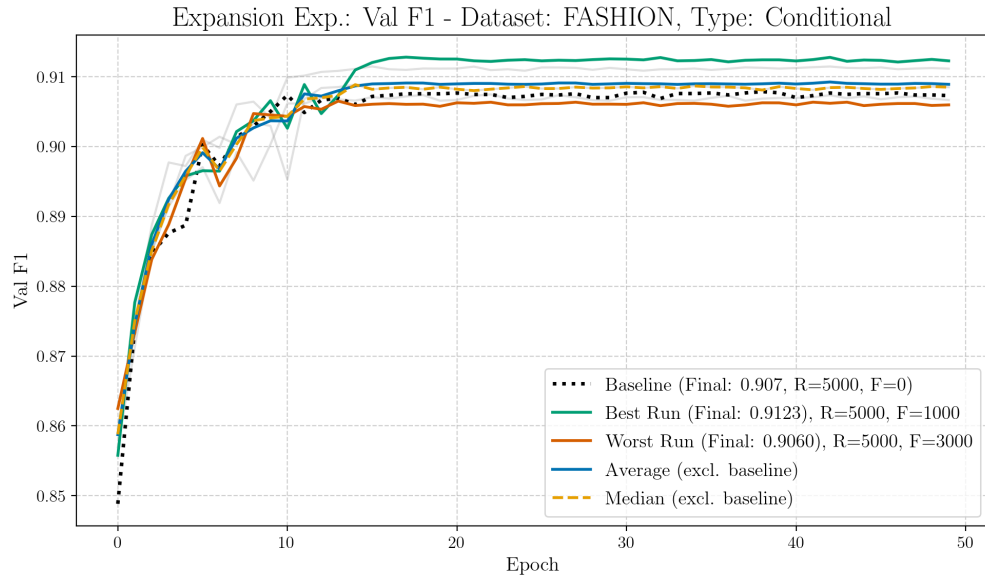
Replacement Experiment:



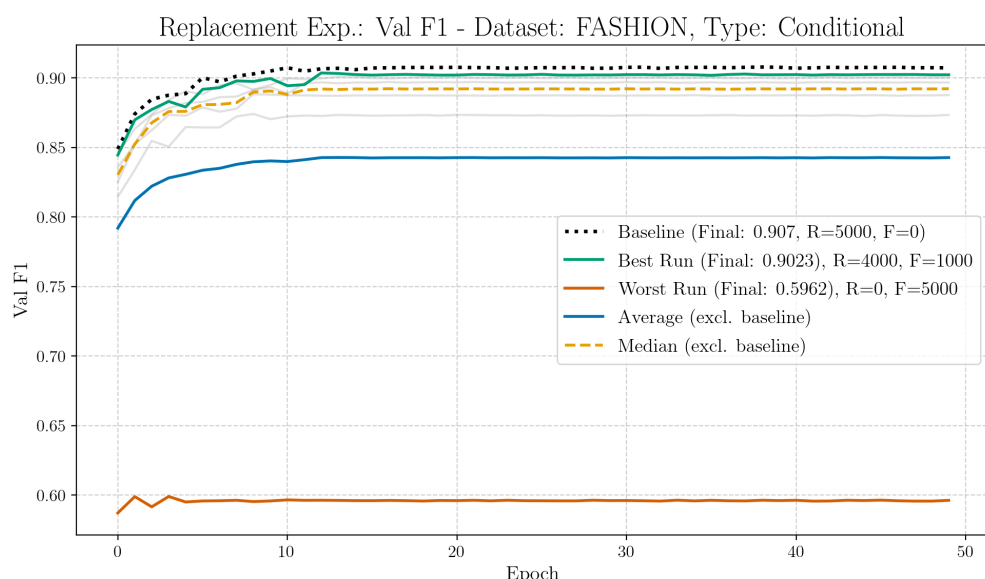
Run Type	Experiment	Performance
best	DC (R:5000, F:1000)	0.9046
worst	DC (R:0, F:5000)	0.8470
median	DC	0.8897
average	DC	0.8823

8.3.8 Dataset: FASHION, Architecture: COND GAN

Expansion Experiment:



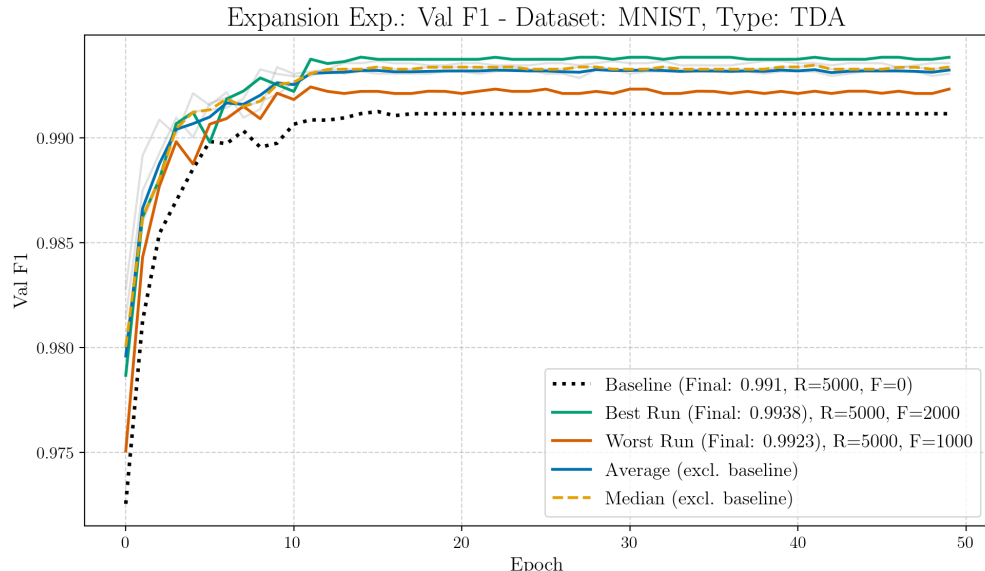
Replacement Experiment:



Run Type	Experiment	Val F1
best	Conditional (R:4000, F:1000)	0.9023
worst	Conditional (R:0, F:5000)	0.5962
median	Conditional	0.8923
average	Conditional	0.8427

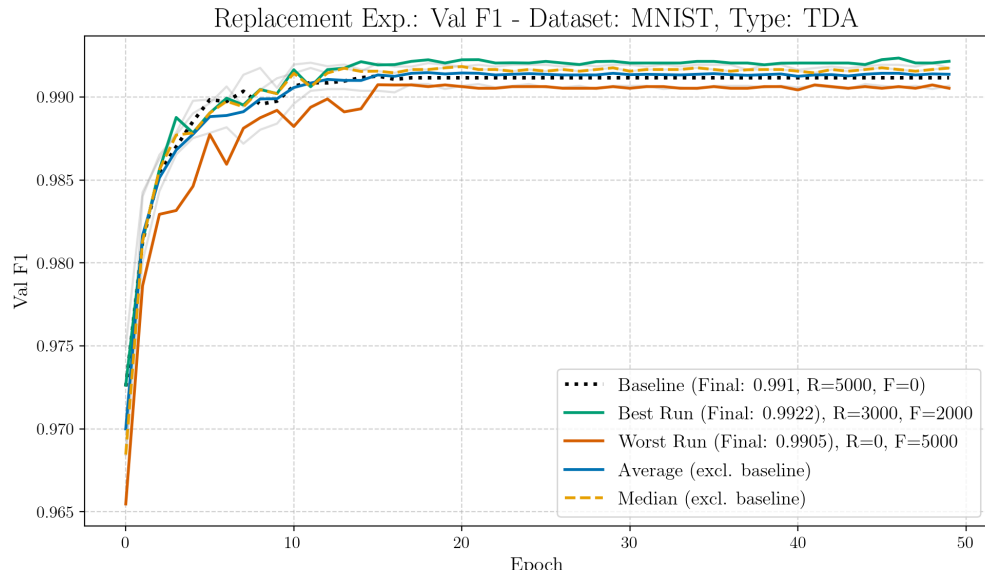
8.3.9 Dataset: MNIST, Architecture: TDA

Expansion Experiment:



Run Type	Metric	Val F1
best	TDA (R:5000, F:2000)	0.9938
worst	TDA (R:5000, F: 1000)	0.9923
median	TDA	0.9934
average	TDA	0.9932

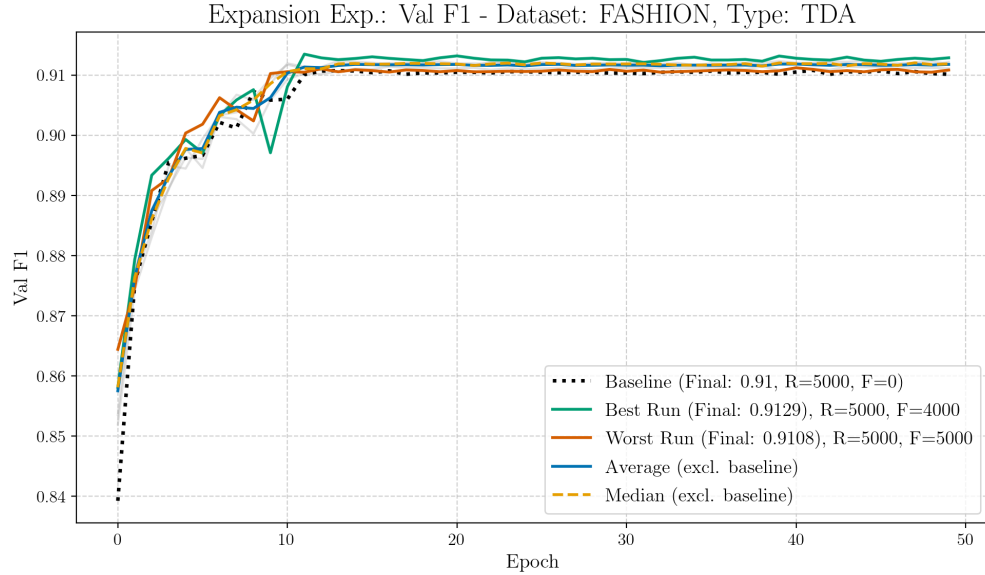
Replacement Experiment:



Run Type	Experiment	Performance
best	TDA (R:3000, F:2000)	0.9922
worst	TDA (R:0, F:5000)	0.9905
median	TDA	0.9917
average	TDA	0.9914

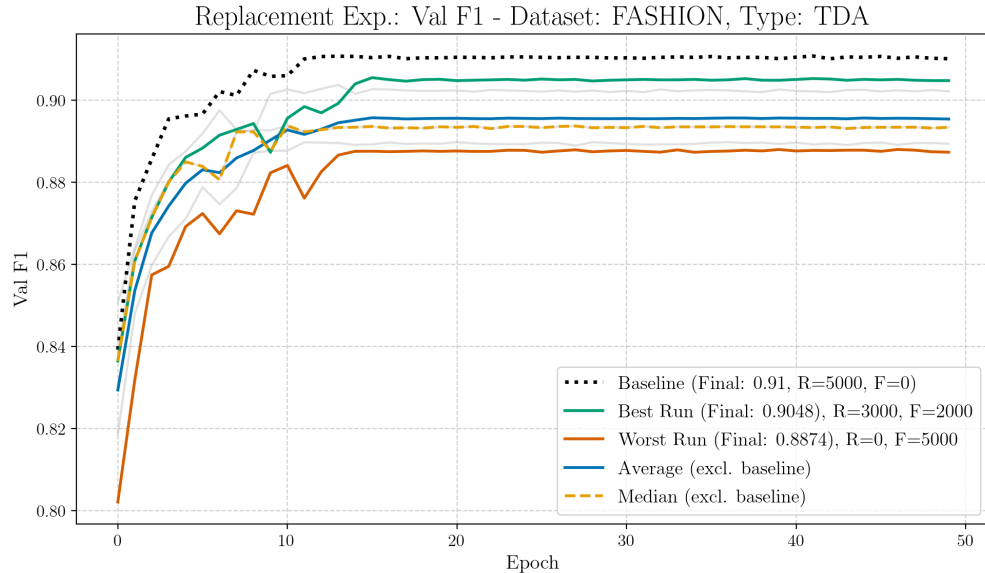
8.3.10 Dataset: FASHION, Architecture: TDA

Expansion Experiment:



Run Type	Experiment	Val F1
best	TDA (R:5000, F:4000)	0.9129
worst	TDA (R:5000, F:5000)	0.9108
median	TDA	0.9119
average	TDA	0.9118

Replacement Experiment:



Run Type	Experiment	Val F1
best	TDA (R:3000, F:2000)	0.9048
worst	TDA (R:0, F:5000)	0.8874
median	TDA	0.8934
average	TDA	0.8955

8.4 Data Creation Histograms

8.4.1 DCGAN MNIST

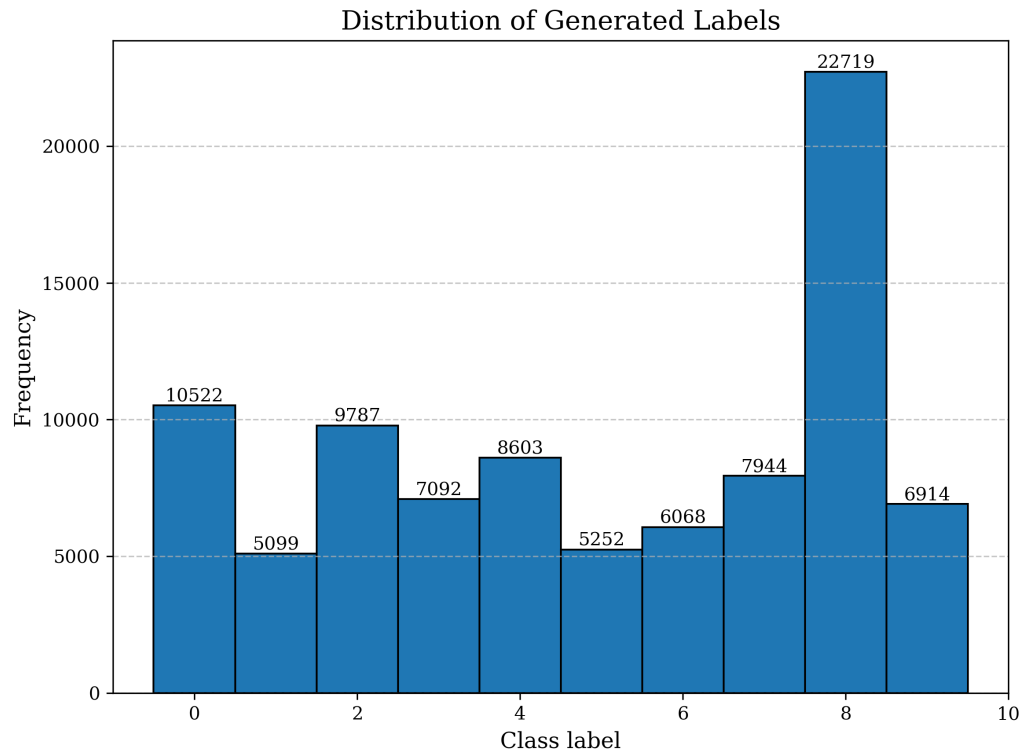


Figure 23: A histogram chart depicting the class distribution of the generated data with the DCGAN generator trained on the **MNIST** dataset. The labels result from an auxiliary classifier as mentioned in 4.1.5.

Declaration of Academic Integrity

Generative Data Augmentation

Multi-Agent Diverse Generative Adversarial Networks for Generative Data
Augmentation.

I hereby declare that I have written this thesis independently. I have properly cited all passages that are taken verbatim or in essence from published or unpublished works of others. All sources and aids used in the preparation of this thesis have been fully acknowledged. Furthermore, this thesis has not been submitted, in whole or in substantial part, to any other examination authority for academic credit.

Signature :

Place, Date :

